COMPARISON OF PERFORMANCE OF SWITCHED RELUCTANCE MOTORS, INDUCTION MOTORS AND PERMANENT MAGNET DC MOTORS

A THESIS SUBMITTED TO
THE GRADUATE SCHOLL OF NATURAL AND APPLIED SCIENCES
OF
MIDDLE EAST TECHNICAL UNIVERSITY

BY

CÜNEYT KARACAN

IN PARTIAL FULFILLMENT OF THE REQUIREMENTS
FOR THE DEGREE OF MASTER OF SCIENCE

IN

ELECTRICAL AND ELECTRONICS ENGINEERING

APRIL 2004

Approval of the Graduate School of Natural and Applied Sciences

_____

Prof. Dr. Canan ÖZGEN
Director

I certify that this thesis satisfies all the requirements as a thesis for the degree of Master of Science.

_____

Prof. Dr. Mübeccel DEMİREKLER
Head of the Department

This is to certify that we have read this thesis and that in our opinion it is fully adequate, in scope and quality, as a thesis for the degree of Master of Science.

_____ _____

Prof. Dr. H. Bülent ERTAN
Co-Supervisor

Prof. Dr. Yıldırım ÜÇTUĞ
Supervisor

Examining Committee Members

Prof.Dr.Muammer ERMİŞ (M.E.T.U. EE) _____

Prof. Dr. Yıldırım ÜÇTUĞ (M.E.T.U. EE) _____

Prof. Dr. H. Bülent ERTAN (M.E.T.U. EE) _____

Assist.Prof.Dr. Ahmet M. HAVA (M.E.T.U. EE) _____

Assist.Prof.Dr.M.Timur AYDEMİR (GAZI UN. EE)_____

I hereby declare that all information in this document has been obtained and presented in accordance with academic rules and ethical conduct. I also declare that, as required by these rules and conduct, I have fully cited and referenced all material and results that are not original to this work.

Cüneyt KARACAN

ABSTRACT

COMPARISON OF PERFORMANCE OF SWITCHED RELUCTANCE MOTORS, INDUCTION MOTORS AND PERMANENT MAGNET DC MOTORS

KARACAN, Cüneyt
M.Sc., Department of Electrical and Electronics Engineering
Supervisor: Prof. Dr. Yıldırım ÜÇTUĞ

April 2004, 124 pages

Since most of the electrical energy is consumed by the electrical motors, it is necessary to use the electrical energy as efficient as possible.

Throughout this study four different types of motors (induction motor, permanent magnet radial flux DC motor, permanent magnet axial flux DC motor, switched reluctance motor) are considered and compared based on their torque per unit volume and speed performance comparison. Torque per unit volume equations are obtained for each of the motor, related to quantities such as magnetic flux density and electric loading and the speed performances are compared by using a washing machine application, which has a wide speed range.

As a result of this study torque per unit volume and speed performance of each of these four types of motors are obtained and motors of different types are evaluated due to their torque per motor volume, torque per ampere, efficiency and etc. over a wide speed range to have an idea about the applications of these motors.

Keywords: permanent magnet motor, induction motor, switched reluctance motor, torque density, performance comparison

ÖZ

ANAHTARLAMALI RELÜKTANS MOTORLARIN, ASENKRON MOTORLARIN VE SABİT MIKNATISLI DC MOTORLARIN PERFORMANS KARŞILAŞTIRMASI

KARACAN, Cüneyt
Yüksek Lisans, Elektrik Elektronik Mühendisliği Bölümü
Tez Danışmanı: Prof. Dr. Yıldırım ÜÇTUĞ

Nisan 2004, 124 sayfa

Elektrik enerjisinin büyük bir kısmı elektrik motorları tarafından tüketildiği için, elektrik enerjisinin olabildiğince verimli kullanılması gerekmektedir.

Bu çalışma boyunca, dört farklı motor (asenkron motor, sabit mıknatıslı radial akılı DC motor, sabit mıknatıslı eksenel akılı DC motor, anahtarlamalı relüktans motor) incelenmiş ve hacim başına tork ve hız performansları karşılaştırılmıştır. Her bir motor için hacim başına tork denklemleri manyetik akı yoğunluğu ve elektriksel yükleme gibi büyüklüklüklerle ilişkilendirilmiş ve hız performansları da geniş bir hız aralığına sahip olan çamaşır makinası uygulaması gözönüne alınarak karşılaştırılmıştır.

Sonuç olarak bu çalışmada dört farklı motor için hacim başına tork değerleri ve hız performansları elde edilmiştir.

Anahtar Kelimeler: mıknatıslı motor, asenkron motor, relüktans motorları, performans karşılaştırması, tork yoğunluğu

ACKNOWLEDGEMENTS

I express sincere appreciation to my thesis supervisor Prof. Dr. Yıldırım Üçtuğ and co-supervisor Prof. Dr. H. Bülent Ertan for their valuable advices and guidance throughout all stages of this study.

I offer sincere thanks to M. Timur Aydemir, who encouraged me during M.Sc. study.

I wish to thank Erdal Bizkevelci for his patience to my questions. Levent Burak Yalçıner for his helps at using the optimization program.

I thank all my friends (Serkan Şedele, Tolga İnan, Akın Acar, Çağlar Özyurt,) and all Tübitak Bilten IEC Group staff for their support and deep understanding during this study.

Special thanks to Hacer Üke for her support and understanding.

Finally I would like to thank my family for their precious support during all stages of my life.

TABLE OF CONTENTS

LIST OF TABLES

TABLE

LIST OF FIGURES

FIGURE

CHAPTER 1

INTRODUCTION

1.1 Introduction

Energy cost and information technology force designers to make more energy efficient and reliable motors. Since, in industrial countries nearly 70% of the electrical energy is consumed by the electrical motors, today it is important to use electrical energy as efficient as possible.

Electrical equipments do much of the work in industry and in the house. In most cases the electrical energy is transformed into mechanical energy. High torque density and efficiency are the most desirable features for an electric motor. In the last decades development of new types of electric motors arise the question, which motor has the highest torque density and is best for a certain application.

The aim of this study is the comparison of four different types of motors, such as induction motor, switched reluctance motor, axial flux permanent magnet brushless DC motor and radial flux permanent magnet brushless DC motor according to their torque per unit volume and applicability to a variable speed washing machine application (typical torque speed curve of a washing machine drum is given in appendix C).

It is evident that, to be able to compare the performance of these four different types of motors a framework should be set. Since it is a dimensionless quantity torque per unit volume can be used as a common basis to compare these motors. However all of these motors need to be electronically driven to achieve the desired speed range. Therefore the ratings of the switches are important from the point of view of drive cost.

For this reason in this study, besides the torque density comparison torque per unit volume, torque per ampere, efficiency etc. of each of the discussed motors are also compared. Such expressions are useful for a broader overlook to the problem to identify which type of motor has an inherent advantage.

To find the torque per unit volume, torque equations should be derived related to volume expressions for each of the four types of motors. Torque equation for each type of the motor includes the magnetic loading, electric loading and motor dimensions [4]. When these torque expressions are divided by the volumes, torque per unit volume (torque density) of each type of motor can be found. Hence by using the torque density expression performance comparison of these motors can be evaluated.

Since a washing machine has a wide speed range of nearly 1:30 (washing mode and spin mode of operation) it is appropriate to use a washing machine application to accomplish this comparison.

1.2 Outline

Chapter 2 includes firstly brief information about well known induction motor. Then the torque and torque density equations for the induction motor are derived by considering sizing equations and magnetic field view point. At the end of the chapter a result section is given.

Chapter 3 is assigned to permanent magnet brushless DC motors, both radial flux and axial flux configurations. At the introduction part of this chapter some aspects of PM excitation are given. Then the first subsection of this chapter constitutes introduction of magnet materials. Second and third subsections of this chapter constitute the basics of permanent magnet brushless DC motor operation and derivation of the torque equations for both of the radial flux and axial flux BLDC motor types respectively. At the end of each subsection, there is a result part that summarizes the work done under that subsection.

Chapter 4 is assigned to the consideration of switched reluctance motors. Chapter starts with the introduction part including some aspects of switched reluctance motor such as design and operation. As was done in previous chapters

torque and torque density equations are derived, related to the magnetic and electric loadings, and at the end of the chapter results are considered.

Chapter 5 evaluates the performances of the motors, considered in the previous chapters for a washing machine application due to its wide speed range.

Chapter 6 is the last chapter of this study and it includes the comparison of the motors and conclusion on the results.

CHAPTER 2

INDUCTION MOTOR

2.1 Introduction

An induction motor is one in which alternating current is supplied to the stator directly and rotor by induction or transformer action from the stator [2]. Thus each coil of the induction motor stator winding with the opposing coils of the rotor winding, may be considered a transformer and whole motor may be thought of as a series of such transformers arranged radialy around the periphery. Rotor of an induction motor may be one of two types, wound rotor or squirrel cage rotor.

Most induction motors are designed to operate from a three phase supply. If variable speed operation of the motor is necessary, the source is normally an inverter.

Slots in the inner periphery of the stator accommodate three phase windings (for three phase induction motor). To have nearly sinusoidal air-gap flux density, windings in the slots are distributed.

This chapter covers the derivation of torque equation related to rotor and motor volume and hence the torque per unit volume of the induction motor for the comparison purposes with the other types of motors, considered in the following chapters. Consideration of the speed range of the induction motor by using the pre-defined washing machine application in a separate chapter after obtaining the torque equations of the other types of motors (torque speed curve is given in appendix section). And chapter ends with the obtained results.

2.2 Derivation of the Torque Equation

Before starting the derivation of the torque equation of an induction motor it is worth to recall some basic equations such as power, back EMF, flux, magnetic loading and electric loading that will be used during the derivation of the torque equation.

$$S = 3 \times E_{ph} \times I_{ph} \times 10^{-3} \text{ kVA} \tag{2.1}$$

$$P_m = S \cos\varphi\eta \tag{2.2}$$

$$T = \frac{S \cos\phi\eta}{w_r} \tag{2.3}$$

Where;

"E_{ph} "and "I_{ph} "are RMS values of back EMF and current respectively.

"w_r" is the mechanical speed in r/s

"η" is the efficiency

"S" is the total power in VA

"P_m" is the real power

$$E_{ph} = 4.44 \times N_{ph} \times f \times k_w \times \phi_p \tag{2.4}$$

$$\Phi_p = B \times A_p = B \times \frac{\pi \times D_i \times L}{P} \tag{2.5}$$

$$f = \frac{n \times P}{120} \tag{2.6}$$

$$B = \frac{2}{\pi} \times B_{\max} = \frac{P \times \phi_p}{\pi \times D_i \times L} \tag{2.7}$$

$$q = \frac{3 \times 2 \times N_{ph} \times I_{rms}}{\pi \times D_i} \tag{2.8}$$

Then by using equation (2.8) phase current can be found as;

$$I_{rms} = \frac{q \times \pi \times D_i}{6 \times N_{ph}} \tag{2.9}$$

Where

"Φ_p "is total flux/pole (Wb)

"A_p "is the pole area

"P" is the number of poles

"n" is the speed in rpm

"k_w "is the winding factor

"f" is the frequency

"N_{ph} "is the turns/phase

"B" is the average magnetic loading (mean flux density over the surface of the air gap)

"q" is the RMS ampere conductors per unit length of air gap periphery

Substituting all equations into equation (2.1), we get the power equation of the motor related to dimensions, magnetic loading and electric loading.

$$S = \left(\frac{\pi^3 \times 10^{-3}}{120 \times \sqrt{2}} \times k_w \right) \times D_i^{\,2} \times L \times n \times B \times q$$

Taking k_w as 0.9;

$$\frac{S}{n} = 1.65 \times 10^{-4} \times B \times q \times D_i^{\,2} \times L \qquad (2.10)$$

Where the unit of S/n is kVA/1000 rpm

- If kVA/1000 rpm increases mean flux density (B) increases too
- If kVA/1000 rpm increases specific electric loading increases too

Hence increase of the S/n ratio increases the machine size.

Torque equation can be obtained by using

1-) Coupled circuit view point

2-) Magnetic field view point

It is appropriate to use magnetic field view point because first one gives no conception of the effects of physical dimensions. The second one should supply some of these missing features.

Currents in the machine windings create magnetic flux in the air-gap between the stator and rotor, the flux paths being completed through the stator and rotor iron. As shown in figure 2.1 magnetic poles of both stator and rotor are centered on their magnetic axes.

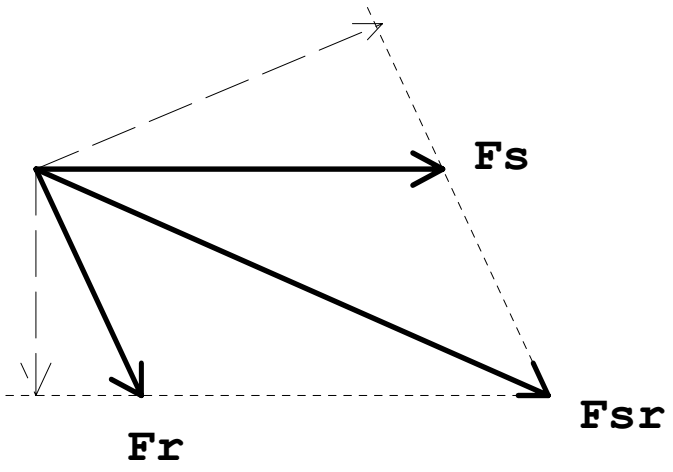

Figure 2 1 Magnetic field vectors

For an induction motor torque is produced by the tendency of the rotor magnetic field (F_r) and the stator magnetic field (F_s) to align.

$$F_{sr} = H_p \times g \tag{2.11}$$

The resultant MMF "F_{sr}" acting across the air-gap is a sine wave and vector sum of the stator and rotor MMFs so the peak value of resultant MMF is:

$$F_{sr} = F_s{}^2 + F_r{}^2 + 2 \times F_s \times F_r \times \cos \delta_{sr} \tag{2.12}$$

And the resultant radial magnetic field density is a sinusoidal with a peak value of:

$$H_p = \frac{F_{sr}}{g} \tag{2.13}$$

$$B_p = \mu_o \times H_p \tag{2.14}$$

$$B = \frac{2}{\pi} \times Bp \tag{2.15}$$

Where;

"Fs"r is the resultant MMF of the stator and rotor windings.

"F's" are the peak values of the stator and rotor magnetic fields.

"g" is the air-gap length

"H_p" is the peak magnetic intensity of the stator.

"δsr" angle between stator and rotor magnetic fields.

"B, H, F" are assumed to be sinusoidally distributed in the space.

To find the torque equation by using the magnetic field view point we should use co-energy concept which is the state function of current and angular distance.

$$dW'_{fld}(i,x) = \lambda di + f_{fld}\,dx \tag{2.16}$$

$$dW'_{fld}(i,x) = \frac{\partial W'_{fld}}{\partial i}\,di + \frac{\partial W'_{fld}}{\partial x}\,dx \tag{2.17}$$

$$\text{Average co-energy density} = \frac{1}{2}B_{rms}H_{rms} = \frac{\mu_0}{2}H_{rms}^2 = \frac{\mu_0}{4}H_{peak}^2 \tag{2.18}$$

Total co-energy = (Average co-energy density) x (Volume of air-gap)

Using equations (2.13), (2.18) total co-energy can be rewritten as;

$$W'_{fld} = \frac{\mu_o}{4} \times \left(\frac{F_{sr}}{g}\right)^2 \times \pi \times D_i \times L \times g \tag{2.19}$$

An expression for the torque can be obtained in terms of interacting stator and rotor magnetic fields by taking the partial derivative of field co-energy with respect to angle.

$$T_{pp} = \frac{\partial W'_{fld}}{\partial \delta_{sr}} \tag{2.20}$$

As a result by using the magnetic field view point the torque for one pole pair becomes:

$$T_{pp} = -\frac{\mu_o \times \pi \times D_i \times L}{2 \times g} \times F_s \times F_r \times \sin\delta_{sr} \tag{2.21}$$

To get the total torque, multiply equation (2.21) by number of pole pairs then the total torque expression becomes:

$$T = -\frac{P}{2} \times \frac{\mu_o \times \pi \times D_i \times L}{2 \times g} \times F_s \times F_r \times \sin \delta_{sr} \qquad (2.22)$$

Negative sign that the torque equation includes, indicates that the fields tend to align themselves.

This total torque expression can be written in two different forms by using the expressions;

$$\begin{aligned} F_s \sin \delta_{sr} &= F_{sr} \sin \delta_r \\ F_r \sin \delta_{sr} &= F_{sr} \sin \delta_s \end{aligned} \qquad (2.23)$$

Using equations (2.13), (2.14), (2.15), (2.22), (2.23)

$$\begin{aligned} T &= -\frac{P}{2} \frac{\pi D_i L}{2} F_r B_{sr} \sin \delta_r \\ &OR \\ T &= -\frac{P}{2} \frac{\pi D_i L}{2} F_s B_{sr} \sin \delta_s \end{aligned} \qquad (2.24)$$

And using flux per pole expression in equation (2.5) we get;

$$T = -\frac{\pi}{2} \left(\frac{p}{2} \right)^2 \phi_p F_r \sin \delta_r \qquad (2.25)$$

Where;

"Φ_p" is the flux/pole.

Now starting with the torque equation of

$$T = -\frac{P}{2}\frac{\pi D_i L}{2} F_r B_{sr} \sin \delta_r$$

Noting that

$$F_{\max} = \frac{4}{\pi} \times k_w \times \frac{N_{ph}}{P} \times I_p$$

$$F = \frac{n}{2} \times F_{\max}$$ (*n* is the number of phases)

By using the above equations

$$F_s = \frac{3}{2} \times \frac{4}{\pi} \times k_w \times \frac{N_{ph}}{P} \times I_p \quad (2.26)$$

Where

$$I_p = \sqrt{2} \times I_{rms}$$

Then assuming that $F_s=F_r$, and taking k_w as "0.9" we get

$$T = \frac{1.3\pi}{4} D_i^2 LBq \quad (2.27)$$

Note that

$$B = \frac{2}{\pi} \times B_p$$

$$B_p = B_{sr}$$

Since the rotor volume can be calculated as

$$V_{rotor} = \frac{\pi \times D_i^{\,2} \times L}{4} \tag{2.28}$$

Then by using equations (2.27) and (2.28) we can get the torque per unit rotor volume as:

$$T_{v-rot} = 1.3Bq \tag{2.29}$$

Now this torque should be related to the motor outer dimensions instead of the rotor only. For this reason the ratio of the stator outer diameter to inner diameter should be determined to find the torque per unit volume expression. Outer diameter calculation of the induction motor is given in "Appendix A". Outer diameter of the induction motor can be approximated as in equation (2.30).

$$D_o = \frac{\pi \times D_i}{P \times K_{br}} + \sqrt{D_i^{\,2} + \frac{4 \times D_i \times q}{K_{cu} \times J}} \tag{2.30}$$

Where

$$K_{br} = \frac{B_{sc}}{B}$$

and

$$K_{cu} = \frac{A_{T-cu}}{A_1}$$

The ratio of the outer diameter to inner diameter can be expressed as;

$$\frac{D_o}{D_i} = \frac{\pi}{P \times K_{br}} + \sqrt{1 + \frac{4 \times q}{K_{as} \times J \times D_i}} \tag{2.31}$$

2.3 Results

- From equation (2.24), torque is proportional to the rotor surface area. Hence larger motors utilize the rotor surface area better.
- In most induction motor drives, the flux density is maintained at or near its maximum value (limited by saturation) so as to obtain maximum torque per ampere of stator current. Thus to get maximum torque for the motor, equation (2.29), B should be as high as possible.
- From equation (2.27), if "B, q, J and rotor volume (D_i, L)" are fixed, then as the number of poles increases torque does not change but D_o/D_i ratio gets smaller, this decrease results decrease in motor size and hence the torque per unit motor volume increases
- From equation (2.27), if "B, q, J and motor volume (D_o, L)" are fixed D_i can be determined from D_o/D_i ratio. As the number of poles increases D_o/D_i decreases (or D_i/D_o increases) so rotor volume increases increasing the torque. Since the motor volume is fixed and we get an increase for the torque with the increasing of the rotor diameter, then the torque per unit motor volume increases.
- As a result of above two conclusions, torque per unit motor volume increases with the increase of the number of poles but this increase saturates after a certain point due to its asymptotic nature (figure 2.2).

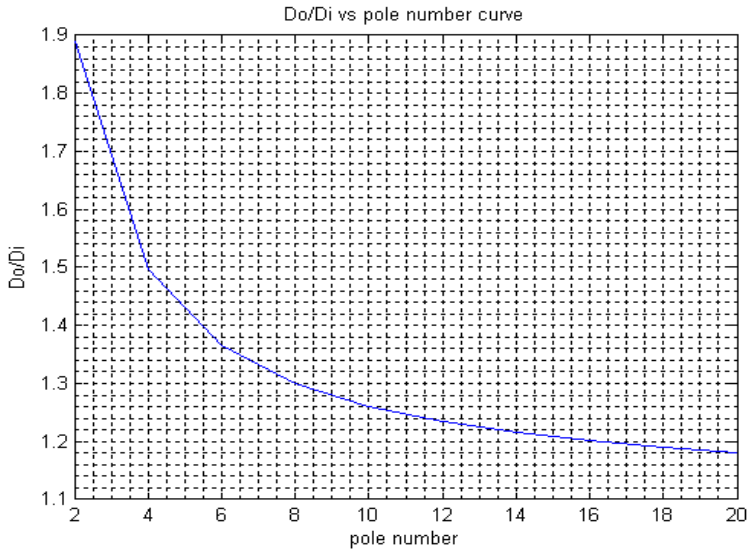

Figure 2 2 Change of the outer to inner diameter with pole number

- As long as the motor volume kept constant, it is necessary to increase the torque per unit rotor volume to get a higher torque per unit motor volume.
- Torque per unit rotor volume is constant as long as "B and q" values are kept constant. It does not depend on number of poles (equation 2.29).
- Maximum "B" value is used during the design stage of the motor. To maintain same flux density in the stator and rotor yokes, yoke thickness should be increased as the number of poles decreases, hence for the same outer diameter the rotor of the motor with smaller number of poles will have smaller diameter than that of larger number of poles. Hence this satisfies that torque production increases with increasing pole number.
- With the increasing of number of poles, the coupling between rotor and stator windings is decreased, increasing the leakage inductance and decreasing the motor losses.
- Torque can be increased by increasing specific electric loading (q) with constant rotor dimensions (D_i, L). To get high value for specific electric loading we should increase I_{ph}, to increase I_{ph} we need high E_{ph} value so choose E_{ph} slightly lower than the maximum AC output of the inverter.
- From equation (2.7) if flux per pole increases magnetic loading also increases. This increase of magnetic loading also increases the torque per unit rotor volume.

CHAPTER 3

PERMANENT MAGNET BRUSHLESS DC MOTOR

3.1 Introduction

There are two common sources of magnetic fields, one being current flowing in a wire and the other is a permanent magnet [6]. Brushless DC (BLDC) motors are sometimes referred to as inside out PM motors with the magnets on the rotor and windings on the stator. The idea of energy transmission between the rotor and the stator is based on excitation of a number of stationary coils interacting with a field created by permanent magnets. These motors have a simpler design than wound field motors and they are lighter and efficient, having no copper losses in the field winding.

PM excitation has some advantages and also disadvantages when compared with the electromagnetic excitation. These advantages and disadvantages of PM excitation are sorted as:

- As diameter decreases, cross-sectional area available for copper decreases with the square of the linear dimension, while the need for MMF decreases linearly hence per unit copper losses increase in smaller motors, decreasing efficiency of electromagnetically excited motors [1].
- As diameter increases magnet volume becomes large and expensive.
- Large motors usually require field weakening operation, which is practically difficult to accomplish.
- With PM excitation, a short circuit in armature winding may cause high braking torques, causing motor destruction or fires.
- For motors with rotor diameter less than 500 mm the magnet volume is less than copper volume. However, cost of high energy magnets is higher than that

of copper. Therefore, only for rotors with diameters less than 20 mm PM excitation will be cheaper than electromagnetic excitation.

- When running costs are taken into account, PM motors will pay for themselves (especially for small motors) in a few months due to electric power savings, since they do not require power to energize the field [1].

After considering these advantages and disadvantages, one can decide whether PM excitation or electromagnetic excitation will be used for the application.

This chapter constitutes brief information about PM materials and properties of these materials. In the following sections of this chapter radial flux brushless DC motor and axial flux brushless DC motor are described and their torque and hence torque density equations are obtained. At the end of each subsection obtained results are summarized to give an idea about the work done so far. It is also possible to find some information about BLDC motor drive circuit throughout this chapter.

3.2 Permanent Magnet Materials

The development of permanent magnet material has been fast during the last decades. Compared with ferrous magnetic materials, the Alnicos have high flux densities (thus producing high output torques) and high coercive force (thus resisting demagnetization from the effects of armature reaction).

The development of commercially useful permanent magnet materials began in the 20^{th} century. In 1930's Aluminum-nickel-cobalt alloy AlNiCo was developed having a low coercive force which is the major drawback for this magnet. In the 1950's ferrite permanent magnets which have higher coercive force and energy product but low remanence. The next milestone in the development of permanent magnetism was the development of Samarium-Cobalt magnets around 1970's. They offer high remanence and high coercive force. However, the high price of the raw materials has prohibited large scale use. And last development in permanent magnet technology is the NdFeB magnets introduced in 1980's. although cheaper than SmCo and of even higher energy density, NdFeB is not always superior due to its lower thermal stability.

With the development of ceramic magnets (barium ferrite and strontium ferrite), lower cost motors could be produced but with a lower output torque due to their lower flux densities. But having much higher coercive forces than that of the Alnicos makes these more resistant to demagnetization force due to the armature reaction.

The most recent developments are the neodymium-iron-boron (Nd-Fe-B) alloys. Magnetic performance of these alloys is about 30% better than that of the samarium cobalt magnets. The usage of Nd-Fe-B magnets is increasing due to their high magnetic performance. During the consideration of the permanent magnet motors either radial flux type or axial flux type Nd-Fe-B magnets are used in this unless otherwise specified.

A demagnetization characteristic for a NdFeB magnet material is shown in figure 3.1. It is characterized by an essentially linear relation with a residual flux density and a slope of approximately μ_o until a point (B_D, H_D), a limit which must not be exceeded if demagnetization to be avoided, is reached.

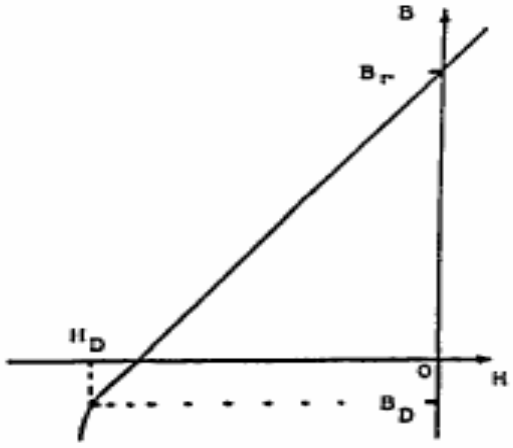

Figure 3 1 Demagnetization characteristics for a typical Nd-Fe-B magnet

Most magnet types are available in both bonded and sintered forms. Bonded magnets are formed by suspending powdered magnet material in a non-conductive, nonmagnetic resin. Magnets formed by this way are not capable of high performance since a substantial fraction of their volume is made up of a

nonmagnetic material. Sintered magnets, on the other hand, are capable of high performance because the sintering process allows magnets to be formed without a bonding agent [6].

Permanent magnet materials are characterized by three specific parameters which are,

- Residual Flux, B_r
- Coercive Force, H_c
- Maximum Energy Product, $(BH)_{max}$

Residual flux is the maximum flux density that can be retained by the magnet itself at a specified temperature.

Coercive force is the value of magnetic flux intensity that brings magnetic flux density "B" to zero.

Maximum energy product is not the actual stored energy, but rather it is a qualitative measure of a magnet's performance capability in a magnetic circuit and this specification is usually the first specification used to compare the magnets. More importantly it gauges how hard the magnet is working to provide flux against the demagnetizing influence of the external circuit. Figure 3.2 shows the development of the $(BH)_{max}$ value with the years.

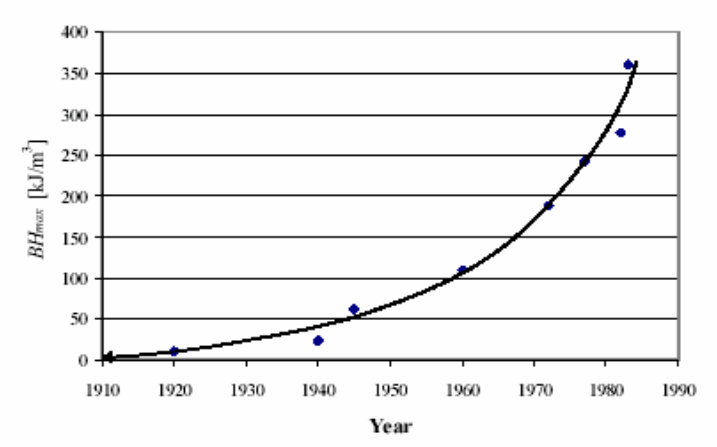

Figure 3 2 Development of permanent magnet materials by the years

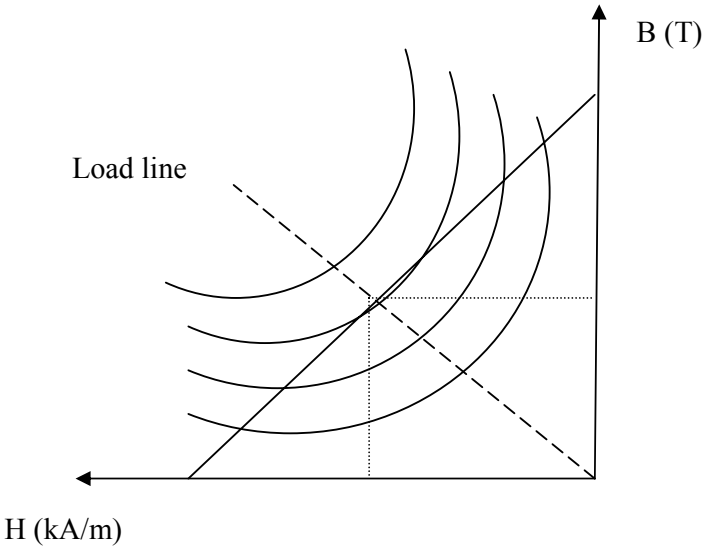

Figure 3 3 Representation of (BH)max point

As seen from the figure 3.3 maximum energy product of a magnet occurs where the intersection of the demagnetization characteristics and load line is tangent to the hyperbola.

In addition to the magnetic performance of the permanent magnet materials, temperature limits must be considered for a proper operation of permanent magnet motor.

Nd-Fe-B magnets can be operated over a wide temperature range. In the normal range of operating temperature as the temperature is increased, the residual flux density and coercivity of the magnet will come down. But this is a reversible process because when the temperature is reduced the flux density and coercivity will return to the original value. This variation in residual flux density of the magnet along with variation in armature resistance of the with temperature, influences the torque capability and efficiency of the PM motor.

Above a critical temperature, it will result in irreversible demagnetization of the magnet. Once this happens the flux density will not come back to its original value as the temperature is reduced.

3.3 Brushless DC motor Drives

A BLDC motor is a motor, which has trapezoidal shaped back EMF waveforms. Since BLDC motor has a trapezoidal back EMF, to have a smooth torque this motor should be fed by rectangular current pulses that are aligned with the flat portions of the back EMF waveform and with the same polarity as shown in figure 3.4.

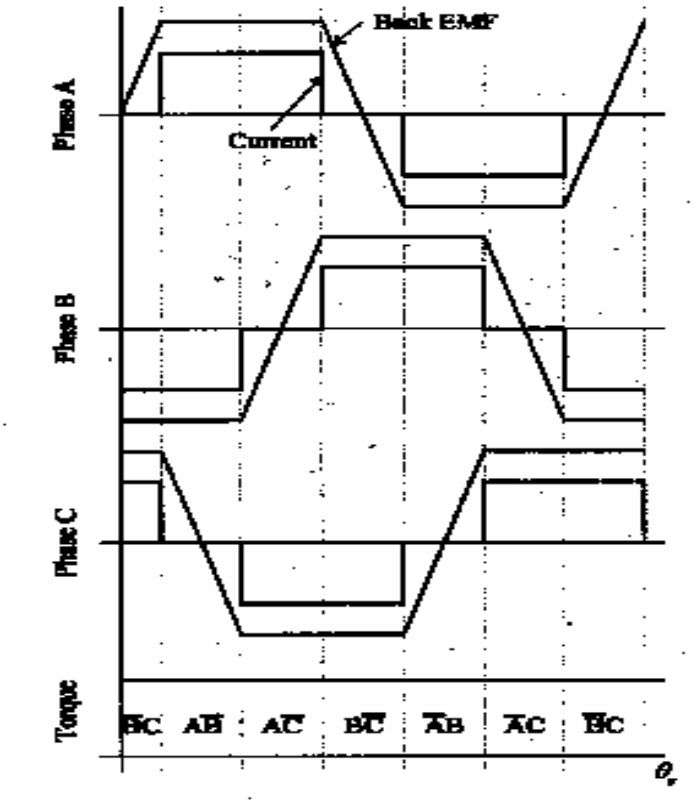

Figure 3 4 Back EMF and current waveforms for BLDC motor

For each 60° positive current flows in one phase, negative current with the same amplitude flows in another phase and no current flows in third phase. Every 60° the current in one phase remains same while the current flowing in another phase goes to zero and the current in the third phase, previously had zero value, becomes nonzero. This action resembles the commutation process that of

commutator DC motor. But for BLDC motor this process is named as electronic commutation.

Electronic commutation is accomplished by opening and closing the six inverter switches. There are six inverter switching actions during each electrical cycle (360°) and two of the six switches, one in the upper and one in the lower, are conducting at any instant as in figure 3.5

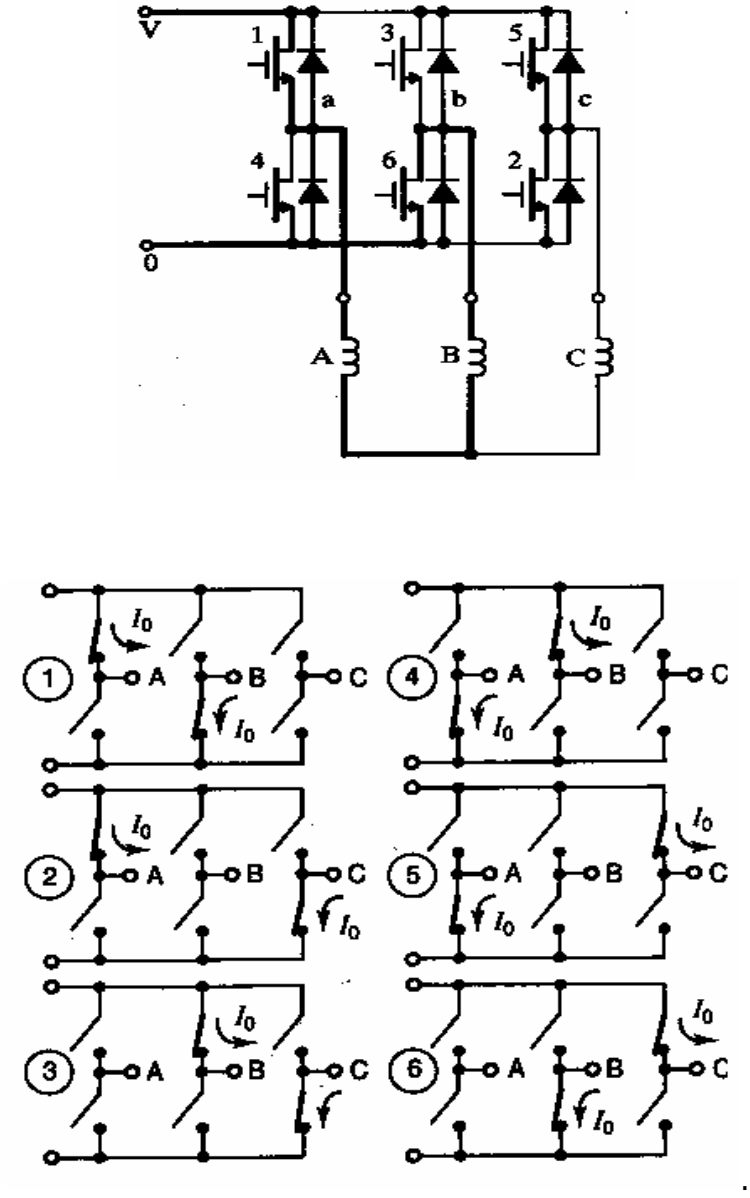

Figure 3 5 Inverter and switching schemes for BLDC motor

To commutate the current from one phase to another, it is necessary to set the switch of the non-conducting phase to 'on' position and simultaneously one of the conducting phases to 'off' position without changing the switch position of the third phase (i.e. Consider figure 3.5, in first stage A and B phases are conducting while phase C has no current flowing on it. When the switching scheme is arranged as in the second stage, current on phase B commutates to phase C and no current change occurs on phase A). for all cases two of the three phases are conducting at the same time with a current of opposite polarity.

To achieve a successful commutation between incoming and outgoing phases, rotor position sensing is necessary. The rotor position is sensed by the help of Hall-effect sensors and the appropriate inverter switches are triggered by the use of the signals coming from Hall-effect sensors.

3.4 Radial Flux Brushless DC Motor

3.4.1 Introduction

New developments in the field of magnet technology have brought great changes in motor design. Brushless design configuration requires PM rotors, magnets producing the air-gap flux and alternating stator currents to produce torque. Since space on the rotor is limited proper utilization of magnetic material is a vital consideration for good designs.

First alternative for the construction of the PM motor is to replace the field winding in a brushed DC motor (figure 3.6 a). In this case stator establishes flux and rotor carries armature winding. Second alternative is to replace the windings on a rotor (figure 3.6 b). In this case armature winding is on the stator. Commutator in a DC motor converts the input DC current into approximately rectangular shaped currents. By applying this rectangular shaped current directly to the stator and field current from the permanent magnets on the rotor surface this motor now becomes a Brushless DC Motor (BLDC) and the current in the stator must be commutated electronically so that this motor can be named as electronically commutated motor.

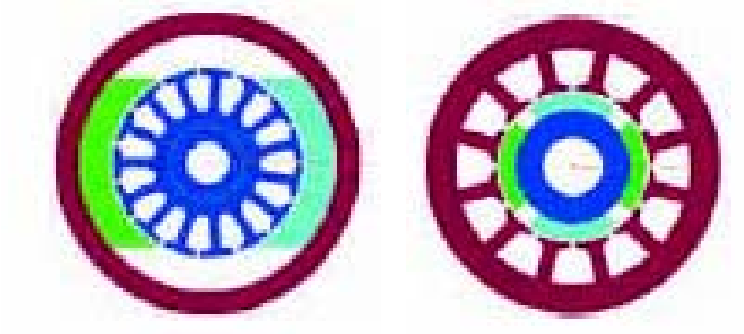

(a) (b)

Figure 3 6 (a) PM DC commutator motor and (b) BLDC motor respectively

The stator windings of the BLDC motor are generally similar to those of an induction motor and synchronous motor except that the conductors of each phase windings [10]. The conductors of each phase winding of BLDC motor are distributed uniformly in slots over two stator arcs (full pitched winding construction) and two of the three windings are excited at the same time to excite the BLDC motor. The winding configuration of a BLDC motor is shown in figure 3.7

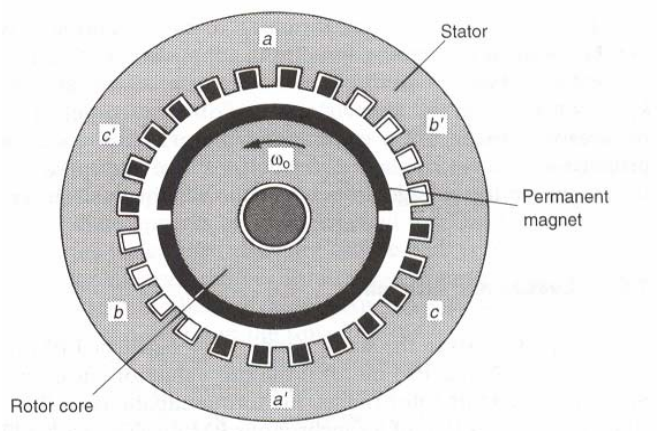

Figure 3 7 Typical BLDC motor with the excitation and configuration of the stator winding

BLDC motors have received wide attention as their performance can be superior to conventional DC commutator motor and induction motors. With the incorporation of microprocessor control it can be programmed to run at various

speeds and provide a large range of torques. The design of BLDC motors have to be carefully considered, taking into consideration the mechanical forces and the electrical and the magnetic balance in the machine.

It is necessary to give a decision whether to use brushless DC motor or DC commutator motor. The reasons for choosing brushless DC motor over the DC commutator motor are well known and include:

- No brushes or commutator so that no sparking, no RFI problems and no maintenance problems for BLDC motors due to brushes.
- Long life time.
- Low noise.
- Wide speed range since the speed is not limited due to the commutators. (Speed is limited by the magnet bonding for surface mounted types)
- High starting torque.
- Higher efficiency.
- Suitable for explosive atmospheres.
- Armature winding is on the stator so that more cross-sectional area exists for armature winding.
- It is easier to cool the armature winding since it is on the stator.
- Reduced motor length and thus low inertia due to the brush removal.
- Requires shaft position sensing.
- Requires complex electronic controller to commutate the armature current.

When there are two alternatives such as brushless DC motor and induction motor for a certain application it is also important to weigh the advantages and disadvantages of the brushless DC motor relative to induction motor [7]:

- Permanent magnet motors have a lower inertia when compared with an induction motor because of the absence of a rotor cage, which causes a faster response for a given electric torque. In other words torque to inertia ratio is higher for permanent magnet motors
- The permanent magnet motor has higher efficiency than an induction motor. This is primarily because of negligible rotor losses in permanent magnet motors.

- The induction motor requires a source of magnetizing current for excitation. While permanent magnet motor has the excitation in the form of rotor magnet.
- The need for magnetizing current and the fact that the induction motor has a lower efficiency necessitates a larger rated drive circuit for the induction motor than for a permanent magnet motor of the same output capacity.
- Permanent magnet motor is smaller in size than an induction motor of the same capacity.
- The rotor losses in a permanent magnet motor are negligible compared with those of induction motor.

Nevertheless the induction motor has the following advantages over permanent magnet motors [7]:

- Larger field weakening range and ease of control in that region.
- Lower cogging torques.
- less expensive feedback transducers such as an incremental rotor position encoder for the induction motor instead of an absolute position encoder that is required by the permanent magnet motors.
- Lower cost
- Much higher rotor operating temperatures are allowed than in permanent magnet motors.

3.4.2 Derivation of Torque Equations

Brushless permanent magnet motors are generally designed for low speed high torque operations. However field weakening methods may be applied to extend the speed range. The basic torque and EMF equations of the BLDC motor resemble those of DC commutator motor, which are

$$T = k \times \phi \times I \tag{3.1}$$

$$E = k \times \phi \times w \tag{3.2}$$

Where

$$k = \frac{4}{\pi} N_{ph}$$
$$\phi = B_g r \pi l$$

Torque is produced by the interaction between the air-gap flux, produced by permanent magnets on the rotor, and stator currents. These types of motors are fed by rectangular current so that rectangular current require a rectangular or trapezoidal PM field distribution in the air-gap in order to reduce torque ripples.

To derive the torque and torque density equation, a simple concept machine is used as shown in figure 3.8 and the waveforms of this concept machine shown in the figure will be helpful to obtain the torque and torque density equation of BLDC motor.

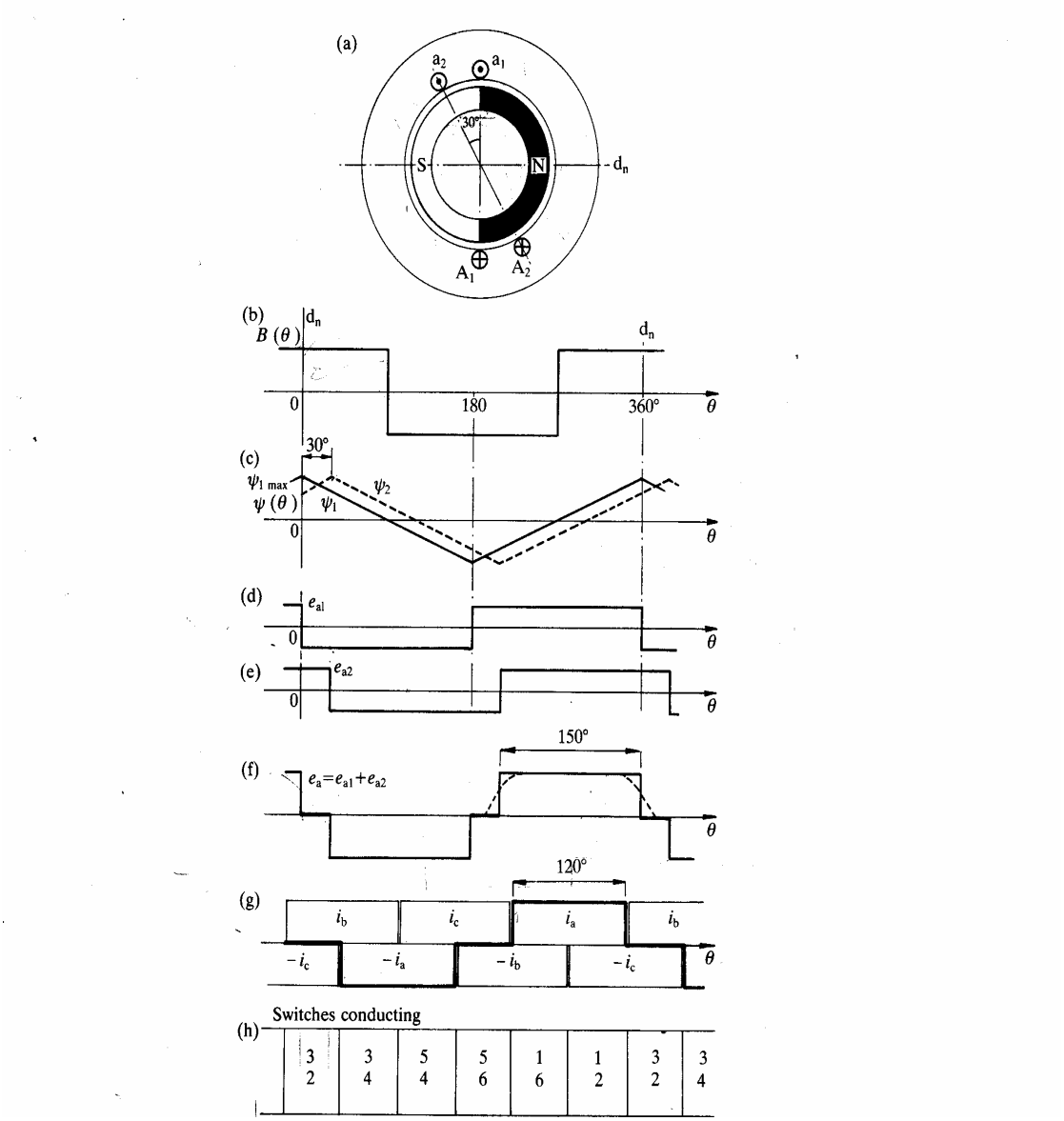

Figure 3 8 BLDC motor with ideal waveforms of flux density, EMF and current

(a) motor with two coils of one phase (b)magnet flux density around the air-gap (c)flux linkages of the coils as the rotor rotates (d),(e)EMF waveform of coil 1 and coil 2 respectively (f)Resultant phase EMF (g)ideal phase current waveform (h)switching pattern of converter switches

As shown in figure 3.8 the air-gap flux density waveform is ideally a square wave but in practice fringing causes the corners to be somewhat rounded. So that flat top portion of the waveform is not 150° as in the figure 3.8 (f), it is nearly 120°.

For the derivation of the torque equation of the radial flux brushless DC motor, consider the flux linkage λ_1 of one coil with "N_1" turns as the rotor rotates. The flux linkage varies linearly with rotor position because the air-gap flux density set up by the magnet is constant over each pole pitch of the rotor. Maximum positive flux linkage occurs at 0° and maximum negative flux linkage occurs at 180°. Flux linkage around the air-gap can be written as:

$$\lambda_{1\max} = N_1 \phi_g \tag{3.3}$$

Where:

"N_1" is the number of turns of full pitch coil

"Φ_g" is the air gap flux (consider one pole pitch)

And the variation of the flux linkage with rotor position can be expressed as:

$$\phi_g = B_g A_g = B_g r \theta_p l = \frac{2\pi}{P} B_g r l \tag{3.4}$$

By using the equation (3.3) and (3.4) the EMF induced on the coil can be found as

$$e_1 = -\frac{d\lambda_1}{dt} = -\frac{d\lambda_1}{d\theta} \times \frac{d\theta}{dt} = -w_e \frac{d\lambda_1}{d\theta}$$

$$e_1 = \frac{P}{2} w_m \frac{2N_1 \phi_g}{\pi} = 2N_1 B_g l r w_m \tag{3.5}$$

$$e_1 = 2N_1 B_g l r \frac{\pi}{30} n$$

Equation (3.5) gives the EMF induced in a coil with "N" turns. The waveform of EMF in this coil is similar in shape to the flux density waveform with respect to position around the rotor. If there are more coils connected in series, as in practical case, the resultant back EMF is the addition of the back EMFs of each coil. Then the equation (3.5) becomes

$$e = 2N_{ph}B_g lrw_m = 2N_{ph}B_g lr\frac{\pi}{30}n \quad \text{Volts} \qquad (3.6)$$

Where;

"N_1" is the number of turns of the coils

"N_{ph}" is the number of turns in series per phase

"n" is the speed in rpm

"w_m" is the mechanical speed in rad/s

"P" is the number of poles

To generalize the EMF expression of equation (3.6) N_{ph} is used instead of N_1. The relation between N_1 and N_{ph} is:

$$N_{ph} = cN_1 \qquad (3.7)$$

Where;

"c" is the number of coils connected in series. (for our concept machine c=2). For the figure 3.9 the value of "c" is 4, so it can be concluded that c is the pole number for this case. (if slots per pole per phase is equal to 1, then c=P)

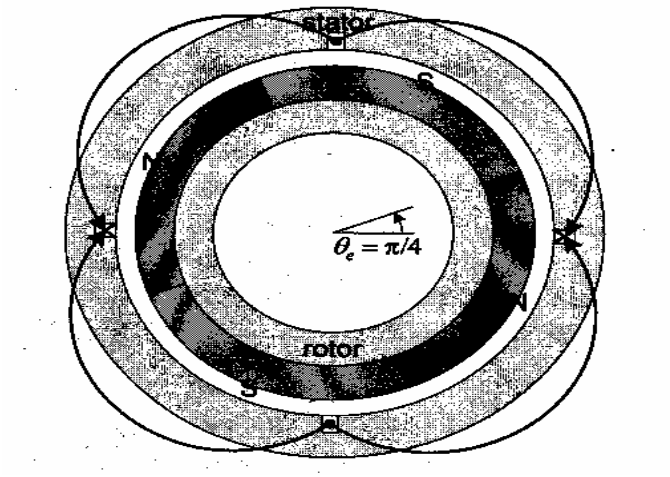

Figure 3 9 Motor with four poles and hence four full pitch coils

From this point torque equation can be derived by using the EMF expression of equation (3.6) and power equation. At any time, two of three phases of a BLDC motor are conducting at the same time (as discussed in section 3.3). By using this fact, instantaneous power being converted from electrical to mechanical can be written as:

$$P = 2eI = w_m T_e \tag{3.8}$$

Hence torque equation becomes:

$$T = \frac{2eI}{w_m} \tag{3.9}$$

Substituting the equation (3.6) in the equation (3.9) gives the torque expression for the BLDC motor as

$$T = 4N_{ph} B_g l I r \tag{3.10}$$

This torque equation is valid for any number of pole pairs (since $N_{ph}=PN_1$)

Where

"B_g" is the average air-gap flux density and can be approximated by using tooth flux density "B_t "as $B_g=B_t/2$. This relation only valid when the stator tooth width is equal to stator slot width as shown in figure 3.10

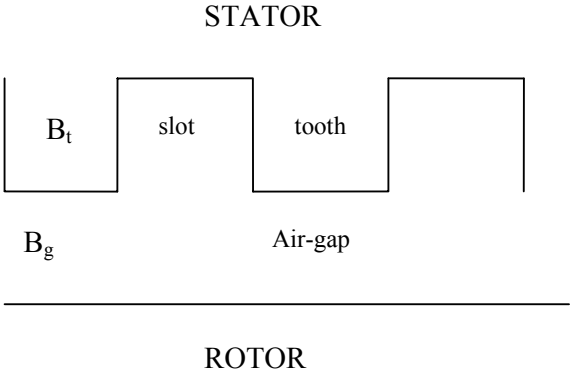

Figure 3 10 Schematic representation of tooth and slot

The achievable value of the air-gap flux density is constrained by the magnet properties and dimensions and by saturation in the stator teeth [1].

$$q = \frac{3 \times 2 \times N_{ph} I_{rms}}{2 \times \pi \times r} = \frac{3 \times N_{ph} \times I_{rms}}{\pi \times r} \tag{3.11}$$

Since the current in torque equation is peak current, it should be converted to RMS current value to relate the torque equation with the electric loading, magnetic loading and dimensions as in the case of the induction motor. Then:

$$I_{rms} = \sqrt{\frac{2}{3}} I_{peak} \tag{3.12}$$

Using the equations (3.10), (3.11), (3.12) and making the necessary modifications, torque equation becomes.

$$T = \sqrt{\frac{8}{3}}\pi r^2 l B_g q = \frac{\pi}{\sqrt{6}} B_g q D_i^2 l \tag{3.13}$$

$$T = \sqrt{\frac{8}{3}} V_{rotor} B_g q$$

Same torque equation for BLDC motor can be derived by using two different methods as starting point.

First one is using the force equation

$$T = 2Fr \tag{3.14}$$

$$F = BIl = B_g I N_{ph} l \tag{3.15}$$

$$T = 2B_g I 2N_{ph} lr = 4N_{ph} B_g Irl \tag{3.16}$$

Substituting equations (3.11), (3.12) and making the necessary modifications the same torque expression as in the equation (3.13) can be obtained.

The second one is to obtain the torque expression by using the air-gap shear stress concept [1].

$$T = 2\pi r^2 l \sigma \tag{3.17}$$

Where

"σ" is the air-gap shear stress and can be formulized as

$$\sigma = B_g q \tag{3.18}$$

Since each phase is energized two-thirds of the time, the RMS value of current density "q" is

$$q = \sqrt{\frac{2}{3}} \times \frac{3N_{ph}I_p}{\pi r} \tag{3.19}$$

Using the equations (3.17), (3.18) and (3.19) torque equation again becomes the same as equation (3.13)

Note that the rotor volume is

$$V_{rot} = \pi r^2 l = \frac{\pi D_i^2 l}{4} \tag{3.20}$$

Then substituting equation (3.20) in equation (3.13) torque per unit rotor volume becomes

$$T_{V-rot} = \sqrt{\frac{8}{3}} B_g q \tag{3.21}$$

Since the stator winding of 3 phase BLDC motor is similar to that of an induction motor, same relation derived for the induction motor can be used to relate the outer diameter to inner diameter.

$$\frac{D_o}{D_i} = \frac{\pi}{pK_{BR}} + \sqrt{1 + \frac{4q}{K_{as} J D_i}} \tag{3.22}$$

3.4.3 Results

- Torque equation depends on rotor volume, air-gap flux density and specific electric loading.
- Different types of magnets can be used on the rotor surface that affects the air-gap flux density which in turn affects the torque and torque per unit motor volume.
- All the parameters including the torque equation for radial flux brushless DC motor are the same as induction motor except the constant value.
- For the same value of magnetic loading and specific electric loading (however BLDC motor has no winding on rotor so specific electric loading may be higher than that of the induction motor) torque of the BLDC motor is higher than that of the induction motor.
- From equation (3.13), if "B, q, J and rotor volume (D_i, L)" are fixed, then as the number of poles increases torque does not change but D_o/D_i ratio gets smaller, due to this the motor size decreases and hence the torque per unit motor volume increases
- From equation (3.13), if "B, q, J and motor volume (D_o, L)" are fixed D_i can be determined from D_o/D_i ratio (equation 3.22). As the number of poles increases D_o/D_i decreases (or D_i/D_o increases) with the increase of "D_i" value therefore rotor volume increases increasing the torque. Consequently since the motor volume is fixed and we get an increase for the torque with the increasing of the rotor diameter, then the torque per unit motor volume increases.
- As a result of two conclusions given above, torque per unit motor volume increases with the increase of the number of poles but this increase saturates after a certain point. Figure 2.2
- From equation (3.13) it is seen that the torque is proportional to rotor volume. Therefore as long as the motor volume kept constant, it is necessary to increase the rotor diameter as far as possible, to achieve a higher torque per unit motor volume.
- Torque per unit rotor volume is constant as long as "B and q" are kept constant. It does not depend on number of poles.

- Maximum magnetic loading (B), which is higher than that of induction motor, is used during the design stage of the motor. To maintain same flux density in the stator and rotor yokes, yoke thickness should be increased as the number of poles decreases, hence for the same outer diameter the rotor of the motor with smaller number of poles will have smaller diameter than that of larger number of poles. This result also satisfies that torque production increases with increasing the pole number.
- With constant rotor dimensions (Di, L) torque can be increased by increasing specific electric loading (q). To get high value for specific electric loading phase current should be increased. Since V=E+RI and voltage is kept constant back EMF should be small for high phase current and hence high specific electric loading.
- As the number of poles increases flux per pole decreases, as the flux per pole decreases E_{ph} decreases. To maintain E_{ph} at pre-determined value increase turns per phase. This increase increases specific electric loading value and hence the torque value.
- From equation (2.4) and equation (2.5) to decrease back EMF flux per pole should be decreased, to decrease the flux per pole number of poles should be increased. This result also satisfies that torque production increases with increasing the pole number.
- BLDC motors have windings only on stator side so that these motors have less copper losses and high efficiency.

3.5 Axial Flux Brushless DC Motor

3.5.1 Introduction

Unlike the radial flux machines, the axial flux permanent magnet machine category actually incorporates a large set of various possible structures.

- Axial flux external rotor non-slotted stator permanent magnet motor. (figure 3.11 a)
- Axial flux external rotor slotted stator permanent magnet motor. (figure 3.11 b)

- Axial flux internal rotor non-slotted stator permanent magnet motor. (figure 3.11 c)
- Axial flux internal rotor slotted stator permanent magnet motor. (figure 3.11 d)

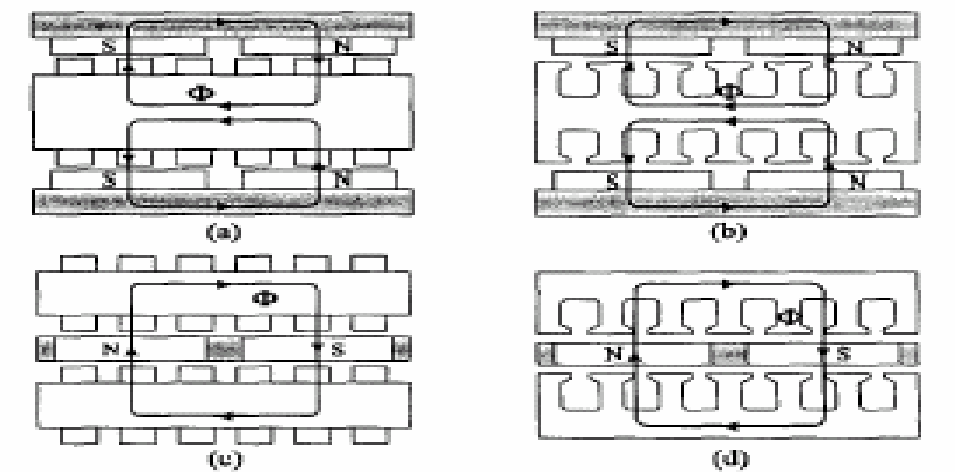

Figure 3 11 Axial flux motor topologies (a) Axial flux external rotor non-slotted stator permanent magnet motor (b) Axial flux external rotor slotted stator permanent magnet motor (c) Axial flux internal rotor non-slotted stator permanent magnet motor (d) Axial flux internal rotor slotted stator permanent magnet motor

This motor is often referred to as a pancake motor. Through out this chapter axial flux external rotor non-slotted stator permanent magnet motor will be examined. Such a motor characteristics can be summarized as follows.

- Because of the slottless design, the permeance component of the flux ripple associated with the slots is eliminated, and the tooth saturation, tooth iron losses and tooth vibrations are also eliminated.
- There are not slots to fix the stator stator windings to position that are stressed by electromagnetic forces and mechanical vibrations.
- Because of the large effective air-gap, the stator winding inductance is very small and the constant power speed range is limited. In addition a large magnet quantity is needed to produce high flux density in the air-gap.

Axial flux machines differ substantially from the conventional radial flux machines due to the direction of the flux in the air-gap, which in this case along the

mechanical axis of the machine and axially polarized permanent magnets on the rotors. Each rotor is connected to the shaft. The basic configuration is shown in figure 3.12

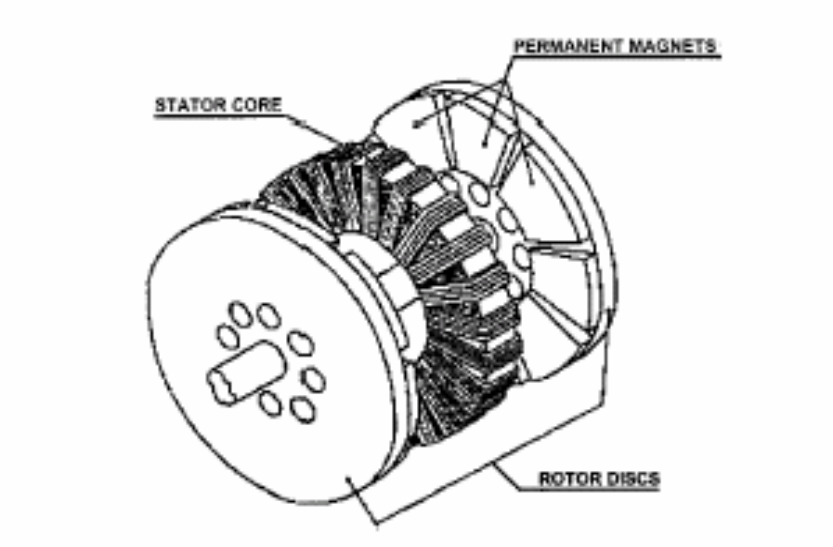

Figure 3 12 Axial flux BLDC shape, stator sandwiched between two rotors

Windings are on the toroidal stator and rotor discs are carrying axially polarized permanent magnets. Flux directions for such types of motors are also shown in figure 3.13.

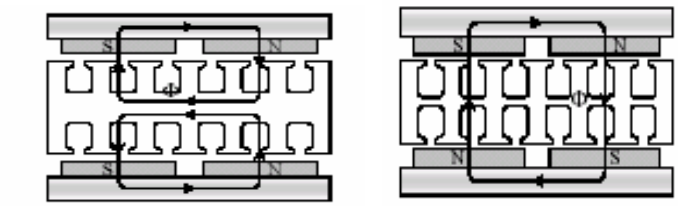

(a) (b)

Figure 3 13 Flux directions of (a) NN type axial flux motor (b) NS type axial flux motor

The major differences between these two topologies, shown in figure 3.8, are the arrangement of the magnet polarity, the arrangement of the armature winding and the thickness of the stator yoke [8]. In NN type, the N pole of the

permanent magnet driven flux enters the stator core through the air-gap travels circumferentially along the stator core and then goes into the rotor core through the S pole of the permanent magnets. In NS type structure, the N pole of the permanent magnet driven flux enters the stator core through the air-gap, travels axially along the stator core, enters the second air-gap and rotor core through the S pole of permanent magnets and closes its path through the N pole of the magnets. NN type motor has a large stator yoke dimension since flux passes through it but allows short end windings, which result in small copper losses. On the other hand NS type motor has small stator yoke and long end windings, which result in small iron losses but high copper losses.

For both type of the constructions, the production of the machine torque is the same. The current commanded in the stator winding coils interacts with the flux generated by the magnets, producing a tangential force and the machine torque results from the contribution of all forces which act on the working surfaces of the toroidal core. Since the working surfaces of the stator core are both used, in comparison with conventional machines, axial flux permanent magnet motors allow the exploitation of a higher percentage of the stator winding for the production of the machine torque.

3.5.2 Derivation of the Torque Equation

For the axial flux type of motors the radial length from the inner radius to outer radius is the motor active part to produce the torque. The cross-section of a 4-pole AF BLDC motor is shown in figure 3.14. The motor consists of a stator, "sandwiched" between two rotors with permanent magnets.

The magnets produce air-gap flux density, which is a square wave in distribution with maximum value B_g over the entire pole pitch at radius "r" and it is assumed that all the winding conductors carry constant current "I", which is the RMS value of the current waveform commanded in the machine phases to be appropriately timed with the flux density distribution at the air-gaps. There are no stator slots and strip wound stator windings are used.

As the winding conductors pass radialy across the face of the stator and wires are placed as close together as possible, the electric loading at radius "r" can be written as [5]:

$$q(r) = \frac{q_i \times R_i}{r} \tag{3.23}$$

Where, the electric loading q_i and the inner radius R_i, are the important design parameter defined as [5]:

$$q_i = \frac{mN_{ph}I}{2\pi R_i} \tag{3.24}$$

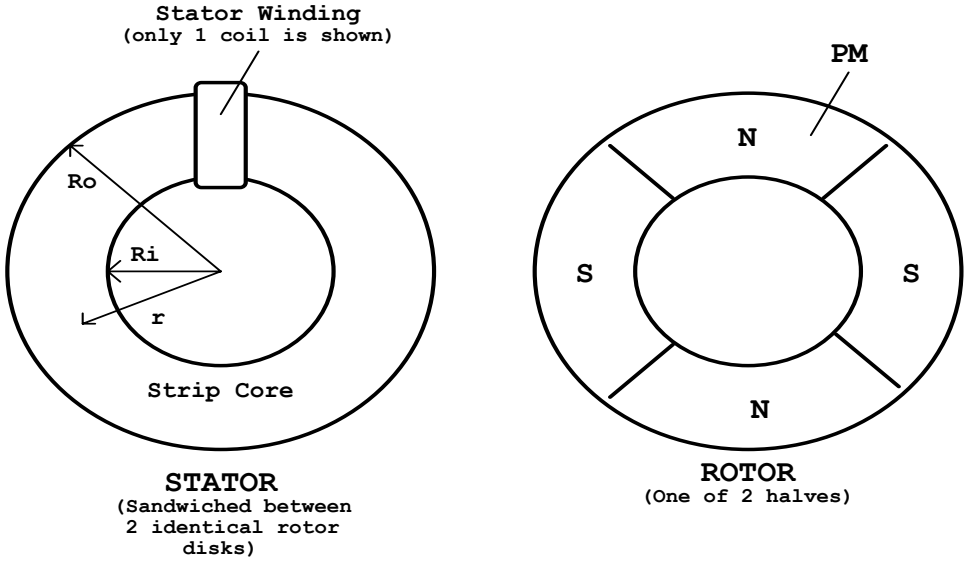

Figure 3 14 Four pole axial flux BLDC motor (radial cross-section)

The current commanded in the winding conductors interacts with the flux generated by the magnets, producing a tangential force. Since the two working surfaces of the stator core are both is used in comparison to conventional machines the structure of axial flux permanent magnets allows the exploitation of a higher

percentage of the stator winding for the production of the machine torque. This is schematically depicted in fig 3.15

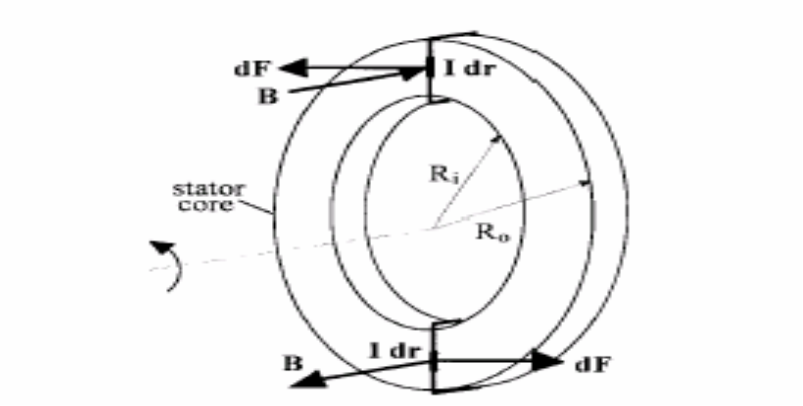

Figure 3 15 Schematic representation of torque production mechanism of AF-BLDC motor

With the above assumptions the machine torque can be calculated by considering the overall contribution to torque resulting from forces "dF" exerted on current excited conductor elements "Idr" located on one stator face at radius "r" and uniformly distributed over the full angular extent [5]. Torque can be written as:

$$dT = 2\pi q(r) B_g r^2 dr = 2\pi q_i R_1 B_g r dr \tag{3.25}$$

Integrating equation (3.25) over the full radial extent of the stator face, contributing the torque production, gives the torque equation for one face of the motor.

$$T = \int_{R_i}^{R_o} 2\pi q_i R_i B_g r dr = \pi B_g q_i R_i (R_o^2 - R_i^2) \tag{3.26}$$

As mentioned, equation (3.26) is the torque equation for one face of the axial flux BLDC motor so that to include the torque contributions of the other faces

this torque equation should be multiplied by the number of faces "h". Then the machine torque equation becomes.

$$T = h\pi B_g q_i R_i (R_o^2 - R_i^2) \tag{3.27}$$

Throughout this chapter one stator sandwiched between two rotors topology is used so that the value of "h" is two. Substituting "h" value gives the torque equation for two faces as

$$T = 2\pi B_g q_i R_i (R_o^2 - R_i^2) = 2\pi B_g q_i R_o^3 K_r (1 - K_r^2) \tag{3.28}$$

Where

$$K_r = \frac{R_i}{R_o}$$

For the axial flux type of motor K_r is an important design parameter. For a fixed magnetic loading, electric loading and outer diameter machine torque only depends on the K_r ratio but this ratio has no effect on torque per unit volume.

Note that the motor volume (and also rotor volume) can be written as:

$$V = \pi R_o^2 L = \pi \frac{D_o^2}{4} L \tag{3.29}$$

Then the torque per unit motor volume equation becomes:

$$T_v = \frac{2\pi B_g q_i R_o^3 K_r (1 - K_r^2)}{\pi L R_o^2} = 2 B_g q_i \frac{R_o}{L} K_r (1 - K_r^2) \tag{3.30}$$

There is a limit on the possible axial length of axial flux BLDC motor (calculation of the axial length is given in appendix B), which is mainly due to the

minimum area required to carry the flux in the core [4]. The axial length is formed of the following components:

- Two rotor back core thickness
- Two permanent magnet thickness
- Two air-gap thickness
- Two stator coil thickness
- Stator back core thickness

Adding all these gives the axial length of an axial flux BLDC motor as;

$$L = \frac{4\pi R_i}{pK_{BR}} + 2\frac{\frac{q_i}{K_{cu}J} + g}{1 - \frac{B_g}{B_r}} \tag{3.31}$$

Where;

"K_{BR}" is the ratio of stator back core flux density to air-gap flux density

"K_{cu}" is the copper fill factor

"B_r" is the permanent magnet's residual flux density

"B_g" is the air-gap flux density

"J" is the current density

The second term of equation (3.31) approximately constant for all types of motors and varies between 3-10 cm [4] and can be neglected for sufficiently large R_i. Substituting equation (3.31) in equation (3.30) gives the torque per unit volume equation, which will be used from now on.

$$T_v = 2B_g q_i \frac{R_o K_r (1 - K_r^2)}{\frac{4\pi R_i}{pK_{BR}} + 2\frac{\frac{q_i}{K_{cu}J} + g}{1 - \frac{B_g}{B_r}}} \tag{3.32}$$

3.5.3 Results

- Torque density is mainly affected by the magnetic loading, electric loading and K_r ratio
- As the number of poles increases the axial flux motor radial active part remains unchanged, but the axial length can decrease and the torque density then increases [9] (For axial flux motors, especially for the large ones torque per unit volume increases dramatically with the increase of the number of poles [4]). But if the pole number is furthermore increased, the torque capability tends to decrease because of increase of the iron losses.
- K_r is an important geometric parameter for the optimization of the machine design and the optimum value for K_r is $1/\sqrt{3}$ for maximized torque so does the torque density [5].
- Torque density equation (3.32) does not include axial length.
- Increasing the number of poles will not change torque value but it will decrease the axial length of the motor and hence the volume of the motor so that torque per unit motor volume increases with the increasing of pole number.
- For small motors second term of equation (3.31) dominates. For large motors the axial length can be approximately determined by the first term.
- Electric loading of the axial flux motor can be higher than that of the radial flux types due to easy cooling by the ventilation effect of the rotors.
- In AF-BLDC motor, the length of stator core and hence the stator mass is inversely proportional to the number of poles, equation (3.31), while the operating frequency is directly proportional to the number of poles. Therefore changing the number of poles does not affect the core loss [4].

CHAPTER 4

SWITCHED RELUCTANCE MOTORS

4.1 Introduction

Switched reluctance motors have been the focus of much research over the last decades. At present, switched reluctance motors are attracting increasing interest by industry because of their simple and rugged motor construction, the capability of running at high speeds, high torque to inertia ratio, their simple uni-polar current drive system, high reliability and low cost [11].

Switched Reluctance motors are similar to the step motors except that they have:

- Fewer poles
- Larger stepping angle
- Higher power output capability

This chapter constitutes brief information about switched reluctance motors as to form a background for the following subsections of this chapter. Then torque and torque density equations will be derived for the switched reluctance motor, related to magnetic loading, electric loading and dimensions of the motor similar to the preceding chapters, as the result of this chapter work done so far will be investigated. Application of the switched reluctance motor to the washing machine will be investigated in chapter 5, taking the torque expressions, derived in this chapter as a starting point.

Since the motors, considered so far are all three phase motors, three phase switched reluctance motor will be considered in this chapter.

4.2 Background

The switched reluctance machine is basically a doubly salient structure in which concentric coils are mounted around the stator poles and rotor has neither windings nor permanent magnets on it. So that it is a doubly salient singly excited motor with different number of stator and rotor poles as shown in figure 4.1.

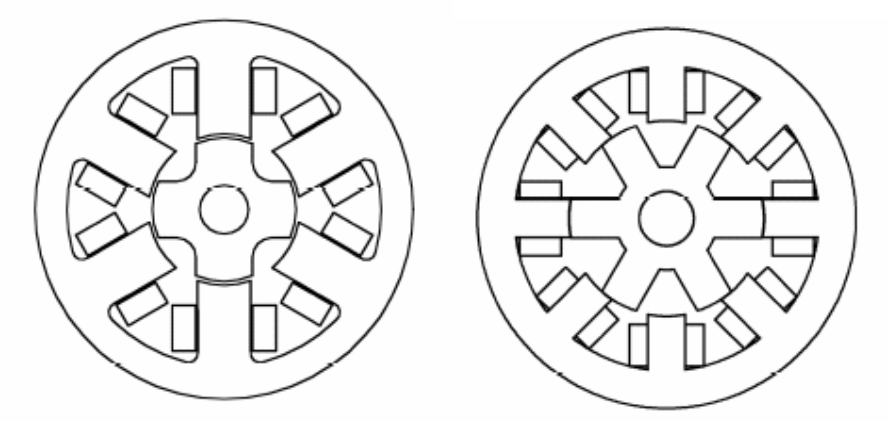

Figure 4 1 Different SR motor configurations
(a) 6/4 pole (**b)** 8/6 pole

Since flux crosses the minimum reluctance path, rotor of the motor comes to alignment with the excited stator poles. The rotor is aligned whenever diametrically opposite poles are excited [12]. While two rotor poles are aligned to the excited two stator poles, other rotor poles become unaligned with respect to the other stator poles. Then another set of stator poles is excited to bring the unaligned rotor poles to align position with the excited stator poles. In the same manner, by exciting the other stator poles sequentially, the movement of the rotor and hence the production of the power and torque can be accomplished. It is better to use figure 4.2 that shows stator windings, to explain the rotor movement.

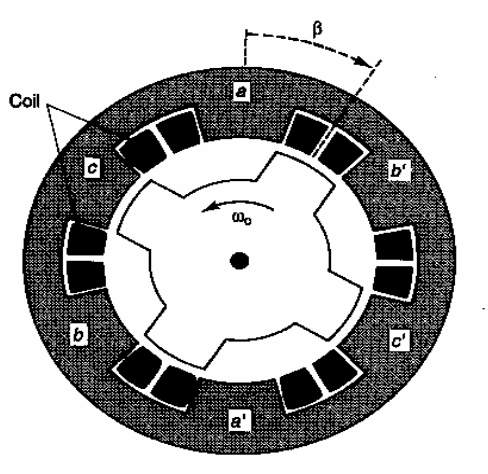

Figure 4 2 Cross-section of a SR motor

For the position shown in figure 4.2, if the coils of phase A are excited, misaligned rotor poles will be exposed to a force, that acts to align the rotor poles with the phase A stator poles. When the nearest rotor poles are aligned with the excited stator phase A poles, if the current is switched to the phase B coils, the counterclockwise force will continue acting on the nearest misaligned rotor poles. As a result rotor rotates in the counterclockwise direction by switching the stator currents sequentially through phases.

Its performance and inherently low manufacturing cost make it a vigorous challenger to these drives. Its particular advantages may be summarized as follows [1], [12], [19]:

- Since there are windings on the stator and there exists no windings or permanent magnets on the rotor, this ensures material saving.
- The rotor is small and has a low moment of inertia, thus giving a large acceleration rate for the motor.
- The rotor is simple and requires relatively low manufacturing steps.
- Since it has no brushes like other AC machines, no maintenance is necessary.
- Since the rotor does not have windings or magnets, it is mechanically robust and therefore suitable for high speed applications.
- Since the windings are only on the stator, it is easy to cool.

Switched reluctance motor configuration does not come with only advantages, it has also disadvantages as:

- High torque ripple
- Acoustic noise generation
- High friction and windage losses at high speeds due to the salient structure of stator and rotor.
- It does not have line start capability
- Position information is required to drive the switched reluctance motor by the use of a converter.
- The motor is a brushless machine like other AC machines.

4.3 Derivation of the Torque Equation

As derived before for induction and permanent magnet motors, the same procedure is applied to obtain the torque and torque density equations for switched reluctance motors related to magnetic loading, electric loading and the main dimensions of the motor. Moreover the experience of machine designers can be used in the design of this machine

To derive the torque equation, some assumptions related to this motor should be done. For the process of the derivation of the torque equation, phase current of the motor is assumed to be trapezoidal as in figure 4.3.

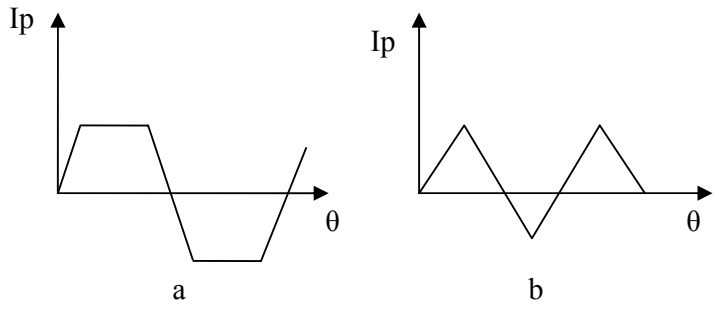

Figure 4 3 Assumed Current waveform (a) at low speed (b) at high speed

In fact the current waveform is not same as mentioned in figure 4.3 and even it can not reach the maximum value due to the back EMF.

Consider the flux linkage vs. current characteristics for the unaligned and aligned position of the stator and rotor poles (figure 4.4). Area enclosed by OABCO denotes the output mechanical energy of the motor for one stroke.

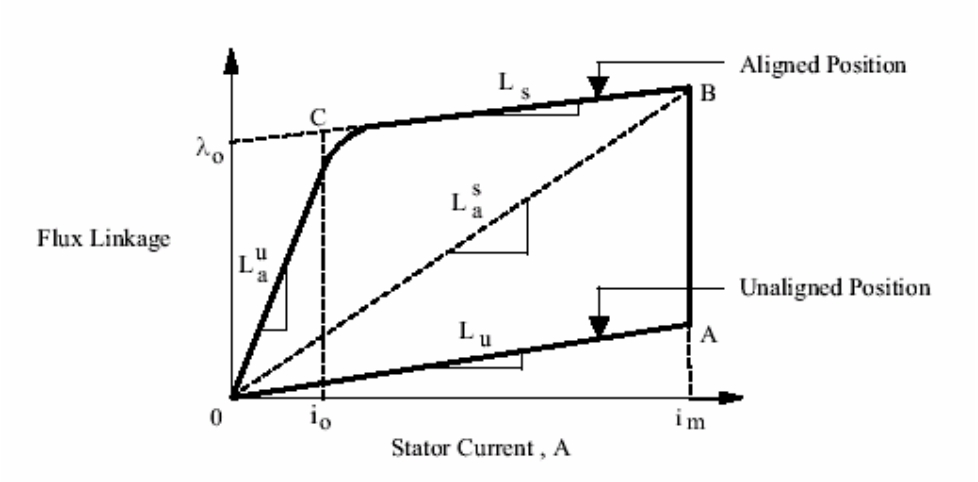

Figure 4 4 Flux linkage vs. stator current of SR motor

When the resistive voltage drop of the windings is neglected, terminal voltage becomes equal to the back EMF of the motor.

$$E = \frac{d\lambda}{dt} = \frac{(\lambda_a - \lambda_u)}{t} = \frac{(L_a^s - L_u)}{t} i \qquad (4.1)$$

Where

"L_a^s" is the aligned saturated inductance per phase ($\lambda_a = L_a^s i$)

"L_u" is the unaligned inductance per phase ($\lambda_u = L_u i$)

"L_s" is the saturated inductance

"L_a^u" is the aligned unsaturated inductance

"V" is the applied voltage

"i" is the phase current

"t" is the time taken for the rotor to move from the unaligned to the aligned position.

To simplify the equation, define two constants "K_1" and "K_2" as;

$$K_1 = \frac{L_a^s}{L_a^u} \quad \text{and} \quad K_2 = \frac{L_a^u}{L_u} \tag{4.2}$$

Then define the time taken for the rotor to move from aligned to unaligned position as;

$$t = \frac{\beta_s}{w_m} \tag{4.3}$$

Where;

"β_s" is the stator pole arc

"w_m" is the rotor speed in rad/sec

Substituting equations (4.2) and (4.3) in equation (4.1), applied voltage, by assuming trapezoidal shape current, expression becomes;

$$E = \frac{w_m}{\beta_s} L_a^s i \left(1 - \frac{1}{K_1 K_2} \right) = \frac{w_m}{\beta_s} L_a^s i K \tag{4.4}$$

Voltage "V" of equation (4.4) can be assumed to be equal to back EMF when resistive voltage drops are neglected. Since equation (4.5) will be used to find the torque equation of switched reluctance motor, power of the motor should be determined.

$$P = T w_m = E i \tag{4.5}$$

Since we have derived the voltage of the equation (4.5) it is necessary to derive the current expression to find the power expression of the motor. flux linkage of the motor can be used to determine the current of the motor.

$$\lambda = L_a^s i = N_{ph} \phi = \frac{1}{2} B D L \beta_s N_{ph} \tag{4.6}$$

Where;

$$\phi = BA_p$$

$$A_p = \frac{\pi DL}{2P_s} = \frac{1}{2}DL\beta_s \tag{4.7}$$

When the equation (4.6) is solved for the current "i" equation (4.8) is obtained for the motor current. This current is valid only for the saturated case and gives the maximum current that can be achieved by the motor.

$$i = \frac{BDL\beta_s N_{ph}}{2L_a^s} \tag{4.8}$$

Since value of the current had found, by putting the equation (4.8) into equation (4.5) and making necessary modifications we can find power and hence the torque expression as;

$$P = \frac{\pi}{4}D^2 L\frac{K}{3}\sqrt{m}Bqw_m \tag{4.9}$$

Where;

"m" is the number of phase and is given as $P_s/2$ (half of the stator poles)

"K" is the constant dependent on the operating point of motor [10], [12].the value of this constant changes from 0.45 (for an unsaturated motor) to 0.75 (for a fully saturated motor).

Optimum value of K maximizes the area OABCO and hence the torque produced by the motor. This is subjected to several constraints such as the ratio of pole pitch to air-gap, stator and rotor tooth pitch to pole pitch, conduction angle, flux density. Optimization of these parameters maximizes the torque [23]. Therefore 'K' can be chosen as 0.75 for maximum torque production [10].

By using the equations (4.5) and (4.9) torque of the switched reluctance motor related to its magnetic loading, electric loading and dimensions can be obtained as in equation (4.10)

$$T = 0.25\sqrt{m}Bq\frac{\pi}{4}D^2L = 0.25\sqrt{m}BqV_{rotor}$$

Since the motor, considered in this chapter is a three phase motor torque equation of this motor becomes:

$$T = 0.433Bq\frac{\pi}{4}D^2L = 0.433BqV_{rotor} \quad (4.10)$$

Then the torque per unit rotor volume is

$$T_{v\_rot} = 0.433Bq \quad (4.11)$$

Torque equation of (4.10) is for the maximum torque that can be produced by the motor. In equation (4.10), effect of the saturation is taken into account. This torque equation is derived for the fully saturated case and hence it can not be used to evaluate this motor over a wide speed range due to its nonlinear behavior. Since this equation is only valid for fully saturated case it can be used to find the dimensions of the motor to meet the maximum torque requirement of the motor.

Equation (4.10) gives the torque equation related to rotor volume. To relate the torque equation outer diameter of the motor should be determined. Outer diameter of the motor consists of bore diameter, stator back core and stator pole height as given in equation (4.12)

$$D_o = D + 2b_{sy} + 2h_s \quad (4.12)$$

Where;

"b_{sy}" is the back core thickness

"h_s" is the stator pole height

As seen from equation (4.12) to determine the outer diameter of the switched reluctance motor, it is necessary to find back core thickness and pole height. Determination of these values necessitates experience.

First start with the determination of pole height. Minimum pole height can be taken as equal to the coil height but the coil has to be held in place and for that a small space is required so that the pole height is taken a little bit more than the coil height. Therefore to determine the pole height, first determine total coil height, starting with the cross-section of the conductor.

$$A_c = \frac{I}{J} \tag{4.13}$$

If "A_c" is the cross-section of one conductor, total conductor cross-section on one pole is" $A_c N_{ph}/2$ "then

$$h_c w_c = A_c \frac{N_{ph}}{2} \tag{4.14}$$

Where;

"h_c" is the coil height

"w_c" is the coil width

Maximum permissible coil width depends on the bore diameter and stator pole arc and can be expressed by the equation (4.15) [12].

$$w_c = \frac{\pi D}{2P_s} - \frac{1}{4} D\beta_s \tag{4.15}$$

Where;

"P_s" is the stator pole number

"β_s" is the stator pole arc

Then using the equations (4.14) and (4.15) coil height can be obtained as:

$$h_c = \frac{A_c N_{ph}}{2 w_c} \tag{4.16}$$

Since the equation (4.18) gives the coil height, it is easy to determine the stator pole height. Experiences show that the optimum value of stator pole height is approximately;

$$h_c < h_s < 1.4 h_c$$

To finalize the outer diameter calculation, stator back iron thickness should be obtained. Since the flux density in the stator back iron is approximately half that of the stator poles, the stator pole arcs have to be chosen appropriately.

$$w_{sp} = 2r \sin(\frac{\beta_s}{2}) \tag{4.17}$$

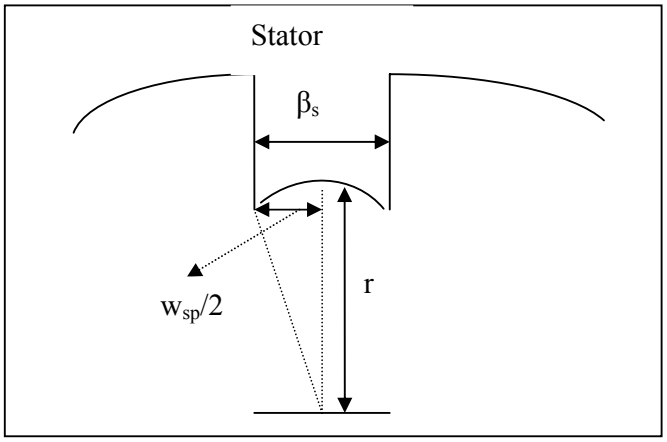

Where;

"w_{sp}" is the pole width

"β_s" is the stator pole arc

Due to the mechanical considerations back iron thickness is in the range of:

$$0.5 w_{sp} < b_{sy} < w_{sp}$$

Since the values of stator back iron thickness and stator pole height are determined, outer diameter and hence the volume of the motor can be easily obtained by using the equation (4.14).

4.4 Results

- Torque equation of the switched reluctance motor is derived related to the main dimensions, electric loading and magnetic loading, as in the case of the permanent magnet motors and induction motor.
- Since this motor is designed to operate in saturation, stator pole flux density of this motor is higher than those of permanent magnet motors and induction motor.
- When the equations (4.4) and (4.5) are considered, it is seen that the torque is independent of the direction of the supply current because it is proportional to the square of the phase current
- Since this motor can be operated in saturation, it has a nonlinear characteristic. Therefore to obtain the torque at various speeds available set of data is used.

CHAPTER 5

EVALUATION OF THE MOTORS FOR WASHING MACHINE APPLICATION

5.1 Introduction

So far during this study four types of motor are considered. Torque equations of four types of motors are evaluated, related to their dimensions and magnetic and electric loading. Since we have torque equations of all the considered motors related to their dimensions, now it is easy to derive the torque per unit volume of each of the motors. Evaluation of the torque per unit volume equation of each type of motor is a good approach to have a basic idea for comparison of these motors but not enough in determining, which one is the best choice.

To evaluate the performance of the motors a washing machine application is appropriate due to its wide speed range (torque speed curve for a typical washing machine is given in appendix section). Over the whole speed range the variation of the efficiency, torque per unit volume, torque per current production and peak current (for the converter switch ratings) are the main issues to be considered for the evaluation of the performance of the motors.

The scope of this chapter is therefore, to analyze these motors not only for their torque per unit volume basis and also to compare the performances of these motors under different speed conditions. That is response of the each motor is considered at low speed and high speed conditions.

During this study in order to have an idea about performance of each motor, copper fill factor, current density, reduction ratio of "10", DC voltage level of 300 volts, and number of poles (different pole numbers will be considered, such as, 2, 6 and 10 poles) are taken as input parameters. While performance of induction motor

and permanent magnet brushless DC motors, both radial flux and axial flux, are considered for different number of pole numbers, switched reluctance motor is considered for two different phases numbers, 3 phase and four phase. For all types of motors, after gathering data at several speed points, the graphs are drawn via piecewise linear approximation.

5.2 Induction motor

The torque equation of the induction motor is derived in chapter 2 as;

$$T = \frac{1.3\pi}{4} D_i^2 LBq \tag{5.1}$$

This torque equation is the starting point of the induction motor performance evaluation for the washing machine application. Electric loading and peak tooth flux density are taken as 28000 A/cond. and 1.7 T respectively. Since stator tooth width is assumed to be equal to stator slot width, magnetic loading "B" in equation (5.1) can be determined. When electric loading and magnetic loading of the motor is determined, the unknowns of this equation become bore diameter and stack length. Since it is assumed that bore diameter and stack length are equal in length, for sake of simplicity, then torque expression of equation (5.1) becomes an equation with one unknown.

The next issue is the determination of the dimensions of the motor so that the torque requirement is met. To meet the maximum torque requirement, determination of the dimensions of induction motor should be performed at a speed where the maximum torque is required. Thus the load torque vs. speed characteristics fits the torque vs. speed characteristics of the motor.

Once the bore diameter and hence the stack length are obtained, volume and mass of the motor and core can be obtained. When obtaining the rotor volume it is appropriate to use bore diameter or for more sensitive approach air-gap length, calculated by using the equation 5.2 [16], can be subtracted from the bore diameter and taking it as the rotor diameter.

$$g = 0.0002 + 0.003\sqrt{rl} \tag{5.2}$$

The next step is to determine the number of turns per phase, that will be used to calculate resistance and hence the necessary voltage to be applied and copper loss of the motor. To determine the number of turns per phase equation (5.3) is used.

$$E_{ph} = 4.44 k_w f N_{ph} B A$$
$$N_{ph} = \frac{E_{ph}}{4.44 k_w f B A} \tag{5.3}$$

The only unknown in this equation is the number of turns per phase. Where

"k_w" is the winding factor and taken as 0.9

"A" is the pole area and can be expressed as $A=\pi D_i L/P$

"E_{ph}" is the maximum phase back EMF (When the resistance voltage drops are considered back EMF value should be determined such a way that applied voltage (V=E+RI) should be less or equal to inverter output).

"f" is the frequency at base speed and proportional to pole number.

Then the turns per phase value is determined at base speed of the motor, where maximum back EMF value is reached as illustrated in figure 5.1.The base speed of the induction motor should be chosen at such a point that the motor torque is greater than or equal to the load torque for every point in the operating speed range and hence the load torque vs. load speed characteristics fits into the torque speed characteristics of induction motor.

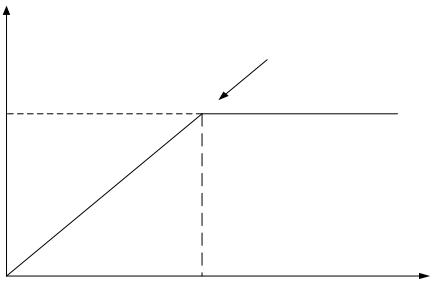

Figure 5 1 Turns per phase calculation

Since the value of turns per phase is determined, it is easy to find the resistance, using equation (5.4) and the maximum value of the current and hence the area of the conductor, which will be used in determination of the resistance, by using the predefined current density value.

$$r = \frac{\rho l}{A_{cu}} = \rho \frac{LMC \times N_{ph}}{A_{cu}} \tag{5.4}$$

Where;

"ρ" is the resistivity of copper

"LMC" is the mean length of one coil and can be given for a full pitch winding as

$$LMC = L + \frac{\pi(D_i + h_s)}{P}$$

"L" is the total length of the conductors for one phase

"A_{cu}" is the copper area and given in equation (5.5)

$$A_{cu} = \frac{I_{rms}}{J} \tag{5.5}$$

Resistance value, found in equation (5.4), is the resistance of the stator side per phase and since the total resistance in the equivalent circuit is the sum of the stator and rotor resistances, for the sake of simplicity the referred rotor resistance is assumed to be equal to the stator resistance value.

From now on the variation of the flux density, electric loading and current with the speed can be determined by using the equations (5.6), (5.7), (5.8) successively.

$$B = \frac{120E}{4.44k_w nN_{ph}\pi D_i L} \tag{5.6}$$

$$q = \frac{4T_m}{1.3\pi D_i^2 LB} \tag{5.7}$$

$$I_{rms} = \frac{q\pi D_i}{6N_{ph}} \tag{5.8}$$

As seen from equations (5.7) and (5.8) the variation of the electric loading affects the variation of the RMS current value over whole speed range so they are similar in shape. The variation of the RMS current with the speed is given in figure 5.2. This figure is helpful to determine the copper loss variation and torque per unit current for the induction motor with speed. Also the current variation is used to determine the applied voltage.

From the voltage equation of (5.3) as the frequency increases voltage should be increased by the same amount to keep flux hence the flux density constant during the constant V/f region (from zero speed to base speed). To determine the applied voltage over the defined speed range (0 to 1250 rpm) equation 5.9 will be used.

$$V = E + IZ \tag{5.9}$$

Where "Z" is the impedance of the motor and it is necessary to determine the variation of the reactance for whole speed range.

Then knowing the variation of the back EMF, current and impedance, due to the variation of reactance, with the speed, the variation of the applied voltage with the speed can easily be determined by using equation (5.9) and the applied voltage and back EMF is given in figure 5.3

To end the evaluation of performance of induction motor, losses of the motor should be considered. Total loss of the induction motor consists of copper loss, friction and windage loss and core loss. The friction and windage loss is assumed to be equal for all motors, and is a function of cube of the speed. Copper loss of the induction motor can be found by using well known equation in 5.10 and the core loss is approximated by using equation (5.11) [21], which includes only hysteresis loss. In the calculation of core loss, it is assumed that powder metal is used for the construction of stator core. So that using powder metal eliminates the eddy current loss.

$$P_{cu} = 3I^2R \tag{5.10}$$

$$P_{core} = K_{cr} f B^2 \tag{5.11}$$

Where

"K_{cr}" is the core loss coefficient and determined at the washing cycle experimentally. Since core of all motors are assumed to be made of same material, this core loss coefficient will be used for the other types of motors.

Variation losses of an induction motor and the efficiency of the motor with speed is given in figure 5.4 and figure 5.5 respectively.

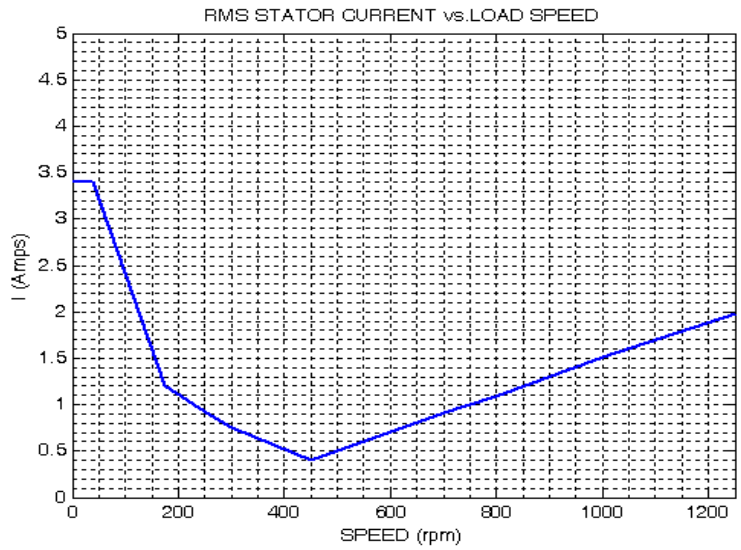

Figure 5 2 RMS stator current of 2-pole IM

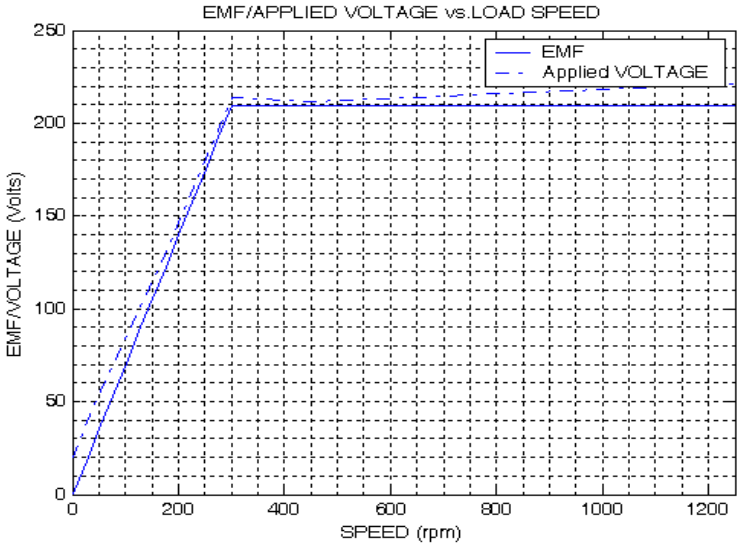

Figure 5 3 Applied voltage and back EMF of 2-pole IM

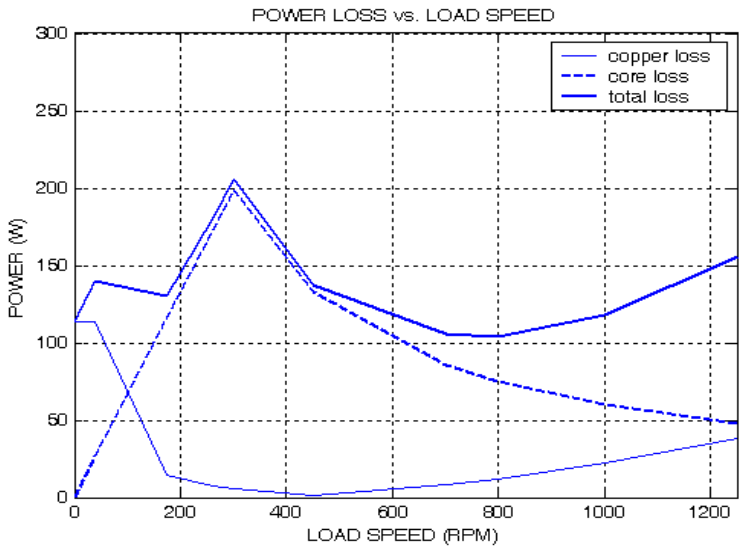

Figure 5 4 Total loss of 2-pole IM

Figure 5 5 Efficiency of 2-pole IM

Figure 5.2, 5.3, 5.4 and 5.5 are determined for a two pole induction motor. For the comparison purposes and to see the effect of the pole number on motor performance, the same graphs for a 6 pole and 10 pole induction motors are given. In order to analyze the performance of induction motor for different number of poles, the same procedure is followed.

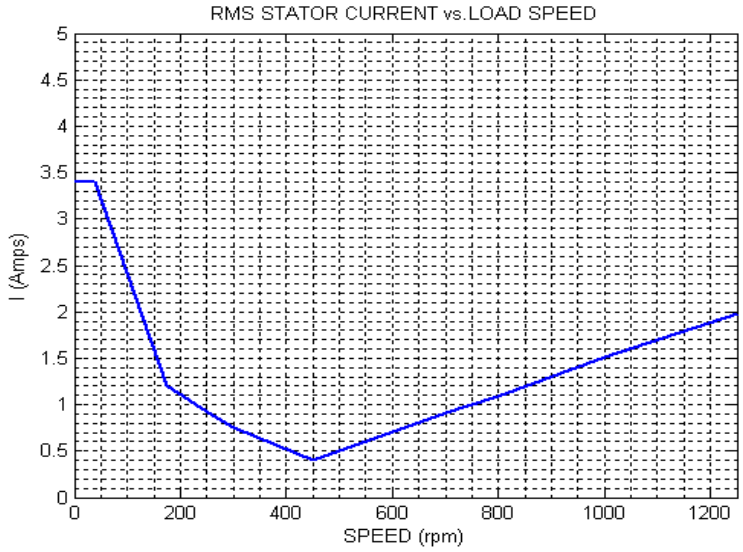

Figure 5 6 RMS stator current of 6-pole IM

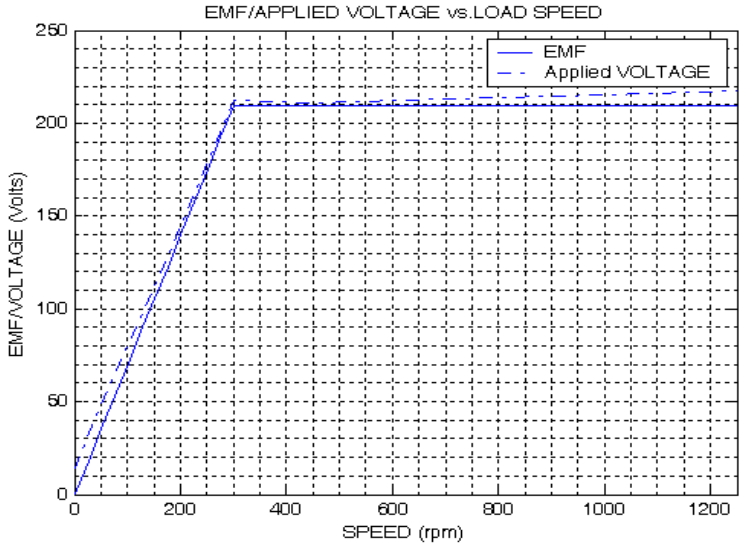

Figure 5 7 Applied voltage and back EMF of 6-pole IM

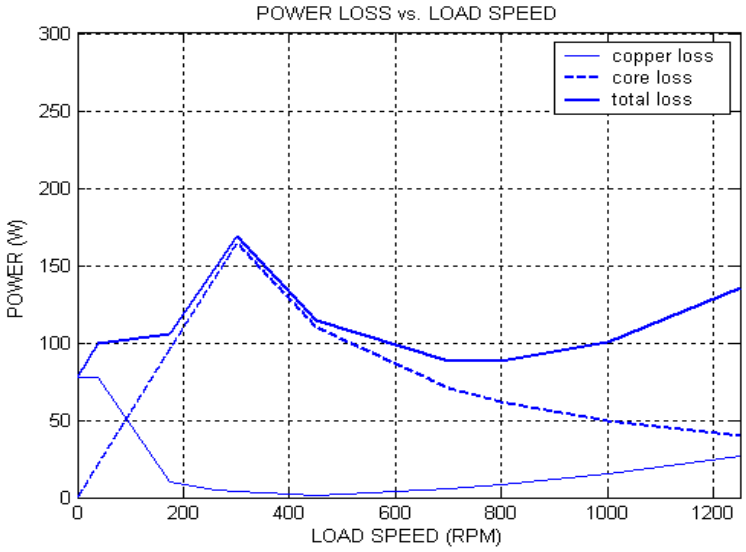

Figure 5 8 Total loss of 6-pole IM

Figure 5 9 Efficiency of 6-pole IM

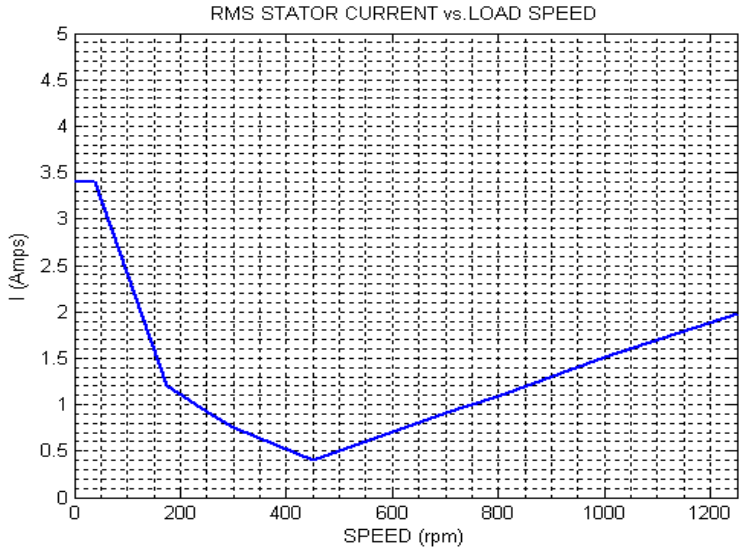

Figure 5 10 RMS stator current of 10-pole IM

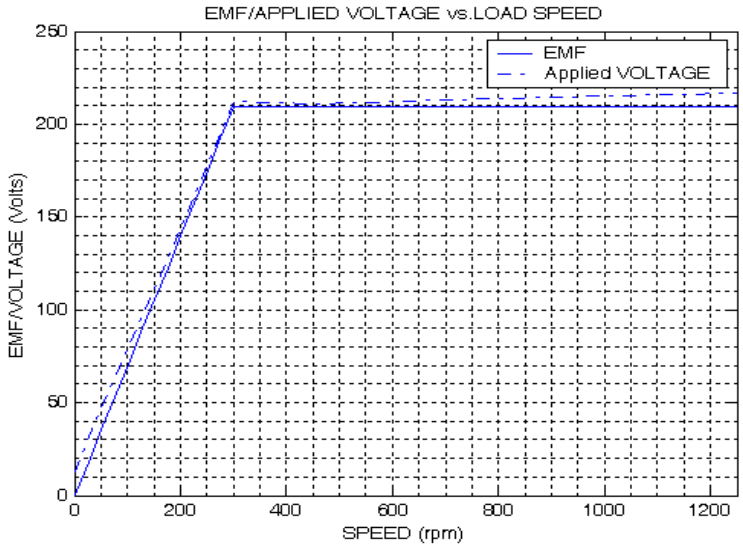

Figure 5 11 Applied voltage and back EMF of 10-pole IM

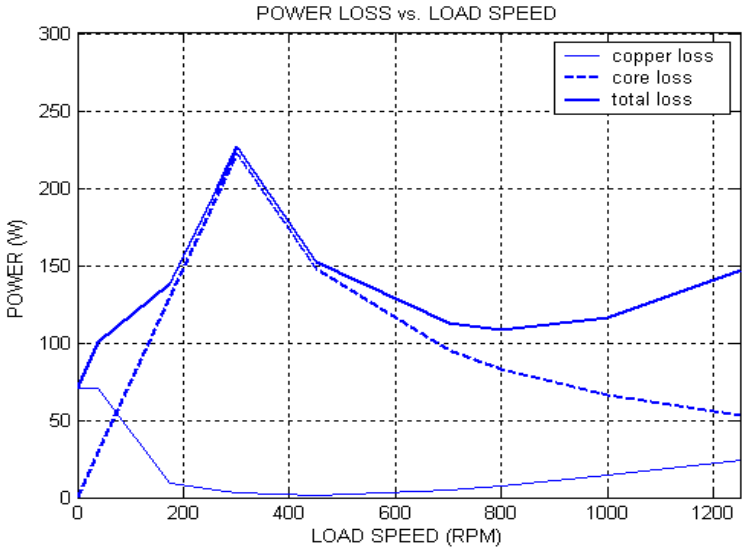

Figure 5 12 Total loss of 10-pole IM

Figure 5 13 Efficiency of 10-pole IM

5.3 Radial flux brushless dc motor

The derivation of the torque equation for the RF-BLDC motor is considered and derived in chapter 3 as;

$$T = \sqrt{\frac{8}{3}}\pi r^2 l B_g q = \frac{\pi}{\sqrt{6}} B_g q D_i^2 l \qquad (5.12)$$

Nearly the same procedure is applied to the RF-BLDC motor as in the case of induction motor. Again Electric loading and peak tooth flux density are taken as 28000 A/cond. and 1.7 T respectively as in the case of induction motor. Since stator tooth width is assumed to be equal to stator slot width, magnetic loading "B" in equation (5.12) can be determined. The air-gap flux is determined depending on the permanent magnet used on the rotor surface but the peak flux density should be limited by the saturation and should not exceed the maximum permissible value (nearly 1.7 T is acceptable)

NEOMAX-35, which is a type of Nd-Fe-B magnet, is used on the rotor surface. This magnet has high residual flux density, nearly 1.2 T, and high energy value. Since the field flux is fixed by the permanent magnet, this means that air-gap flux density is constant over whole speed range, this motor can produce the same torque at all speeds.

To find the main dimensions of this motor equation (5.12) is used. For the sake of simplicity and to reduce the number unknowns to 1 stack length is chosen to be equal to the bore diameter. Then to meet the maximum torque requirement of the motor, dimensions are chosen accordingly.

Now the number of turns should be determined for this motor. Calculation of turns per phase value of RF-BLDC motor is similar to that of the induction motor. Maximum value of the number of turns per phase is necessary at the base speed of the motor (since no field weakening is considered for this motor base speed is chosen as the highest speed), where back EMF of the motor is reached. Only difference between induction motor and RF-BLDC motor in calculating the turns per phase is the back EMF expression. Equation (5.13) is used to determine the number of turns per phase of RF-BLDC motor.

$$e = 2N_{ph}B_g lrw_m = 2N_{ph}B_g lr\frac{\pi}{30}n$$

$$N_{ph} = \frac{e}{B_g lD_i w_m} \tag{5.13}$$

Where;

"e" is the phase back EMF and since in an RF-BLDC motor two phases are conducting at the same time, the value of phase back EMF should not exceed the half of the inverter output voltage value (for our case since the inverter output is limited to 300 volts back EMF can not be more than 150 volts)

"w_m" is the speed of the motor and s mentioned before for the calculation of the turns per phase, it is chosen as the base speed of the motor.

Since all the parameters of equation (5.13) are known turns per phase of the motor can easily be obtained. To calculate the resistance of one phase equation (5.4) can be used (Note that total resistance is two times of the calculated since two phases are conducting at the same time).

Now the variation of flux density, electric loading and current with the speed can be calculated in a straightforward manner by using the equations (5.14), (5.15), (5.16).

$$B_g = \frac{e}{N_{ph}lD_i w_m} \tag{5.14}$$

$$q = \frac{\sqrt{6}T_m}{\pi D_i^2 lB_g} \tag{5.15}$$

$$I_{rms} = \frac{q\pi D_i}{6N_{ph}} \tag{5.16}$$

Applied voltage also varies with the speed of the motor depending on the variation of the current value. Putting the current expression in equation (5.16) into the equation (5.17), variation of applied voltage can be obtained

$$V = E + RI \tag{5.17}$$

Note that the resistance expression of equation (5.17) is the total resistance (two times the calculated resistance by using equation (5.4).

The variation of the stator current and the applied voltage, including the back EMF, with the speed are given in figures 5.14 and 5.15 respectively.

The same losses exist in RF-BLDC motor as in induction motor. Therefore friction and windage losses, copper losses and core losses should be considered for this motor to evaluate the efficiency of the motor.

The same loss data with the induction motor is used for the calculation of the friction and windage loss. Copper loss can be found by using the equation (5.18). Note that the resistance value is two times the phase resistance because two phases are conducting simultaneously.

$$P_{cu} = I^2 R \tag{5.18}$$

In order to obtain the core loss of RF-BLDC motor same procedure is used as in the case of induction motor so that equation (5.11) can be applicable. Since no field weakening is considered, as mentioned before, this motor is expected to have high core loss at high speed.

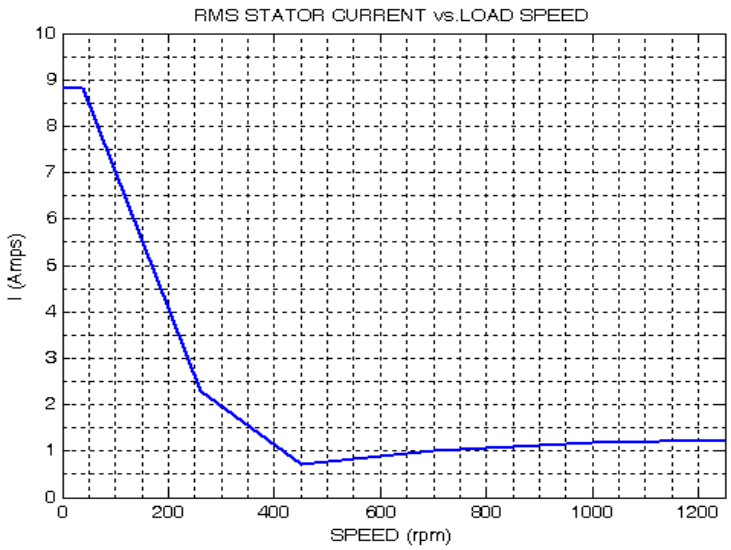

Figure 5 14 RMS stator current of 2-pole RF-BLDC

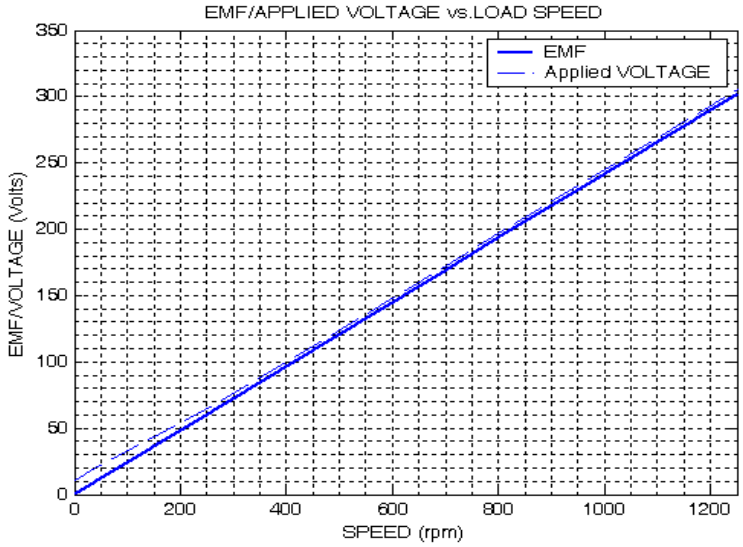

Figure 5 15 Applied voltage and back EMF of 2-pole RF-BLDC

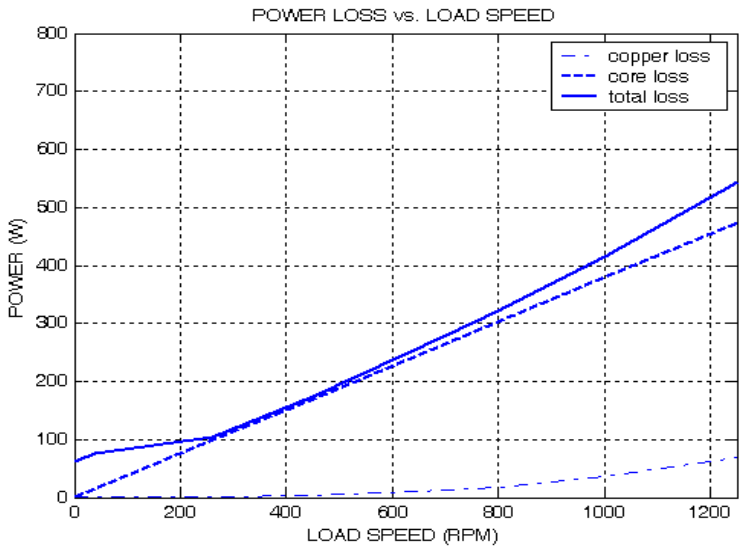

Figure 5 16 Total loss of 2-pole RF-BLDC

Figure 5 17 Efficiency of 2-pole RF-BLDC

Above figures for RF-BLDC are for 2 pole motor, so that in order to enlarge this evaluation for different pole numbers, graps of 6 and 10 pole numbers are given.

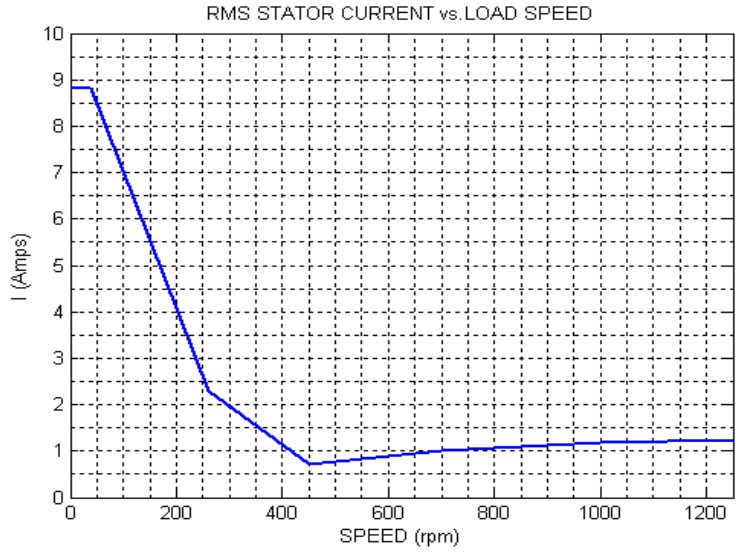

Figure 5 18 RMS stator current of 6-pole RF-BLDC

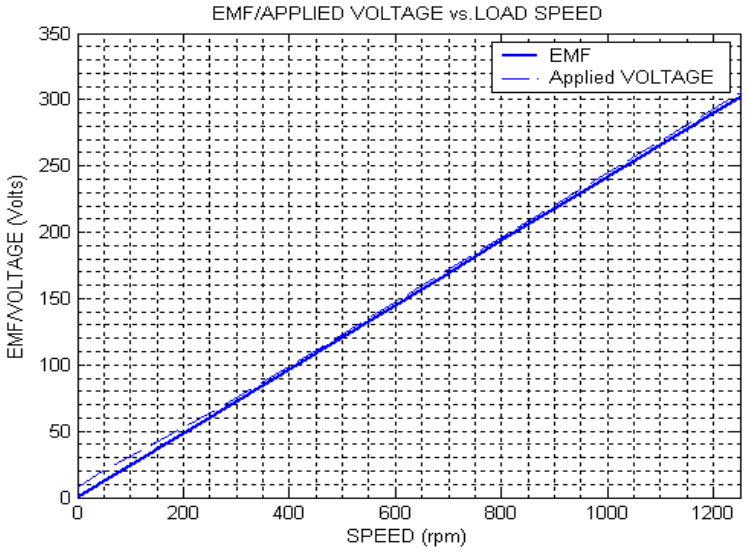

Figure 5 19 Applied voltage and back EMF of 6-pole RF-BLDC

Figure 5 20 Total loss of 6-pole RF-BLDC

Figure 5 21 Efficiency of 6-pole RF-BLDC

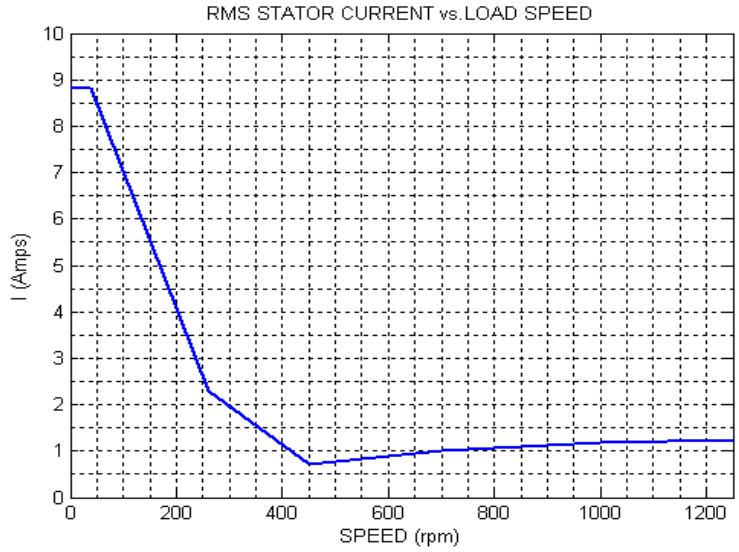

Figure 5 22 RMS stator current of 10-pole RF-BLDC

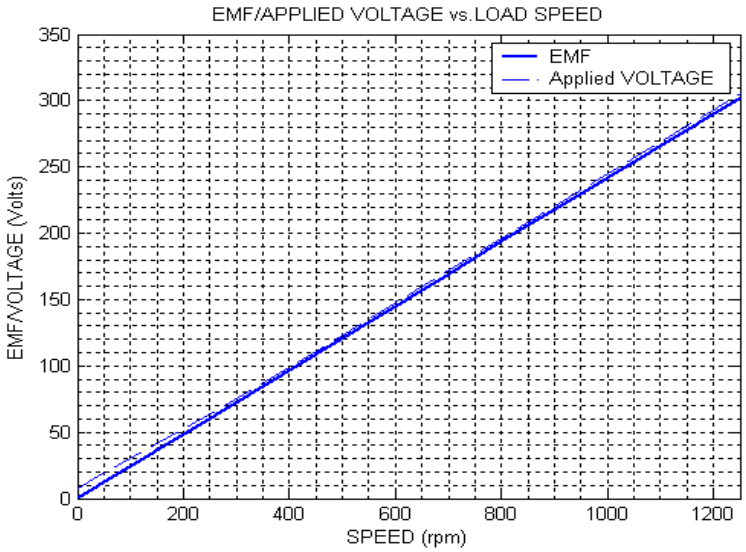

Figure 5 23 Applied voltage and back EMF of 10-pole RF-BLDC

Figure 5 24 Total loss of 10-pole RF-BLDC

Figure 5 25 Efficiency of 10-pole RF-BLDC

5.4 Axial flux brushless dc motor

Torque equation of AF-BLDC motor was derived in chapter 3 and given in equation (5.19).

$$T = 2\pi B_g q_i R_i (R_o^2 - R_i^2) = 2\pi B_g q_i R_o^3 K_r (1 - K_r^2) \quad (5.19)$$

"Kr" in equation (5.19) is the ratio of inner radius to outer radius and chosen to be "0.578" as the optimum value [5]. NEOMAX-35 is used on the rotor surface of this motor. This motor is very similar to RF-BLDC motor except the flux path. So that the procedure also very similar. Same electric loading value (28000 A/cond.) is used. Knowing all the unknown values of equation (5.19), it is easy to find the outer radius of the motor to satisfy the maximum torque requirement. Then using predefined outer radius to inner radius ratio, inner radius and hence the mass and volume of the motor and stator core can be obtained.

Number of turns per phase can be found by solving the back EMF equation for the turn per phase value as in the equation (5.20), choosing the base speed as the highest speed as in the case of RF-BLDC motor.

$$N_{ph} = \frac{e}{B_g R_o^2 (1 - K_r^2) w_m} \quad (5.20)$$

Number of turns per phase should be calculated at the base speed of the motor and phase EMF (e) of the motor should not exceed the half of the inverter output as mentioned in the RF-BLDC case. After calculating the turns per phase by using the equation (5.4), resistance of one phase can be found (note that two phases are conducting at the same time so that take two times of the calculated resistance value for the calculations)

Now the variation of flux density, electric loading and current with the speed can be calculated in a straightforward manner by using the equations (5.21), (5.22), (5.23).

$$B_g = \frac{e}{N_{ph} R_o^2 (1 - K_r^2) w_m} \quad (5.21)$$

$$q = \frac{T}{2B_g \pi R_o^3 K_r (1 - K_r^2)} \tag{5.22}$$

$$I_{rms} = \frac{q \pi D_i}{3 N_{ph}} \tag{5.23}$$

The necessary voltage, should be applied, can be obtained by using the equation (5.17) remembering that the value of resistance is two times the calculated.

Figure 5.26 and 5.27 show the mentioned variation of current and applied voltage with the speed.

The losses of an AF-BLDC motor consists of the same losses as those of the induction motor and RF-BLDC motor such as friction and windage loss, copper loss and core loss. Friction and windage loss is taken the same. To find the copper loss of AF-BLDC motor, equation (5.18) of RF-BLDC motor can be used, for the core loss calculation equation (5.11) can be used, considering the same assumptions mentioned for induction motor and RF-BLDC motor. Then the total loss and efficiency of the AF-BLDC motor varies with the speed as in figures 5.28 and 5.29.

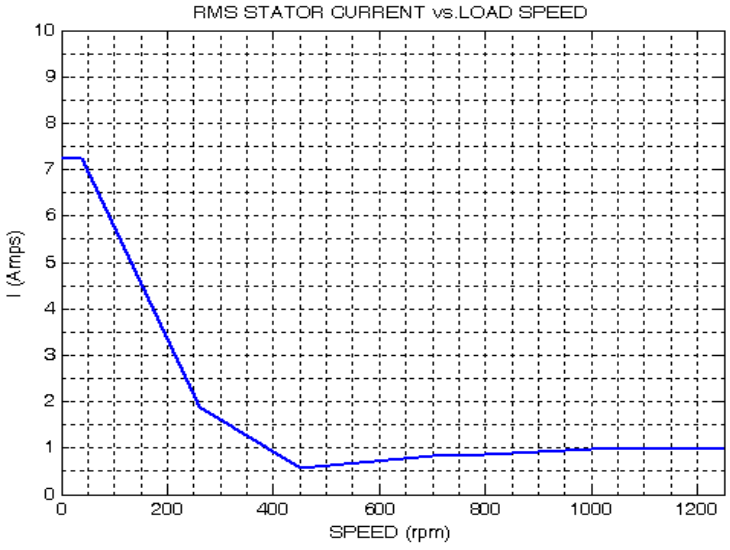

Figure 5 26 RMS stator current of 2-pole AF-BLDC

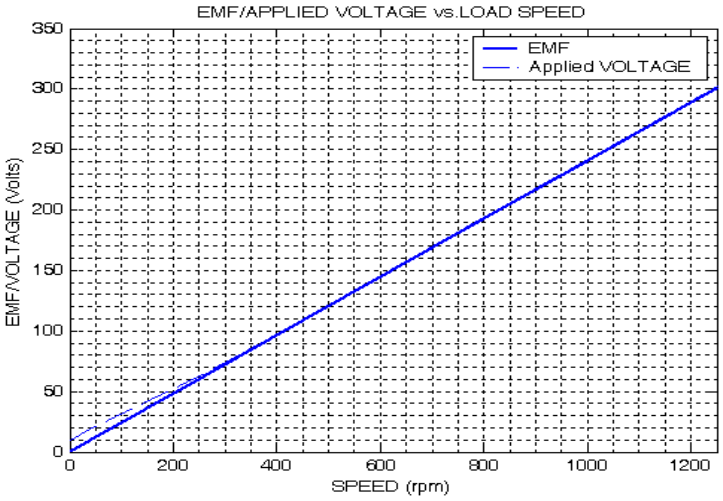

Figure 5 27 Applied voltage and back EMF of 2-pole AF-BLDC

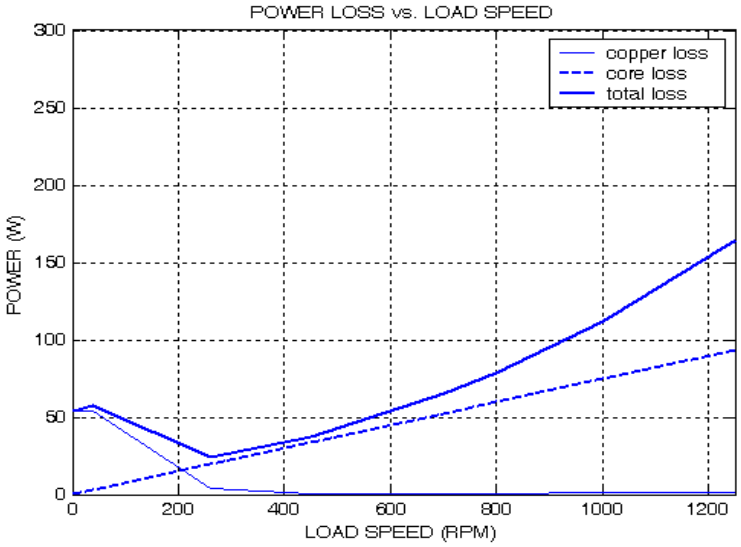

Figure 5 28 Total loss of 2-pole AF-BLDC

Figure 5 29 Efficiency of 2-pole AF-BLDC

Figure 5.26, 5.27, 5.28, 5.29 are for 2 pole AF-BLDC motor and graphs for 6 and 10 pole AF-BLDC motor are also given respectively.

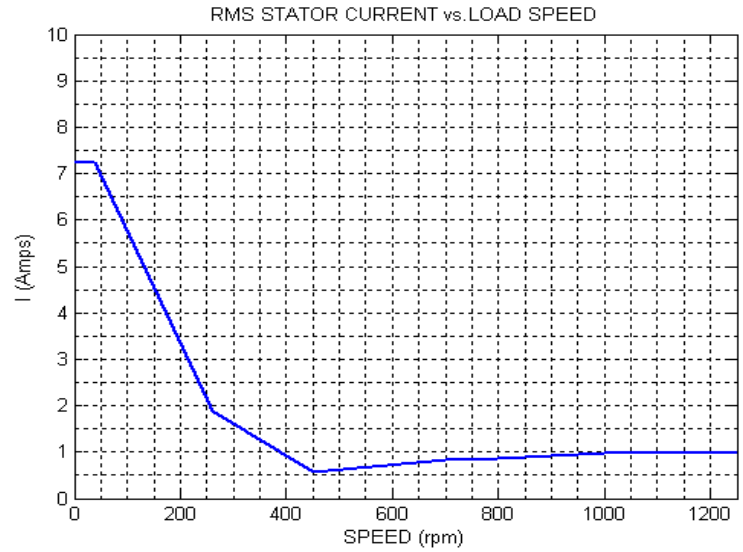

Figure 5 30 RMS stator current of 6-pole AF-BLDC

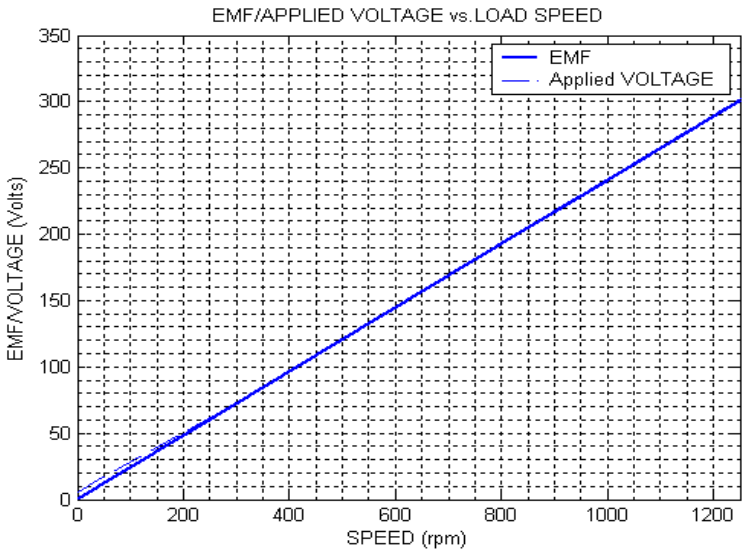

Figure 5 31 Applied voltage and back EMF of 6-pole AF-BLDC

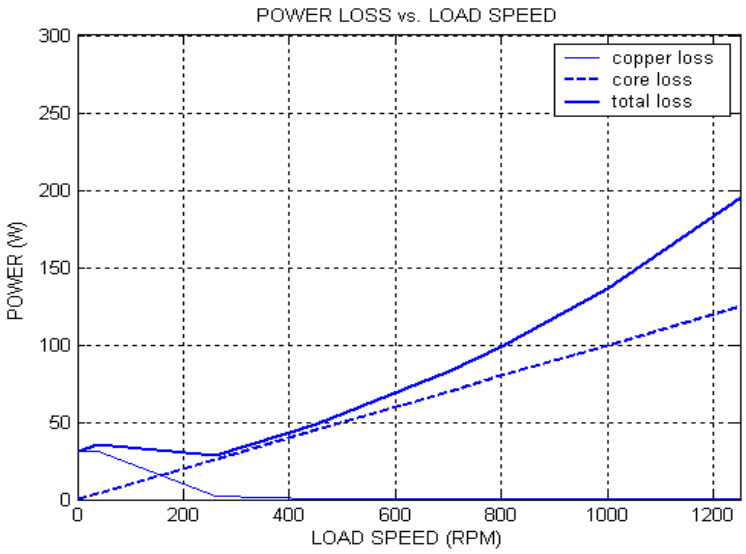

Figure 5 32 Total loss of 6-pole AF-BLDC

Figure 5 33 Efficiency of 6-pole AF-BLDC

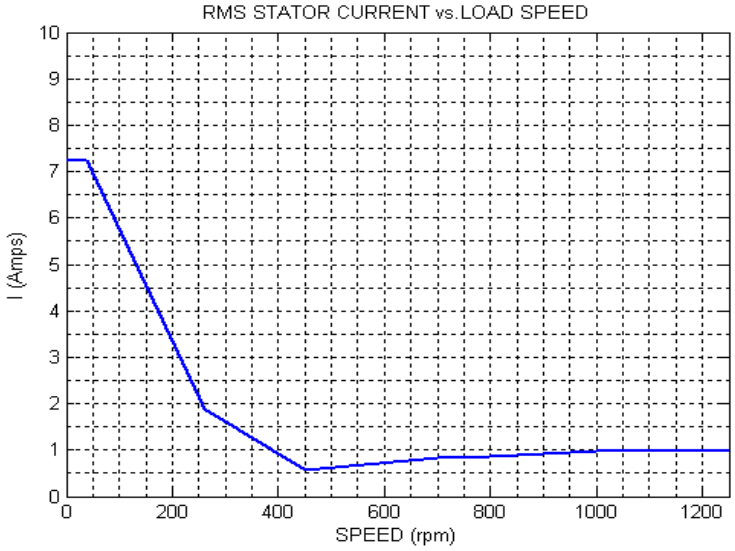

Figure 5 34 RMS stator current of 10-pole AF-BLDC

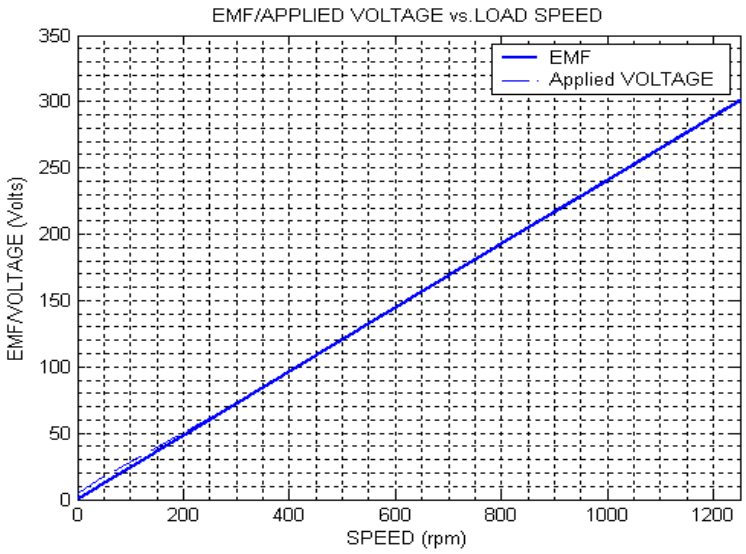

Figure 5 35 Applied voltage and back EMF of 10-pole AF-BLDC

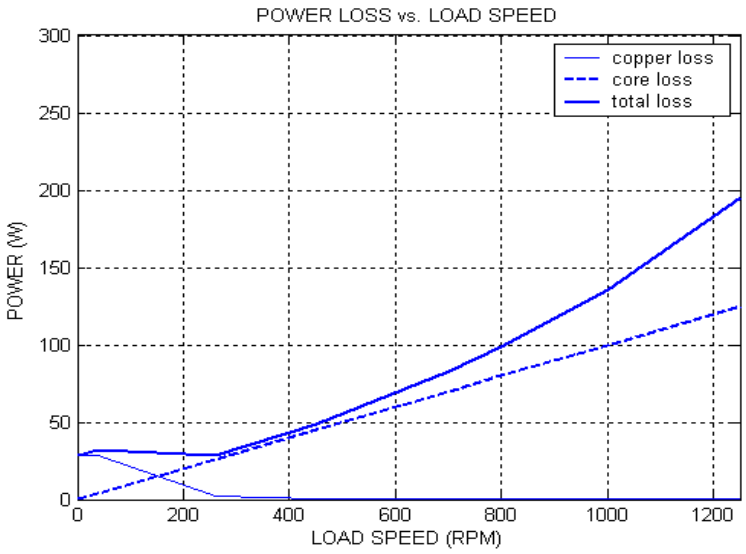

Figure 5 36 Total loss of 10-pole AF-BLDC

Figure 5 37 Efficiency of 10-pole AF-BLDC

5.5 Switched Reluctance Motor

The torque equation of switched reluctance motor is derived in chapter 4 as:

$$T = \frac{K}{\sqrt{3}} Bq \frac{\pi}{4} D_i^{\,2} L = \frac{K}{\sqrt{3}} BqV_{rotor} \qquad (5.24)$$

This torque equation is the starting point for the performance calculation of switched reluctance motor. Since the electric loading and stator pole flux density of the motor are taken as 28000 A/cond and 1.7 T respectively, it is necessary to find the dimensions of the motor where it meets the maximum torque requirement (2.5 Nm washing cycle and 0.35 Nm at spin cycle). For the sake of simplicity, as in the case of the other motors considered before, stack length of the motor is taken to be equal to the bore diameter.

The next step is the determination of number of turns per phase. Number of turns per phase should be determined at the base speed of the motor, where the flux linkage and hence the back EMF is at its maximum value. Number of turns per phase is found by using the equation (5.25). While writing the equation (5.25),

resistive voltage drops are neglected, that is applied voltage is assumed to equal to the induced voltage.

$$N_{ph} = \frac{V\pi}{\phi_p P_r w_b} \tag{5.25}$$

Where

"w" is the base speed of the motor (taken the same as that of induction motor)

"Φ_p" is the maximum flux (B_pA)

"P_s" is number of stator poles

"P_r" is number of rotor poles

When the number of turns per phase is obtained, calculation of the resistance can be done as in the case of induction motor. The next step for the performance evaluation of this motor is to determine the variation of the flux density, electric loading and phase current with the speed.

In order to determine the variation of the flux density, it is necessary to determine the flux variation with the speed. Equation (5.26) can be used to determine the flux density, assuming no resistive voltage drop, variation with the speed [22].

$$B = \frac{V}{kA}$$
$$where$$
$$k = \frac{N_{ph} P_r}{\pi} w \tag{5.26}$$

After dimensions are determined two different approaches are used to analyze the performance of the motor. In both approaches, the dimensions found, by using equation (5.24) are used. The differences are the approximations applied to find the current waveforms and losses. First approach uses the approximation applied to induction motor, i.e. same core

loss coefficient and core loss calculation. However the second approach is an optimization program that uses the equations derived for the nonlinear case of this motor.

5.5.1 Approach 1

Since the variation of flux density with speed is found and the torque requirement of the motor at different speeds is known, it is a simple matter to calculate the electric loading and hence the stator current by using the equations (5.27) and (5.28).

$$q = \frac{4\sqrt{3}T}{BK\pi D^2 L} \tag{5.27}$$

$$I_{peak} = \frac{q\pi D_i}{6N_{ph}} \tag{5.28}$$

In this study current is assumed to be trapezoidal and hence the rms value of the stator current can be calculated by using the equation (5.29).

$$I_{rms} = \frac{I_p}{\sqrt{m}} \tag{5.29}$$

Since the variation of current (figure 5.38) with the speed and the value of the resistance is obtained and applied voltage to the motor can be found by using:

$$V = E + RI \tag{5.30}$$

The variation of back EMF and the applied voltage to the motor is given in figure 5.39.

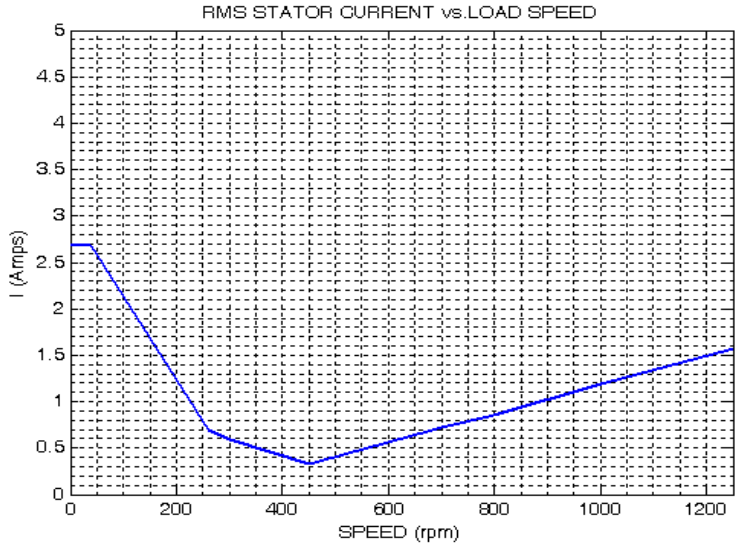

Figure 5 38 RMS stator current of 3-phase SR

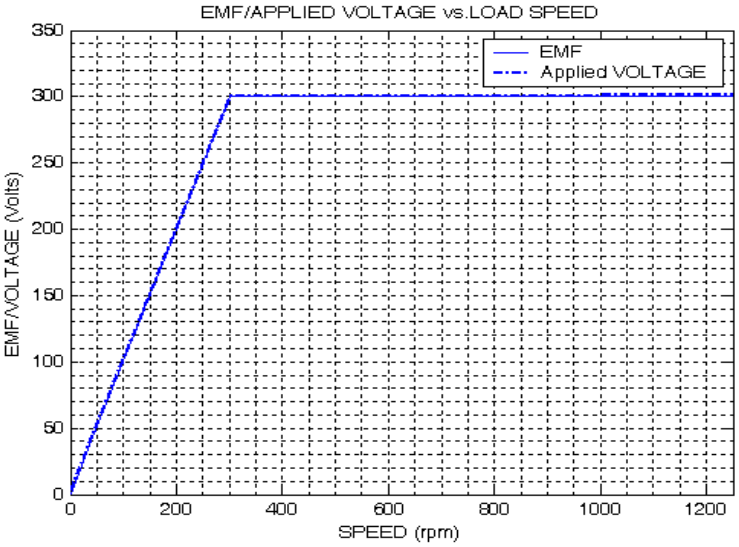

Figure 5 39 Back EMF and applied voltage of 3-phase SR

In order to determine the total loss of the switched reluctance motor friction and windage loss, copper loss and core loss are considered. Copper loss is determined in same manner as in the case of the induction motor and permanent magnet motors, using the equation given below.

$$P_{cu} = 3{I_{rms}}^2 R \tag{5.31}$$

In order to calculate the switched reluctance motor core loss, it should be noted that the flux density and frequency are different at different parts of the motor. When it is assumed that the flux density of the stator pole is "B_t" then back core flux density and rotor pole flux density are represented as [24]:

$$B_{BC} = \frac{0.5 B_t t_s}{b_{sy}}$$
$$B_r = \frac{B_t t_s}{D_i - 2h_r} \tag{5.32}$$

Where;

"B_{BC}" is the back core flux density

"B_r" rotor pole flux density

"t_s" stator tooth width

"b_{sy}" stator back core thickness

"h_r" rotor pole depth

To complete the determination of the core loss, frequencies of the fluxes at different parts of the motor should also be determined by using the equations given below.

$$f1 = \frac{P_r n}{60}$$
$$f2 = \frac{P_s n}{60} \tag{5.33}$$

Where;

"f1" is the frequency of back core flux and stator pole flux

"f2" is the frequency of rotor pole flux

"P_r" is the number or rotor poles

"P_s" is the number of stator poles

The resultant core loss is the sum of the losses determined individually by the help of equation (5.31), at different sections of the motor at different frequencies.

$$P_{core} = K_{cr} f B^2 \tag{5.34}$$

When calculating the core loss of the motor it should be kept in mind that the maximum flux density in the rotor core will be low compared to the flux densities in the other sections, so that rotor core iron losses can be neglected [24]. Results of the loss calculation and the efficiency are given respectively.

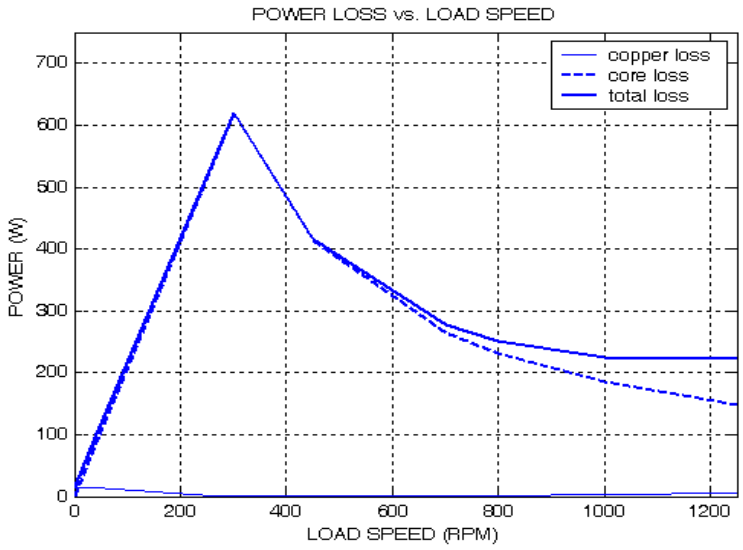

Figure 5 40 Total loss of 3-phase SR

Figure 5.40 is a result of the core loss calculation using equation (5.34). In fact the calculation of core loss by using this equation gives errors. In reference [24] core loss was determined, experimentally at base frequency. Since the flux waveforms and frequencies are different at different parts of the motor, core loss of the material was obtained at different frequencies and under different excitations (i.e. for a 8/6 SR motor, at base frequency rotor poles experiences flux waveform of 200 Hz stator poles and stator back core experience flux waveform of 150 Hz). Experimental result for such a motor is given in figure 5.41 [24].

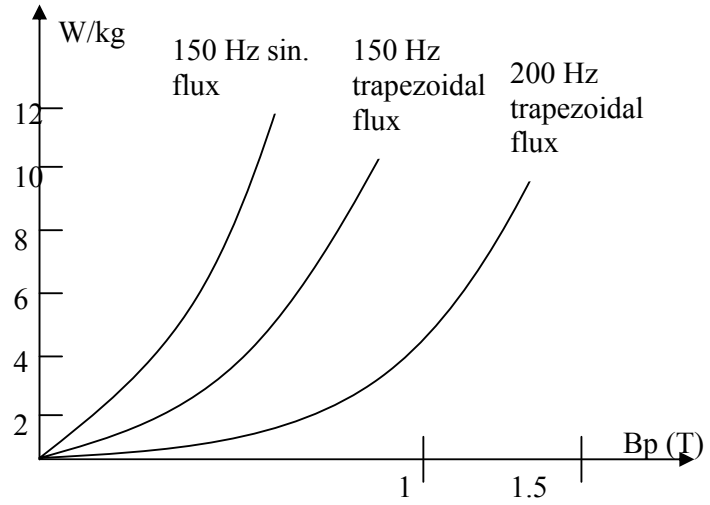

Figure 5 41 Core loss per unit weight vs peak flux density [24]

Figure 5 42 Efficiency of 3-phase SR motor

5.5.2 Approach 2 (Optimization Program)

Figures 5.38, 5.39, 5.40, 5.42 are the results of our approach. In order to check the appropriateness of the procedure mentioned so far, an optimization program, developed in TUBITAK-BILTEN is used. In this program non-linear case is considered. For this program flux linkage and current curve is necessary for the

solution. If these curves are ready then, can be entered manually if not, dimensions of the motor and magnetic properties of the motor (B-H curve) are entered and then program predicts the flux linkage current curve by using the predefined normalized permeance data, motor dimensions and magnetic properties.

Since the flux linkage current curve of the motor is determined, by using one of the differential equation solution methods (i.e. runge kutta) starting from switch on position to the end of the conduction period, current position waveform, instant torque position waveform, flux linkage position waveform and flux linkage current locus can be obtained.

- From flux linkage position curve core loss is obtained
- From current position curve copper loss and RMS value of the current is obtained
- From instantaneous torque position curve, average torque and torque ripple is obtained.

For the non-linear case terminal voltage equation, used in this program, is given as.

$$V = \frac{d\phi(\theta,i)}{dt} + RI$$
$$then$$
$$\frac{d\varphi(\theta,i)}{d\theta} = \frac{V - RI}{w} \qquad (5.32)$$

Where;

"Φ(θ,i)" is the flux linkage of a phase winding

Since the flux linkage vs. current curve is known, change in co-energy and hence the torque of the motor can be found by applying the equations (5.33) and (5.34) respectively.

$$W_c = \int_{i1}^{i2} \phi(i,\theta)di \qquad (5.33)$$

$$T = \frac{\Delta W_c(i,\theta)}{\Delta\theta} \tag{5.34}$$

In order to compare the results obtained so far with the results of the optimization program, applied voltage, advance angel and excitation period are so arranged that flux value of stator pole and torque requirement is satisfied at both wash cycle and spin cycle. Note that the peak current value for the switched reluctance motor should be entered and makes chopping around this value and due to excitation angle and conduction period RMS value of the current changes. The corresponding results of the optimization program are given below.

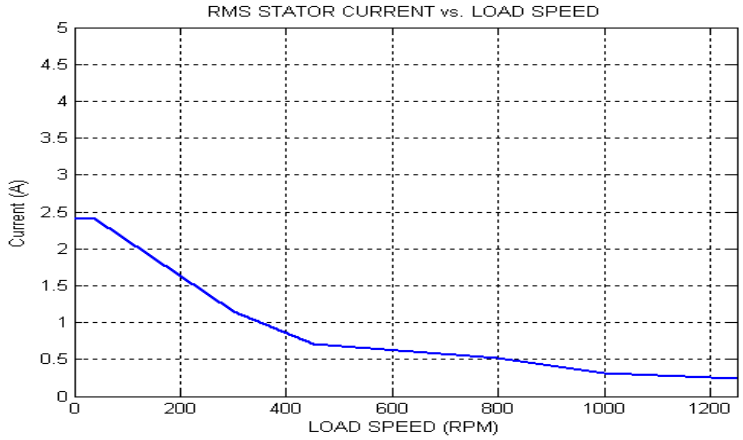

Figure 5 43 RMS stator current of 3-phase SR with optimization program (B=1.7T)

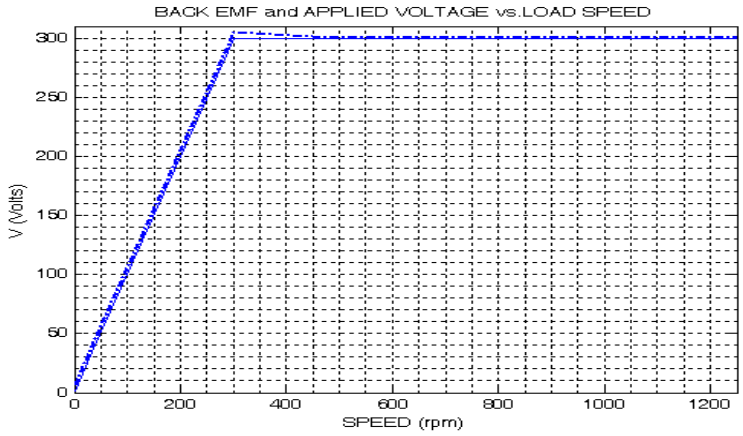

Figure 5 44 Applied voltage and bak EMF of 3-phase SR with optimization program (B=1.7T)

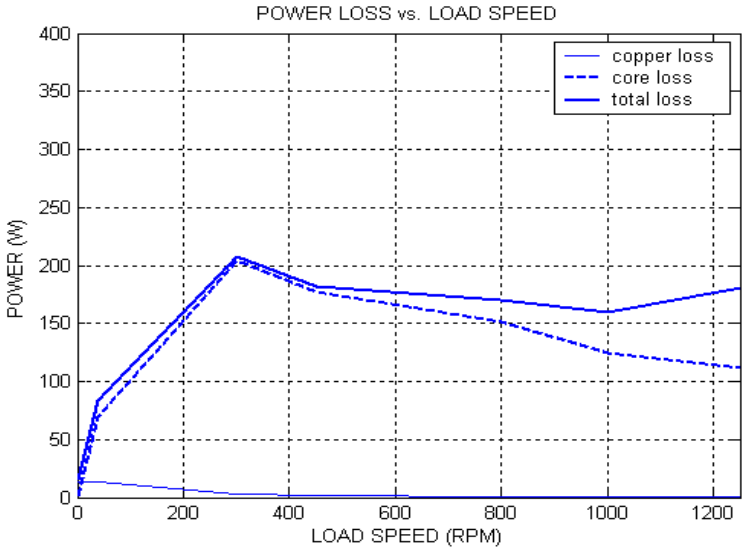

Figure 5 45 Total loss of 3-phase SR with optimization program (B=1.7T)

Figure 5 46 Efficiency of 3-phase SR with optimization program (B=1.7T)

The results of both approaches are given in table for the comparison. Since the optimization program considers the non-linear behavior of the switched reluctance motor, it is more reliable to use optimization program for the analysis of the switched reluctance motor.

Table 5 1 Comparison of the results of SR motor approaches

	Approach 1	Approach 2 (opt. Prog.)
I_{peak} (A) wash cycle	4,65	4
I_{peak} (A) spin cycle	2,7	0,3
I_{rms} (A) wash cycle	2,68	2,4
I_{rms} (A) spin cycle	1,56	0,21
P_{loss} (W) wash cycle	95,8	83,4
P_{loss} (W) spin cycle	222,4	181,1
η (%) wash cycle	52,2	55,58
η (%) spin cycle	67,3	71,3

As the last part of this chapter, analysis results of a 3 phase motor for a peak flux density of "2.1 T" and 4 phase switched reluctance motor are given both for taking flux density as "1.7 T" and "2.1 T" respectively. For all cases the dimensions of the motors are determined by the help of equation (5.24) and the calculations are performed by using the optimization program supplied by Tubitak-Bilten. When the dimensions are calculated, it is checked that whether they satisfy the torque requirement at wash cycle and spin cycle.

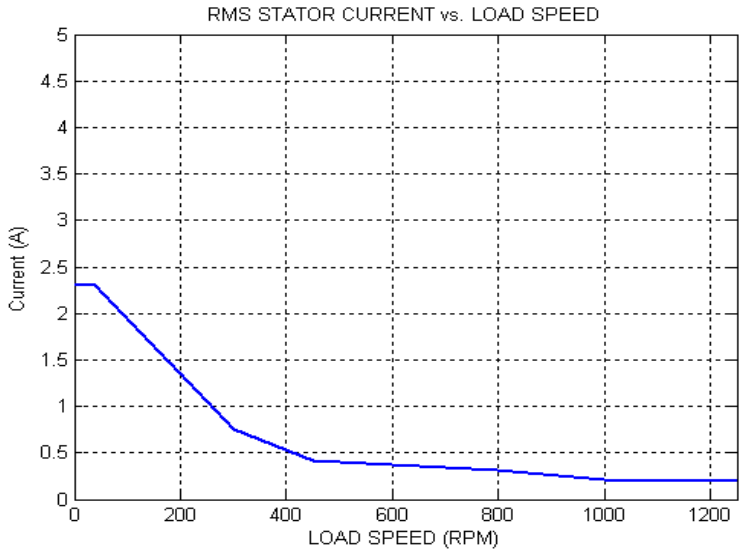

Figure 5 47 RMS stator current of 3 phase SR with optimization program (2.1 T)

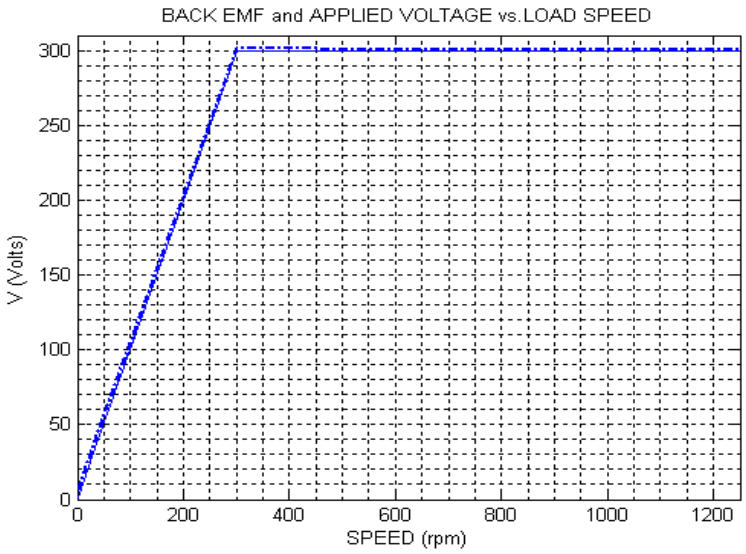

Figure 5 48 Applied voltage and back emf of 3-phase SR with optimization program (2.1 T)

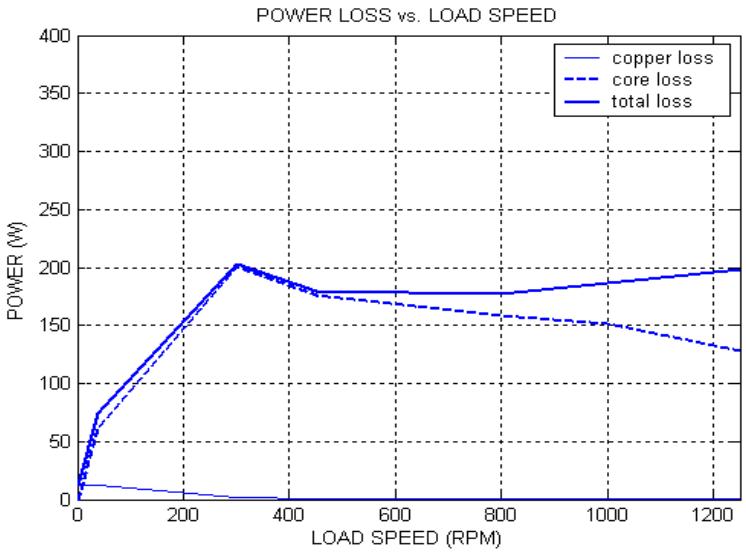

Figure 5 49 Total loss of 3-phase SR with optimization program (2.1 T)

Figure 5 50 Efficiency of a 3-phase SR with optimization program

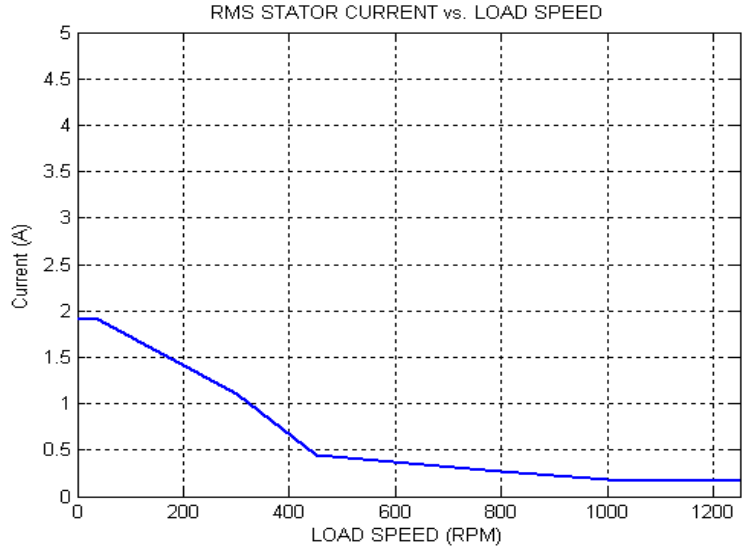

Figure 5 51 RMS stator current of 4-phase SR with optimization program (B=1.7T)

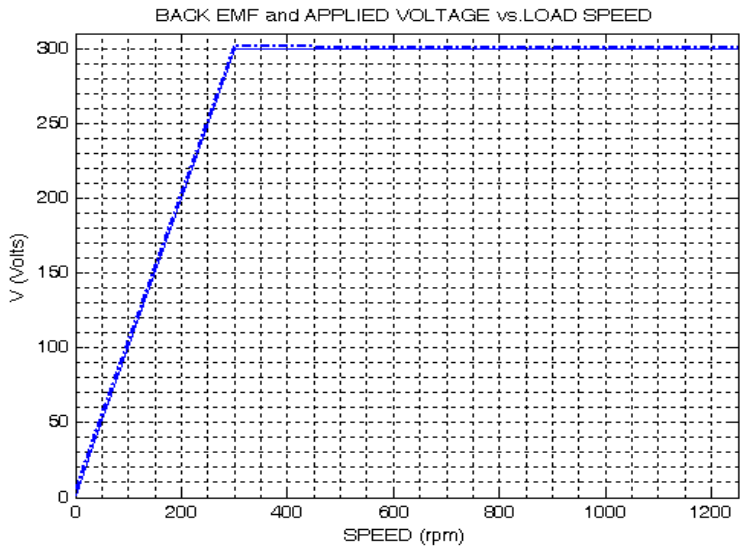

Figure 5 52 Applied voltage and back EMF of 4-phase SR with optimization program (B=1.7T)

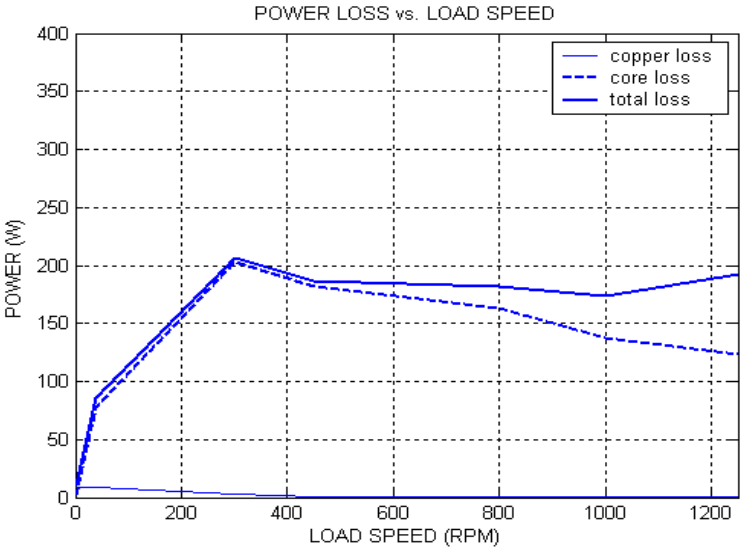

Figure 5 53 Total loss of 4-phase SR with optimization program (B=1.7T)

Figure 5 54 Efficiency of 4-phase SR with optimization program (B=1.7T)

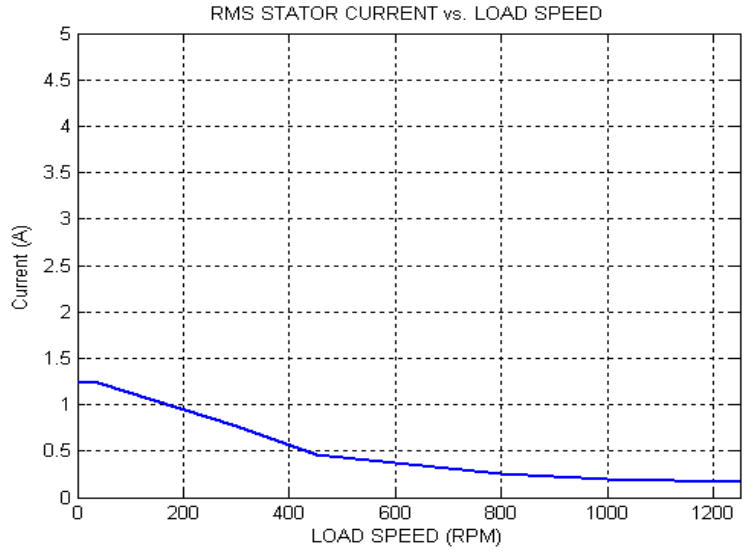

Figure 5 55 RMS stator current of a 4-phase SR with optimization program (2.1 T)

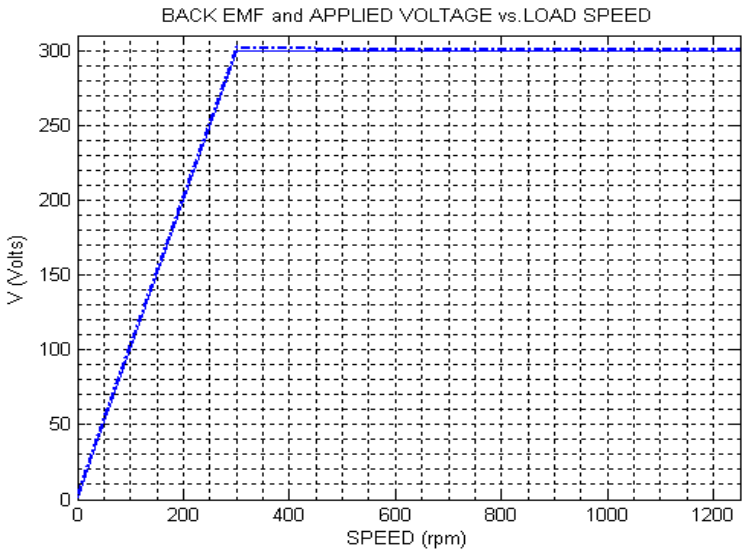

Figure 5 56 Applied voltage and back EMF of a 4-phase SR with optimization program (2.1 T)

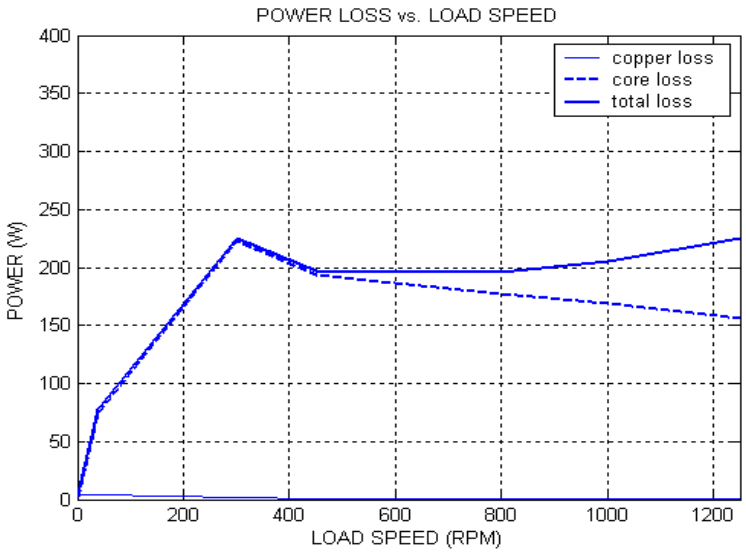

Figure 5 57 Total loss of a 4-phase SR with optimization program (2.1 T)

Figure 5 58 Efficiency of a 4-phase SR with optimization program (2.1 T)

In this chapter, induction motor, permanent magnet brushless dc motors, both radial and axial flux types, and switched reluctance motor are considered and analyzed. Induction motor and permanent magnet motors are considered for three different pole numbers (2, 6, 10) and switched reluctance motor is considered for two different phase numbers (3 phase and 4 phase). Next chapter is arranged for the comparison of these motors, to have an idea about the motors.

CHAPTER 6

CONCLUSION

6.1 General

In chapters 2, 3 and 4 torque equation of the induction motor, permanent magnet brushless dc motors (both radial and axial flux type) and switched reluctance motor are derived in terms of dimensions. In chapter 5 these motors are analyzed for a washing machine application at low speed (wash cycle) and at high speed (spin cycle). In order to see the affects of the number of poles on motor performance, this analysis is also made for different number of poles for each motor (for induction motor and permanent magnet brushless dc motor) and for different phase numbers (for switched reluctance motor).

Before starting the comparison of the motors, it is worth to recall the requirements and assumptions of this application.

- The washing machine drum requires 25 Nm during wash cycle (40 rpm), and 3.5 Nm during spin cycle (1250 rpm)
- Motors are fed with a DC link voltage of 300 volts.
- A reduction ratio of 1/10 is used.
- Specific electric loading of 28000 is used
- Maximum current density is taken as 7 A/mm^2
- For the sake of simplicity bore diameter is assumed to be equal to core length for induction motor, RF-BLDC and SR motor.
- In the calculations induction motor is assumed to be rotating at synchronous speed.
- Demagnetization is neglected for BLDC motors

- Field weakening is not considered for permanent magnet brushless dc motors. Therefore the highest motor speed is taken as base speed for BLDC motors (both radial flux and axial flux type).
- Base speed for SR motor and induction motor are chosen as the same.
- Magnetic loading "B" of induction motor is taken as 0.54 T and air-gap flux density of PM BLDC motors are taken as 0.6 T.
- Switched reluctance motor is considered for 2 different peak stator pole flux density values (1.7 T and 2.1 T)
- For SR motor, SR-CAD, supplied by Tubitak Bilten and makes a detailed analysis of SR motor, is used to analyze the performance.
- Dimensions of each motor are determined at wash speed then checked whether they satisfy the torque requirement at spin speed. If not design process is repeated for the spin speed.
- Induction motor AF-BLDC motor and RF-BLDC motor are designed at wash cycle and determined dimensions satisfy the torque requirement at spin cycle. But dimensions of the SR motor, determined at wash cycle did not satisfy the torque requirement at spin cycle. So that SR motor is designed at spin cycle.
- Since switched reluctance motor is designed to satisfy the torque requirement of the load at spin cycle, at wash cycle it gives more torque than required, by changing the advance angle and conduction period of optimization program. So that torque per unit volume of switched reluctance motor is determined by using the maximum torque that it can give at specified speed.

We have derived the torque equation of each motor in preceeding chapters. In order to compare the torque per unit rotor volume of the motors, we can write the torque equations, assuming axial length is equal to the bore diameter, of each motor in the form of

$$T = KBqD_i^3 \tag{6.1}$$

The motors and corresponding torque equations are tabulated in table 6.1. In table;

"B" is the magnetic loading of induction

"B_p" is the peak stator flux density of SR motor

"B_g" is the air-gap flux density of BLDC motors

Note that; "B_p" of the SR motor is nearly 3.5 times of the "B" of induction motor and "B_g" of BLDC motors. The term in the paranthesis for SR motor, takes this into account.

Table 6 1 Torque per unit rotor volume capabilities of each motor

MOTOR	TORQUE EQUATION
Induction Motor	$1.02\,BqD_i^3$
SR Motor	$0.34B_pqD_i^3 = \left(1.19\,BqD_i^3\right)$
RF-BLDC Motor	$1.3B_gqD_i^3$
AF-BLDC Motor	$1.56\,B_gqD_i^3$

It is seen from the table that AF-BLDC is expected to produce the same torque with a smallest inner diameter as compared to other motors. Induction motor may be expected to have the largest volume for the same torque, since the constant in its torque equation is the smallest. The SR motor and RF-BLDC may be expected to have roughly the same volume. Once the tabulated results are studied in detail it is seen that the expectations due to the torque per unit rotor volume are satisfied. Results of the performance analysis of the motors for different number of poles at wash cycle and at spin cycle are given in the tables 6.2 and 6.3. In the tables the variables used are as follows:

"V_{motor}" is the motor volume

"I_{peak}" is the peak stator current

"T" is the motor torque

"P_{core}" core loss

"P_{cu}" Copper loss

"D_i" is the bore diameter

"L" is the axial length

"D_o" is the outer diameter

Table 6 2 Results of the analysis at low speed (wash cycle)

WASH CYCLE $n=400$ rpm, $T= 2.5$ Nm, $P_{out}=104,7$ W													
	Induction Motor			**RF-BLDC Motor**			**AF-BLDC Motor**			**SR Motor**			
Number of poles (phase)	2	6	10	2	6	10	2	6	10	3 ph (1.7T)	3 ph (2.1T)	4 ph (1.7T)	4 ph (2.1T)
D_i (mm)	54,5	54,5	54,5	48,8	48,8	48,8	45,6	45,6	45,6	53,7	50	56,3	52,5
L (mm)	54,5	54,5	54,5	48,8	48,8	48,8	98,7	51	41,4	53,7	50	56,3	52,5
D_o (mm)	106,8	84	79,5	105	79,3	74,2	79	79	79	109	104	96,8	91,8
V_{motor} ($*10^{-4}m^3$)	4,875	3,01	2,69	4,21	2,41	2,11	4,83	2,49	2,03	5,05	4,28	4,14	3,47
I_{peak} (A)	4,7	4,7	4,7	10,8	10,8	10,8	8,86	8,86	8,86	4	3,6	3,5	3.2
T/V_{motor} (N/m^2)	5128	8300	9293	5938	10373	11848	5175	10040	12315	6728	7920	8933	11180
T/I_{peak} (Nm/A)	0,53	0,53	0,53	0,23	0,23	0,23	0,28	0,28	0,28	0,625	0,69	0,71	0,8
f (Hz)	6,6	20	33,3	6,6	20	33,3	6,6	20	33,3	26,6	26,6	40	40
P_{core} (W)	14,77	20	26,5	9,9	11,3	13,8	4	4	4	69,6	61,9	77,5	73,92
P_{cu} (W)	103,5	73,6	67,65	63,6	43,2	39,13	43,75	29,5	26,7	14,5	12	8,7	4,7
η (%)	46,9	52,78	52,65	58,7	65,7	66,4	68,6	75,7	77	55,5	58,4	54,8	57,4
P_{loss}/surface	3285	3744	5397	2227	2477	2646	1404	1522	1353	2272	2239	2693	2800

Table 6 3 Results of the analysis at high speed (spin cycle)

SPIN CYCLE **n=12500 rpm, T= 0,35 Nm, P_{out}=458 W**													
	Induction Motor			**RF-BLDC Motor**			**AF-BLDC Motor**			**SR Motor**			
Number of poles (phase)	2	6	10	2	6	10	2	6	10	3 ph (1.7T)	3 ph (2.1T)	4 ph (1.7T)	4 ph (2.1T)
D_i (mm)	54,5	54,5	54,5	48,8	48,8	48,8	45,6	45,6	45,6	53,7	50	56,3	52,5
L (mm)	54,5	54,5	54,5	48,8	48,8	48,8	98,7	51	41,4	53,7	50	56,3	52,5
D_o (mm)	106,8	84	79,5	105	79,3	74,2	79	79	79	109	104	96,8	91,8
V_{motor} (*$10^{-4}m^3$)	4,875	3,01	2,69	4,21	2,41	2,11	4,83	2,49	2,03	5,05	4,28	4,14	3,47
I_{peak} (A)	2,8	2,8	2,8	1,51	1,51	1,51	1,01	1,01	1,01	0,51	0,45	0,37	0,36
T/V_{motor} (N/m^2)	718	1162	1301	831	1452	1658	724	1136	1724	744	958	1053	1181
T/I_{peak} (Nm/A)	0,125	0,125	0,125	0,231	0,231	0,231	0,346	0,346	0,346	0,68	0,7	0,94	0,97
f (Hz)	208	625	1041	208	625	1041	208	625	1041	833	833	1250	1250
P_{core} (W)	26,6	36,14	47,8	310	355	430	124	124	124	111,6	128,4	123	156
P_{cu} (W)	35,16	25	23	1,24	0,84	0,76	0,85	0,57	0,5	0,2	0,13	0,15	0,1
η (%)	79	77	76,6	52,9	51,8	47,76	70	70	70	71,3	69,8	70,4	67
P_{loss}/surface	1715	2445	3078	9424	16136	21500	3672	5662	6200	3016	3890	3842	5570

From now on the aim is to select the best choice for the washing machine application. In order to compare motors, torque per unit volume, torque per unit current and efficiency of the motors are considered.

In order to simplify the comparison procedure, first a selection is made between motors of the same type. To be able to make this selection, plots of each criteria against number of poles (phases for SR motor) are drawn. After the most appropriate motor of each type is chosen, they are also compared with each other.

6.2 Results

6.2.1 Induction motor

In this section the three different induction motors with different pole numbers will be evaluated from the point of view of chosen criteria. In figures 6.1 to 6.5 plots of efficiency, torque per unit motor volume and torque per unit current are given against motor speed for each motor. Then by the help of these plots we will choose the most appropriate induction motor for the washing machine application.

In the selection it should be kept in mind that energy efficiency is an important criteria for a washing machine application. Typically a washing machine spends nearly 90% of its time at wash cycle. Therefore the efficiency at wash cycle is more important than spin cycle efficiency.

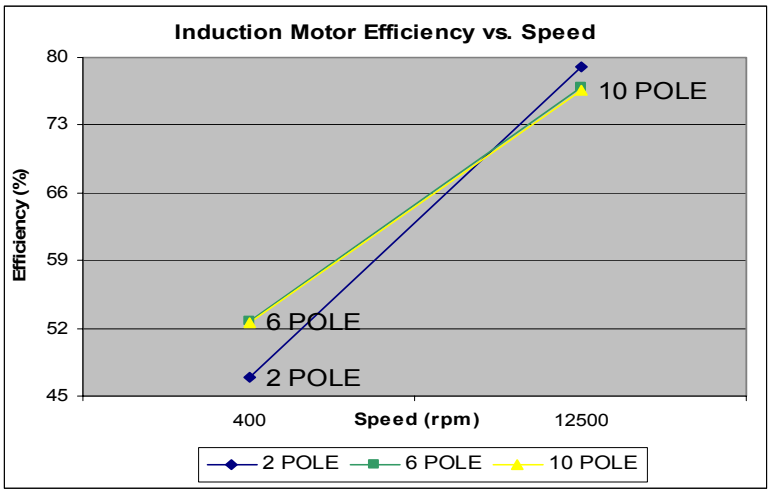

Figure 6 1 Induction motor efficiency vs. speed variation with the number of poles

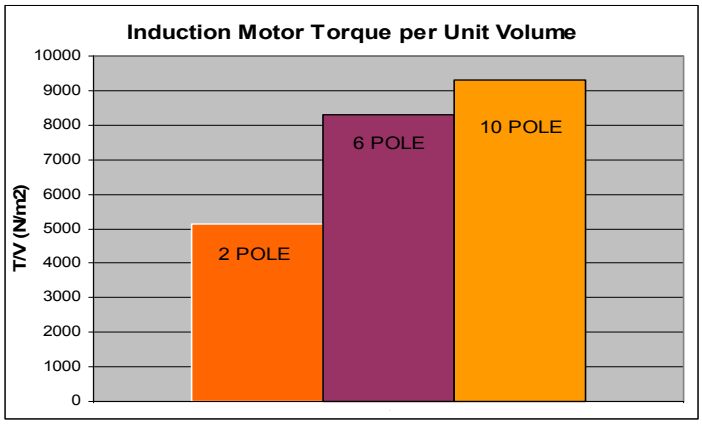

Figure 6 2 Torque per unit motor volume of induction motor at wash cycle

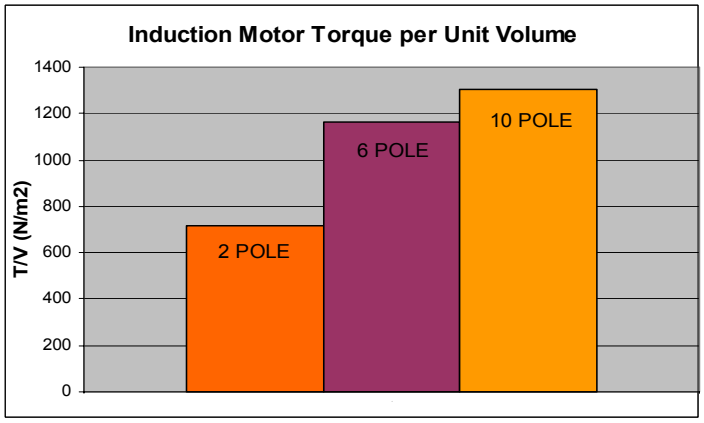

Figure 6 3 Torque per unit motor volume of induction motor at spin cycle

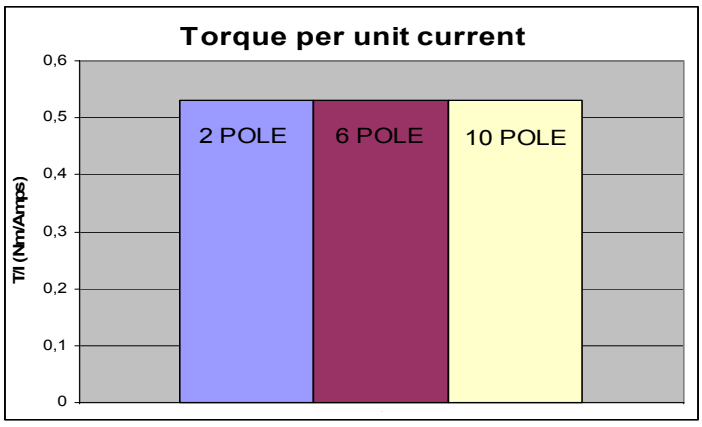

Figure 6 4 Torque per unit current of induction motor at wash cycle

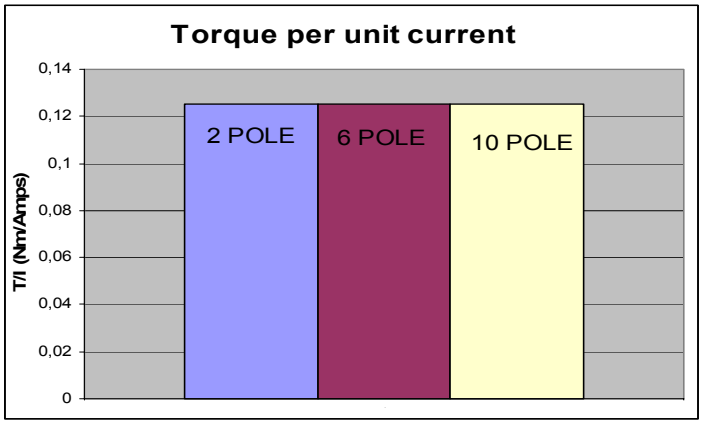

Figure 6 5 Torque per unit current of induction motor at spin cycle

Once the figures are considered, it is seen that ten pole induction motor and six pole induction motor have nearly the same efficiency. But from the point of view of torque per unit motor volume criterion ten pole induction motor gives the best result. Therefore it is appropriate to choose ten pole induction motor among the induction motor types for the washing machine application.

6.2.2 RF-BLDC motor

In this section the three different RF-BLDC motors with different pole numbers will be evaluated from the point of view of chosen criteria. In figures 6.6 to 6.10 plots of efficiency, torque per unit motor volume and torque per unit current are given against motor speed for each motor. Then by the help of these plots we will choose the most appropriate RF-BLDC motor for the washing machine application.

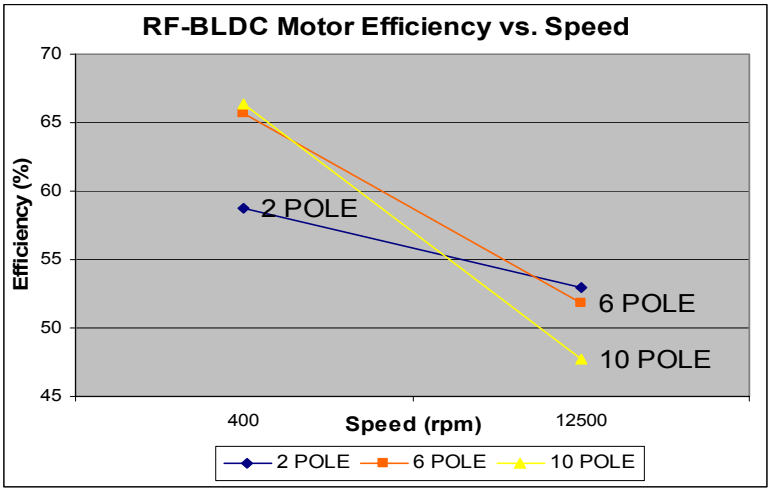

Figure 6 6 RF-BLDC motor efficiency vs speed variation with the number of poles

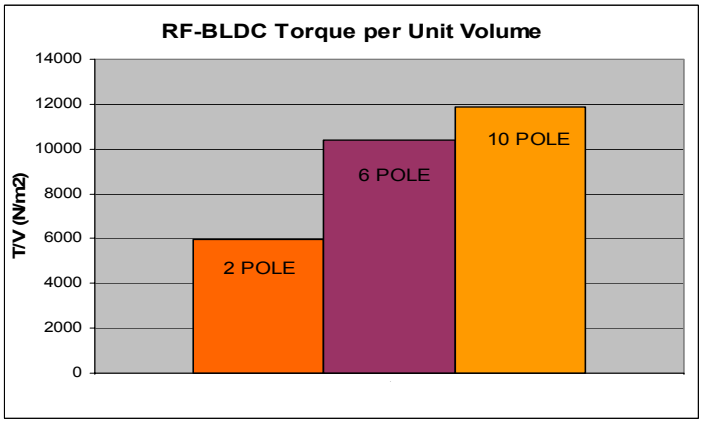

Figure 6 7 Torque per unit motor volume of RF-BLDC motor at wash cycle

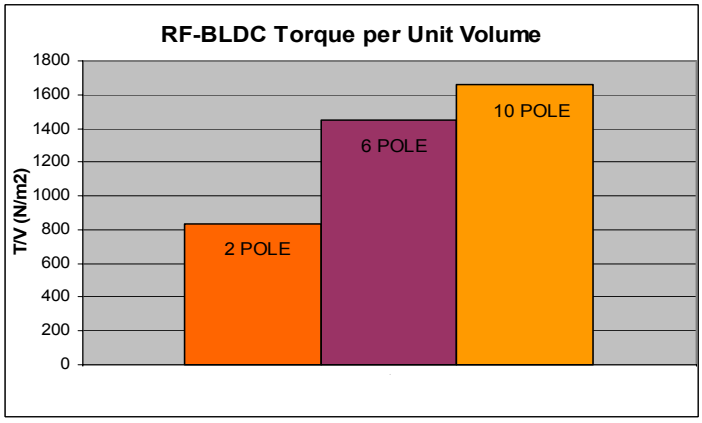

Figure 6 8 Torque per unit motor volume of RF-BLDC motor at spin cycle

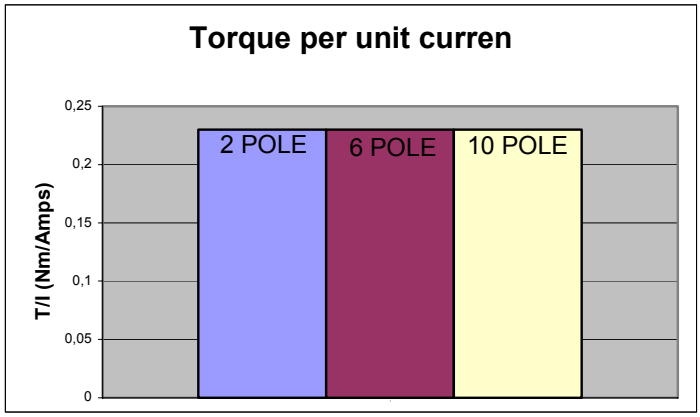

Figure 6 9 Torque per unit current of RF-BLDC motor at wash cycle

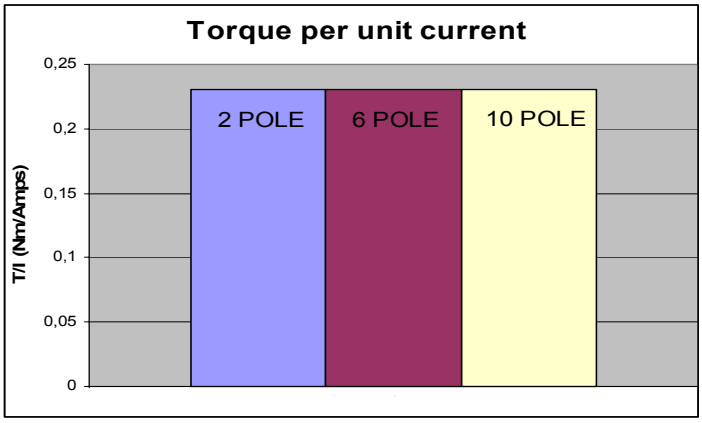

Figure 6 10 Torque per unit current of RF-BLDC at spin cycle

Although ten pole RF-BLDC motor has the lowest efficiency at spin cycle, its efficiency at wash cycle is high. Also torque per unit motor volume of ten pole RF-BLDC motor is the highest. Combining these, it will be appropriate to choose ten pole RF-BLDC motor among the RF-BLDC motor types for the washing machine application.

6.2.3 AF-BLDC motor

In this section the three different AF-BLDC motors with different pole numbers will be evaluated from the point of view of chosen criteria. In figures 6.11 to 6.15 plots of efficiency, torque per unit motor volume and torque per unit current are given against motor speed for each motor. Then by the help of these plots we

will choose the most appropriate AF-BLDC motor for the washing machine application.

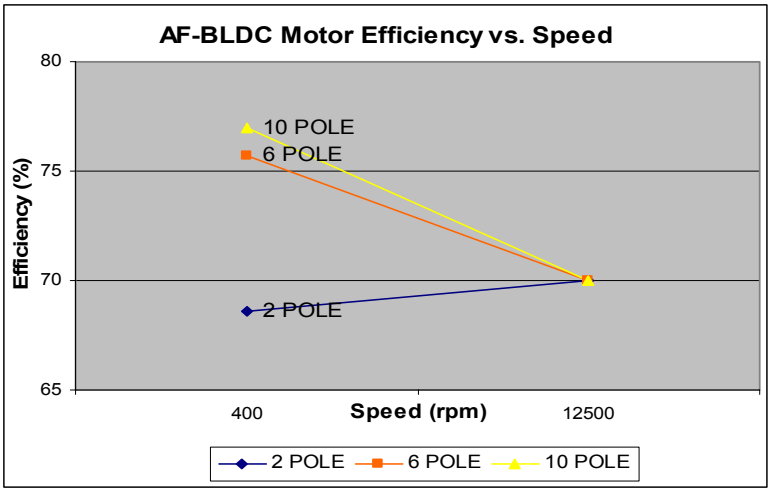

Figure 6 11 AF-BLDC motor efficiency vs. speed variation with the number of poles

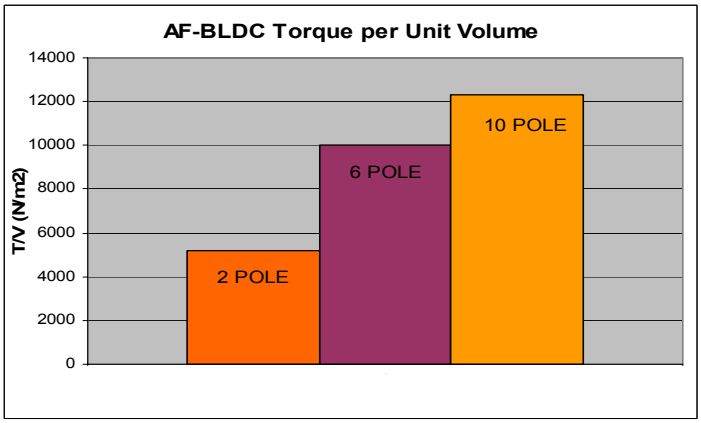

Figure 6 12 Torque per unit motor volume of AF-BLDC motor at wash cycle

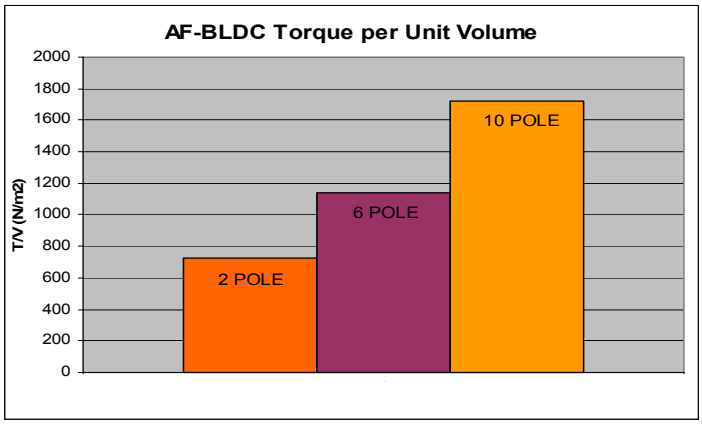

Figure 6 13 Torque per unit motor volume of AF-BLDC motor at spin cycle

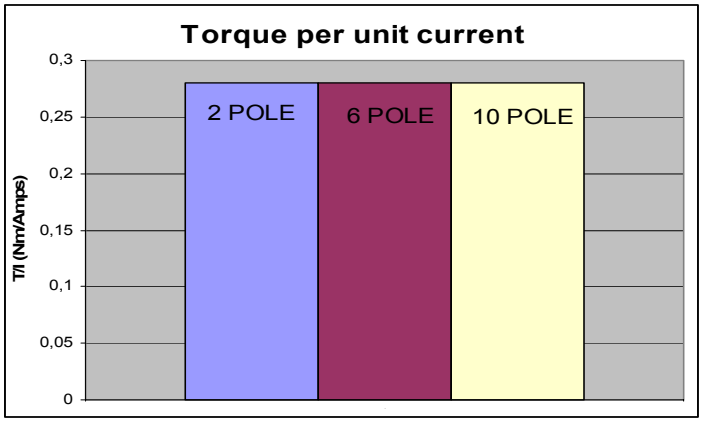

Figure 6 14 Torque per unit current of AF-BLDC motor at wash cycle

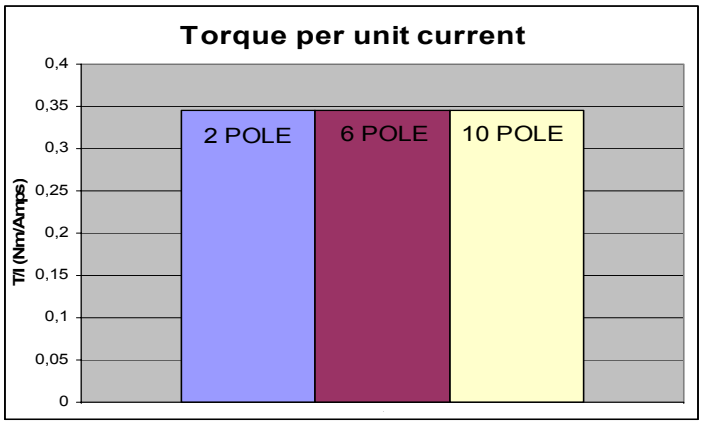

Figure 6 15 Torque per unit current of AF-BLDC motor at spin cycle

Once the figures are considered, it is seen that ten pole AF-BLDC motor is the best choice from the point of view of all the comparison criteria. It gives the best results both at wash cycle and at spin cycle. So that ten pole AF-BLDC motor is chosen among the AF-BLDC motor types.

6.2.4 SR motor

As the last part of the selection procedure, in this subsection we will consider the SR motor. In this section the four different SR motors with different phase numbers will be evaluated from the point of view of chosen criteria. In figures 6.16 to 6.20 plots of efficiency, torque per unit motor volume and torque per unit current are given against motor speed for each motor. Then by the help of these plots we will choose the most appropriate SR motor for the washing machine application.

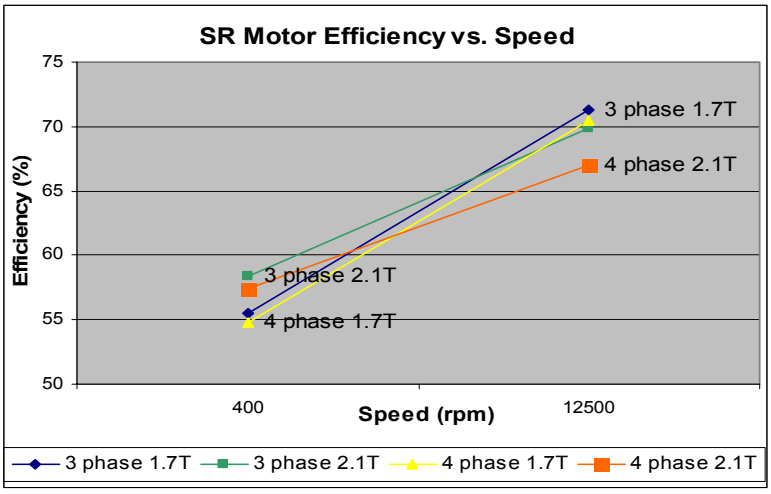

Figure 6 16 Efficiency vs. speed variation of SR motor types

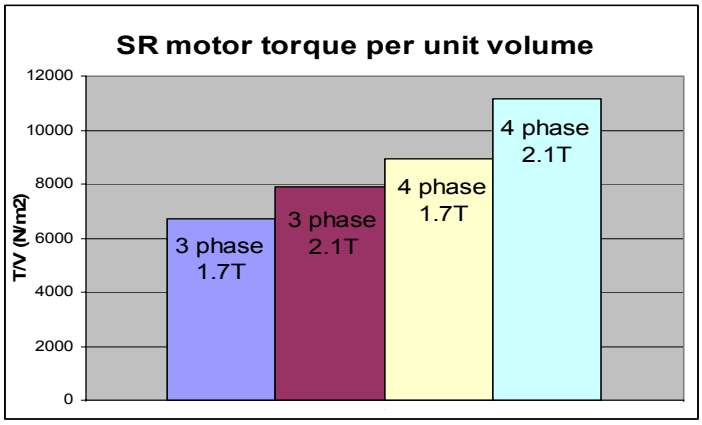

Figure 6 17 Torque per unit volume of SR motor at wash cycle

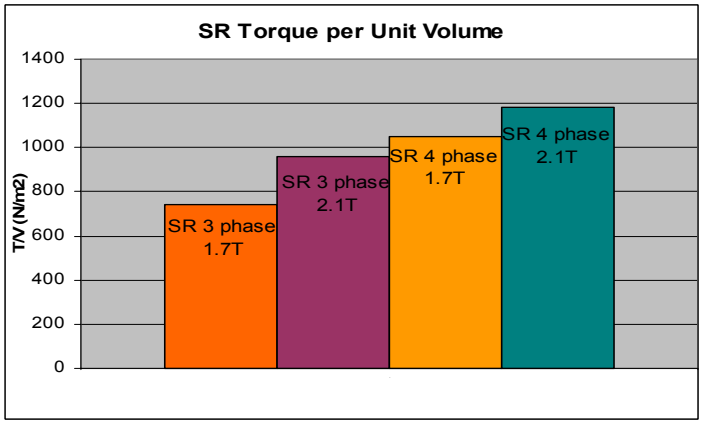

Figure 6 18 Torque per unit motor volume of SR motor at spin cycle

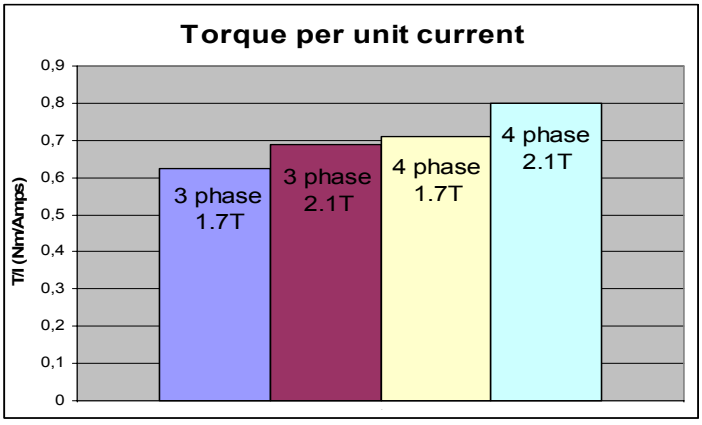

Figure 6 19 Torque per unit current of SR motor at wash cycle

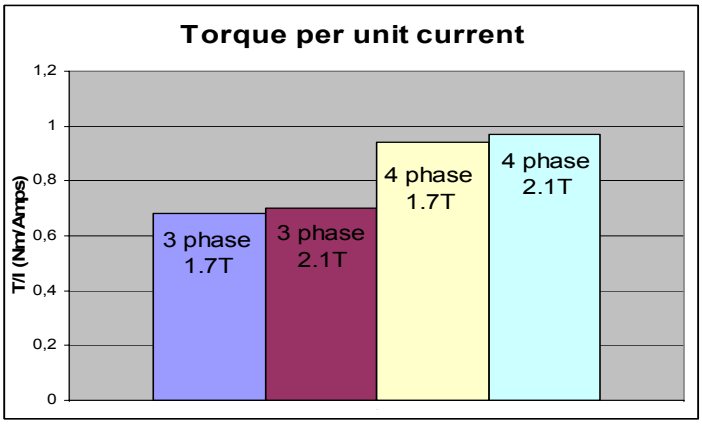

Figure 6 20 Torque per unir current of SR motor at spin cycle

Once the SR motor figures are considered, four phase SR motor designed at a peak stator flux density of 2.1T seems to be the best choice for the washing machine application. Its only drawback is the efficiency at spin cycle. Therefore considering all advantages and dis advantages, we can hoose this motor.

6.2.5 Comparison

So far we have chosen the most appropriate motors of each type for the washing machine application. They are;

- Ten pole induction motor
- Ten pole RF-BLDC motor
- Ten pole AF-BLDC motor
- 4 phase SR motor designed at a peak stator flux density of 2.1T

In this section we will compare these previously selected motors from the point of view of chosen criteria. In figures 6.21 to 6.25 plots of efficiency, torque per unit motor volume and torque per unit current are given against motor speed for the selected motors.

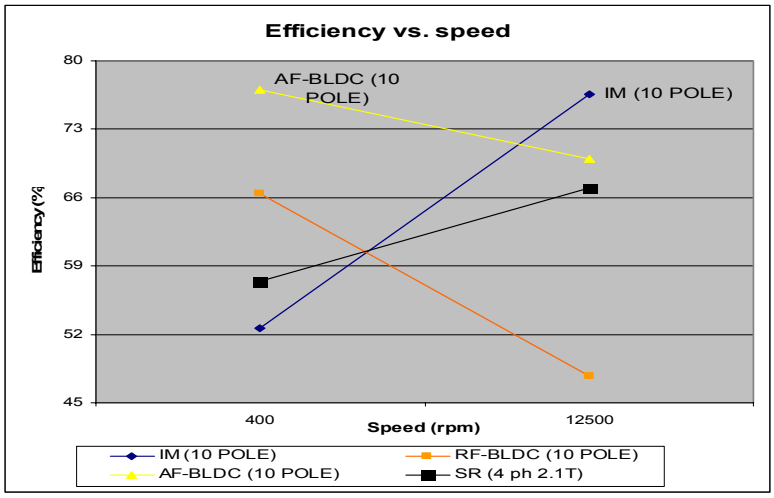

Figure 6 21 Efficiency vs speed of selected motors

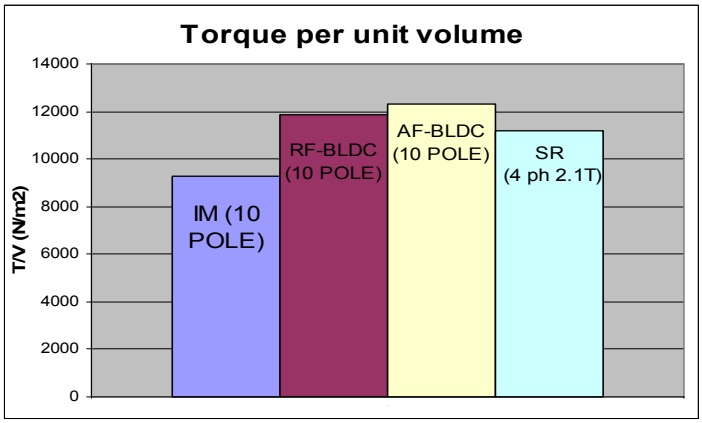

Figure 6 22 Torque per unit motor volume of the selected motors at wash cycle

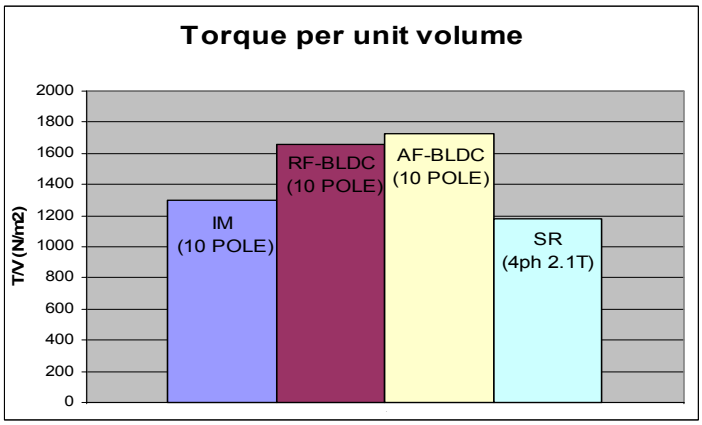

Figure 6 23 Torque per unit motor volume of selected motors at spin cycle

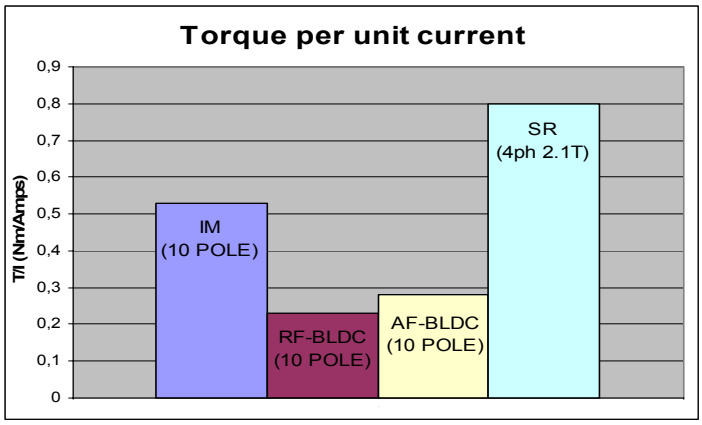

Figure 6 24 Torque per unit current of the selected motors at wash cycle

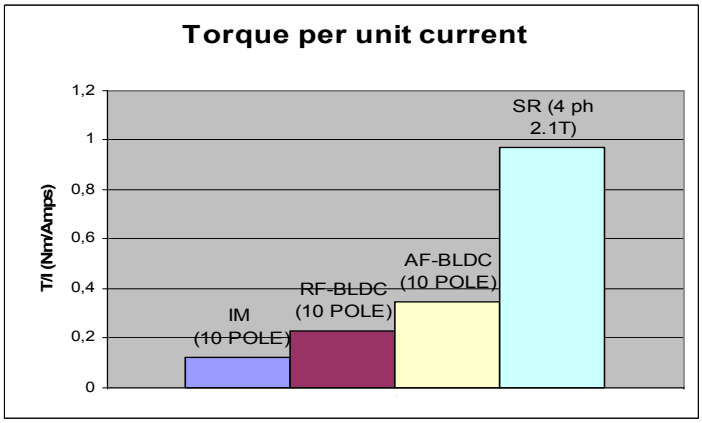

Figure 6 25 Torque per unit current volume of the selected motors at spin cycle

Once the figures are studied in detail, it is seen that efficiency of ten pole AF-BLDC motor is the highest at wash cycle. AF-BLDC motor also has good efficiency at spin cycle, its only competitor at spin cycle is the induction motor. However induction motor could not be a good choice becouse of its low efficiency at wash cycle. Therefore from the point of view of efficiency ten pole AF-BLDC motor is the most appropriate motor for washing machine application.

From the point of view of torque per unit motor volume criterion, figure 6.22 and 6.23 show that ten pole AF-BLDC motor has the highest torque per unit motor volume both at wash cycle and at spin cycle. Especially at wash cycle ten pole RF-BLDC motor and four phase SR motor can also be good competitors since they have high torque per unit motor volume values.

From the point of view of torque per unit current criterion, four phase SR motor gives the best results both at wash cycle and at spin cycle. In this case AF-BLDC and RF-BLDC motor does not seems to be good choices.

The results mentioned above demonstrate the superiority of AF-BLDC motor over the other types of motors. Especially from the point of view of energy efficiency both at wash cycle and at spin cycle. Since SR motor has lower current rating, it can also be another competent for the washing machine application when the converter cost is taken into account.

6.3 Future work

These theoretical studies will be compared with the results obtained in the laboratory environment in order to see the reliability of the equations. This is achieved by using the prototype BLDC motors, SR motor and induction motor, present in the laboratory.

REFERENCES

[1] T.J.E. Miller, "Brushless Permanent Magnet and Reluctance Motor Drives", 1989, Oxford University Press

[2] A.E. Fitzgerald, C. Kingsley, S.D. Umans, "Electric Machinery", Fifth ed. McGraw Hill

[3] Funda Şahin, "Design and Development of a High Speed Axial Flux Permanent Magnet Machine", 2001, Technische Universiteit Eindhoven

[4] N.Balkan Şimşir, H. Bülent Ertan, " A Comparison Between the Torque Production Capabilities of Axial Flux and Radial Flux Type of BLDC Motors for Adjustable Speed Drives", Proceedings of the IEEE 1999 International Conference on power electronics and drive systems

[5] F. Caricchi, F. Crescimbini, O. Honorati, "Low Cost Compact Permanent Magnet Machine for Adjustable Speed Pump Application", IEEE Transactions on Industry Applications, Jan/Feb 1998, pp. 464-470

[6] D. Hanselman, "Brushless Permanent Magnet Motor Design", Second ed. Writers' Collective,2003

[7] P. Pillay, R. Krishnan, "Application Characteristics of Permanent Magnet Synchronous and Brushless DC Motors for Servo Drives", IEEE Transactions on Industry Applications, Sep/Oct 1991, pp. 986-996

[8] S. Huang, M. Aydın, T.A. Lipo, "Torus Concept Machines: Pre-prototyping Design Assessment for Two Major Topologies", IEEE Industry Applications Conference, 2001, pp. 1619-1625

[9] F. Profumo, Z. Zhang, A. Tenconi, "Axial Flux Machines Drives: A New Viable Solution for Electric Cars", IEEE Transactions on Industrial Electronics, 1997, pp. 39-44

[10] B.K. Bose, "Power Electronics and Variable Frequency Drives", IEEE Press, 1997

[11] Y. Li, J.D. Lloyd, G.E. Horst, "Switched Reluctance Motor with DC Assisted Excitation", IEEE Industry Application Conference, 1996, pp. 801-807

[12] R. Krishnan, "Switched Reluctance Motor Drives: Modeling, Simulation, Analysis, Design and Applications", Magna Physics Publishing,

[13] E. Spooner, B.J. Chalmers, "Toroidally Wound Slotless Axial Flux Permanent Magnet Brushless DC Motors", ICEM 88, pp. 81-86

[14] S. Huang, J. Luo, F. Leonardi, T.A. Lipo, "A General Approach to Sizing and Power Density Equations for Comparison of Electrical Machines", IEEE Transactions on Industry Applications, Jan/Feb. 1998, pp.92-97

[15] V.B. Honsinger, "Sizing Equations for Electrical Machinery", IEEE Transactions on Energy Conversion, March 1987, pp.116-121

[16] G.R. Slemon, "On the Design of High Performance Surface Mounted PM Motors", IEEE Transactions on Industry Applications, Jan/Feb 1994, pp.134-140

[17] G.R. Slemon, "Electrical Machines for Variable Frequency Drives", IEEE Proceedings, August 1994, pp. 1123-1139

[18] H. Moghbelli, G.E. Adams, R.G.Hoft, "Performance of a 10 Hp Switched Reluctance Motor and Comparison with Induction Motors", IEEE Transactions on Industry Applications, May/June 1991, pp. 531-537

[19] K.M.Rahman, S.E.Schulz, "Design of High Efficiency and High Torque Density Switched Reluctance Motor for Vehicle Propulsion", IEEE Transactions on Industry Applications, Nov/Dec 2002, pp. 1500-1507

[20] G.R.Slemon, A.Straughen, "Electric Machines", 1980, :Addison Wesley Publishing Company

[21] B.S.Guru, H.R.Hızıroglu, "Electric Machinery and Transformers", 2001, Oxford University Press

[22] H.B.Ertan, M.Y.Üçtuğ, R.Colyer, A.Consoli, "Modern Electrical Drives", 2000, NATO ASI Series

[23] H.B. Ertan, Ö.F. Yagan, A. Diriker, "Optimum Parameters for Doubly Salient Motors Driven by a Voltage Source Drive", Proc. of the International Conference on Electrical Machines, pp. 806-811

[24] L.B. Yalçıner "A Software for Analysis & Design Optimization of Switched Reluctance Motor" MSc Thesis, M.E.T.U. Electrical Electronics Engineering, 2004

APPENDIX A

OUTER RADIUS CALCULATION OF RF-PMSM AND INDUCTION MOTOR

To calculate the outer diameter, we assume D_i is known.

$$D_o = D_i + 2W_{sy} + 2h_s \tag{1}$$

Where;

W_{sy} is the stator back core thickness

h_s is the slot depth

R_i is known so that to find the R_o, h_s and W_{sy} should be determined. First find the slot height. Let the total area occupied by the stator conductors be;

$$A_{T-cu} = 6N_{ph}A_{cu} = 6N_{ph}\frac{I}{J} \tag{2}$$

Where;

A_{cu} is the cross-section for one conductor

$A_{T\text{-}cu}$ is the total conductor area

If the total slot area is A_1 then by using copper fill factor K_{cu} and total conductor area the slot area becomes

$$A_1 = \frac{A_{T-cu}}{K_{cu}} = \pi\left(\frac{D_i}{2} + h_s\right)^2 - \pi\left(\frac{D_i}{2}\right)^2$$
$$A_1 = \pi h_s\left(D_i + h_s\right) \tag{3}$$

When equation (3) is solved

$$h_s = \frac{\sqrt{D_i^2 + \frac{4D_i q}{K_{cu} J}}}{2} - \frac{D_i}{2} \tag{4}$$

Where;

"K_{cu}" is the copper fill factor

"J" is the current density in A/m2

From now on the only unknown of the equation (1) is stator back core thickness. To find stator back core thickness area of the stator core can be used so that our starting point, when finding the back core thickness, is the stator core flux.

$$\phi_{sc} = \frac{\phi_p}{2} \tag{5}$$

Where;

Φ_p is the flux per pole

Φ_{sc} is the stator back core flux

As we know

$$\phi = B \times A$$

If we know Φ_p we can find Φ_{sc} by using equation (2.30)

If we know B_p we can find B_{sc} approximately (B_{sc}=2B by assuming tooth width=slot width) with the reference of figure 2.2.

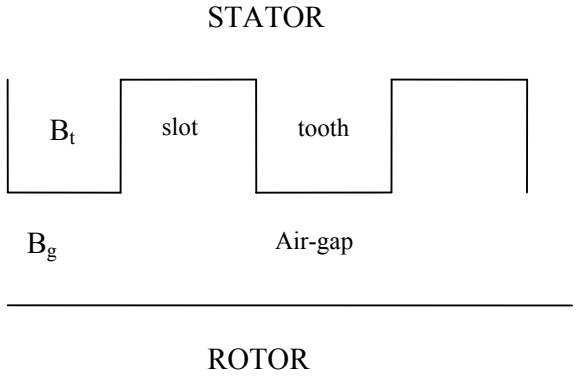

Figure A 1 Schematic representation of tooth and slot

We can find stator back core area A_{sc} as;

$$A_{sc} = W_{sy}L = \frac{\phi_{sc}}{B_{sc}} = \frac{\phi_p/2}{K_{BR}B} = \frac{B\frac{\pi D_i L}{P}}{2K_{BR}B} = \frac{\pi D_i L}{2PK_{BR}} \tag{6}$$

$$W_{sy} = \frac{\pi D_i}{2PK_{BR}} \tag{7}$$

Then using equation (1), (4) and (7) outer diameter can be found as:

$$D_o = \frac{\pi D_i}{PK_{BR}} + \sqrt{D_i^2 + \frac{4D_i q}{K_{cu}J}} \tag{8}$$

APPENDIX B

AXIAL LENGTH OF AXIAL FLUX MOTOR

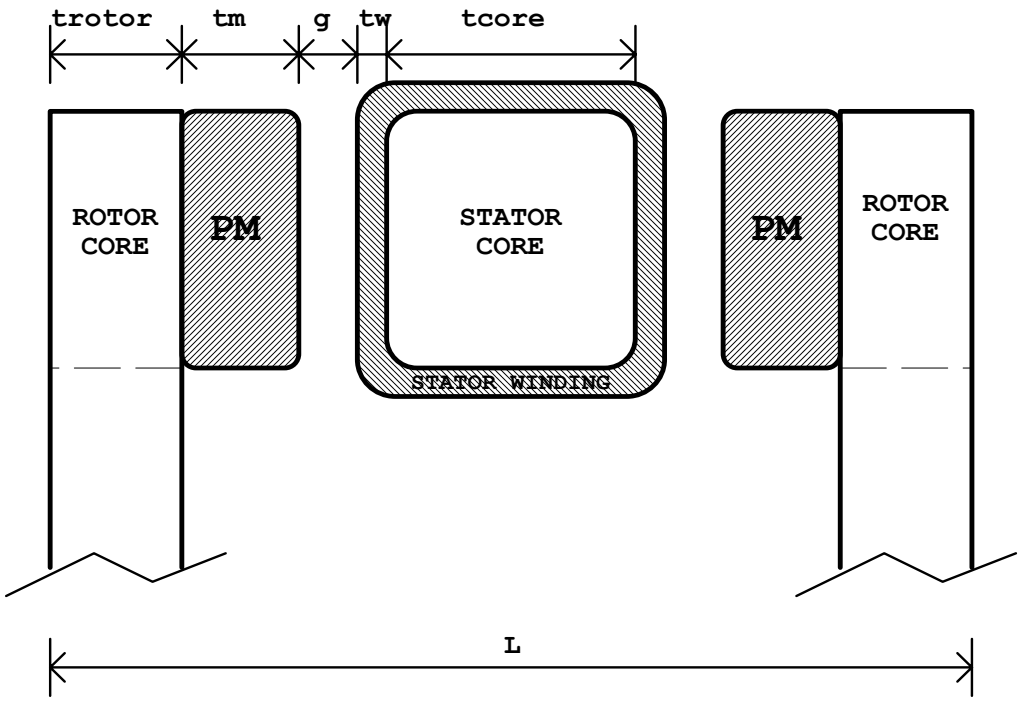

Figure B 1 Axial Length Calculation

As seen from the figure total axial length constitutes of rotor back cores, permanent magnets, air-gaps, stator coils and stator back core. To find axial length, it is necessary to find these values.

$$L = 2t_{rotor} + t_{core} + 2t_m + 2t_w + 2g \quad (1)$$

Air-gap flux density, produced by the magnets can be found using the formula:

$$B_g = \frac{t_m}{t_w + g + t_m} B_r \quad (2)$$

Where

B_r is the remenant flux density of the permanent magnet.

Rearranging the terms magnet thickness can be found as:

$$t_m = (t_w + g) \frac{B_g / B_r}{1 - B_g / B_r} \quad (3)$$

The minimum value for air-gap is determined from mechanical constraints while winding thickness is determined from current loading and current density as:

$$t_w = \frac{q}{JK_{cu}} \quad (4)$$

The stator core thickness can be written as:

$$t_{core} = w \frac{B_g}{B_{core}} \quad (5)$$

Where

$w = \frac{2\pi R_i}{p}$ is the tangential magnet width

When the core thickness is found it can be assumed that

$$t_{rotor} = \frac{t_{core}}{2} \tag{6}$$

Then by combining these equations axial length of the motor can be written as:

$$L = \frac{4\pi R_i}{pK_{BR}} + 2\frac{t_{w+g}}{1 - B_g / B_r} \tag{7}$$

APPENDIX C

WASHING MACHINE DATA

The washing machine requires 25 Nm at 40 rpm (during wash cycle) and 3.5 Nm at 1250 rpm (during spin cycle) or so. The speed range of the drum is then nearly 1:30.

Typical torque speed curve of the sample washing machine, by using piecewise linear approximation is given in the figure shown below